# 國立交通大學

## 電控工程研究所

## 博士論文

### 基於腦波建置一通用型瞌睡預測系統

### Development of Generalized EEG-based
### Drowsiness Prediction System

研 究 生：林富章

指導教授：林進燈　教授

中 華 民 國 一 百 零 一 年 四 月

# National Chiao Tung University

## Department of Electrical Control Engineering
## **Dissertation**

基於腦波建置一通用型瞌睡預測系統

Development of Generalized EEG-based

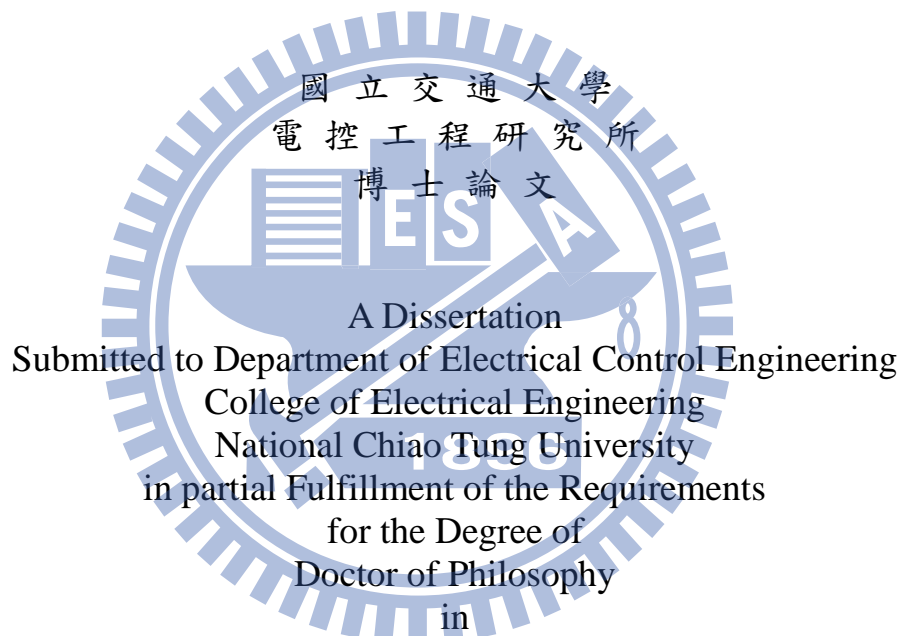Drowsiness Prediction System

Student: Fu-Chang Lin
Advisor: Prof. Chin-Teng Lin

**April, 2012**

基於腦波建置一通用型瞌睡預測系統

# Development of Generalized EEG-based Drowsiness Prediction System

研 究 生：林富章　　Student: Fu-Chang Lin

指導教授：林進燈　　Advisor: Chin-Teng Lin

國 立 交 通 大 學

電 控 工 程 研 究 所

博 士 論 文

A Dissertation
Submitted to Department of Electrical Control Engineering
College of Electrical Engineering
National Chiao Tung University
in partial Fulfillment of the Requirements
for the Degree of
Doctor of Philosophy
in

Electrical Control Engineering

April 2012

Hsinchu, Taiwan, Republic of China

中華民國一百零一年四月

# 基於腦波建置一通用型瞌睡預測系統

學生: 林富章　　　　　　　　　　　　　　　　指導教授:林進燈教授

國立交通大學電控工程所博士班

## 摘　　要

本論文主要提供一套自組織式模糊類神經網路技術(Self-organizing Neural Fuzzy Inference Network)，使用腦波建構一通用型瞌睡預測系統與應用。近年來，證據顯示疲勞駕駛是造成車禍發生的重大原因之一。因此，許多關於如何監測駕駛者精神狀態，並提供警示的輔助系統(Assistant Monitoring System) ，包含人機介面(Brain Computer Interface, BCI)等研究應運而生。而開發這些輔助系統的最大難題,首在如何取得最即時(Real Time)、直接(Direct)且明顯(Significant)與駕駛者精神狀態相關的指標(Index)，以作為該系統判別瞌睡程度的依據；另外並需要同時克服在動態的實際駕駛環境中，所帶來的雜訊干擾 (Noise Disturbance)。本論文利用虛擬實境技術之動態駕車裝置，來模擬真實之駕車環境，透過高速公路行車場景的設計，結合腦電波(Electroencephalogram, EEG)分析來取得駕駛者在疲勞駕車行為下，人類的腦部認知功能與反應變化。研究發現，駕駛者的疲勞程度與其腦波的 Occipital Component 的能量分布(Power Spectra)有極大的關聯，並與駕駛者在高速公路行車場景所設計的車輛偏移事件實驗(Event-Related Lane Departure Experiment)的反應時間(Reaction Time)有直接的相關性。在本論文中，我們將六個參與高速公路行車場景所設計的車輛偏移事件實驗的駕駛者的腦波，透過獨立成份分析演算法(Independent Component Analysis, ICA)，分離出多個獨立訊號源後，採用 Occipital Component 的能量分布，加上相

對應的駕駛反映時間，作為四種腦波瞌睡預測系統的模型建置(Model Construction)依據。研究發現，當使用相同駕駛者的腦波及反應時間所建立的四種反應時間估測模型(RT Estimation Models)，其系統的運作性能(Performance)運用在相同駕駛者的反應時間預測上，皆可以達到相當好的效果；然而當使用不同駕駛者的腦波所建立的四種反應時間估測模型，其系統的運作性能運用在不同駕駛者的反應時間預測上，只有所提出的自組織式模糊類神經網路的架構，仍能保持一定的性能。此獨特的優勢(p-value < 0.038)，可將此基於腦波建置的通用化瞌睡預測系統，廣泛應用在一般的生活當中。

# Development of Generalized EEG-based Drowsiness Prediction System

Student: Fu-Chang Lin                    Advisor: Prof. Chin-Teng Lin

Institute of Electrical Control Engineering
National Chiao Tung University

## ABSTRACT

A generalized EEG-based Neural Fuzzy system to predict driver's drowsiness was proposed in this study. Driver's drowsy state monitoring system has been implicated as a causal factor for the safety driving issue, especially when the driver fell asleep or distracted in driving. However, the difficulties in developing such a system are lack of significant index for detecting the driver's drowsy state in real-time and the interference of the complicated noise in a realistic and dynamic driving environment. In our past studies, we found that the electroencephalogram (EEG) power spectrum changes were highly correlated with the driver's behavior performance especially the occipital component. Different from presented subject-dependent drowsy state monitor systems, whose system performance may decrease rapidly when different subject applies with the drowsiness detection model constructed by others, in this study, we proposed a generalized EEG-based Self-organizing Neural Fuzzy system (SONFIN) to monitor and predict the driver's drowsy state with the occipital area. Two drowsiness prediction models, subject-dependent and generalized cross-subject predictors, were investigated in this study for system performance analysis. Correlation coefficients and root mean square errors are showed as the experimental results and interpreted the performances of the proposed system significantly better than using other traditional Neural Networks (p-value <

0.038). Besides, the proposed EEG-based Self-organizing Neural Fuzzy system can be generalized and applied in the subjects' independent sessions. This unique advantage can be widely used in the real-life applications.

# 致　　謝

# Table of Contents

# List of Tables

# List of Figures

# Abbreviations

BCI   : brain computer interface

EEG   : electroencephalograms

ICA   : independent component analysis

EOG   : electrooculography

HRV   : heart-rate variability

VR   : virtual reality

3D   : three degree

RT(s)   : reaction time (s)

Dev-on   : deviation onset

Rps-on   : response onset

Rps-off   : response offset

MLPNN   : multi-layer perceptron neural network

SVR   : support vector regression

SVM   : support vector machine

RBF   : radial basis function

RBFNN   : radial basis function neural network

SONFIN   : self-organizing neural fuzzy inference network

PPMCC   : pearson product moment correlation coefficient

RMSE   : root mean of square error

BSS   : blind source separation

OLS   : orthogonal least squares

# I  Introduction

## 1.1. Motivation

Drowsy driving is unsafe and dangerous to result in mounts of fatal accident every year. Many traffic accidents have been implicated to drivers' fatigue that is the causal factor among these accidents. Driving safety has been escalated to receive a prior attention of the publics during the past years because of the growth of traffic accidents caused by the declination in the drivers' capability of perception, recognition and vehicle control abilities while sleepy. The 2009 Sleep Report of National Sleep Foundation (NSF) in America poll shows that 1% or as many as 1.9 million drivers have had a car crash or a near miss due to drowsiness in the past year. Even more surprising, 54% of drivers (105 million) have driven while drowsy at least once in the past year, and 28% (54 million) do so at least once per month [1].

Therefore, the development of a human drowsy state monitoring system for drivers has become a major focus in the field of safety driving and accident prevention in recent years. The development of countermeasures against a serious threat to driver safety is an urgent necessity. Such an in-vehicle system requires the capabilities of continuously monitoring the arousal state of the driver, accurately predicting the potential impact on the driving performance, and delivering a timely warning before dropping asleep.

The difficulties in developing such a system are lack of significant index for detecting drowsiness and complicated noise interferences in a realistic and dynamic driving environment. Development of the drowsiness monitoring technology for preventing accidents behind the steering wheel has become a major interest in the field of safety driving. Thus, developing accurate and non-invasive real-time driver drowsiness monitoring system would be highly desirable, particularly if this system can be further integrated into an automatic

warning system.

## 1.2. Literature Survey and Problem Statement

Many studies related to drowsy state monitoring and detection technologies have been developed during the last decade. Kozak et al. [2] and Rimini-Doering et al. [3] proposed a similar lane-departure warning system via tracking lane marks by camera systems for the assisted drivers. A different approach is to monitor the activities of the drivers themselves such as yawning, head positions, or eye blink duration by using optical sensors or video cameras [4]-[5]. However, image- or video-based techniques are sensitive to external weather conditions, e.g., rain or snow, and are easily influenced by the driver's posture inside the car. McGregor et al. [6] introduced a technique to monitor the drivers' physiological states by directly acquiring and analyzing subject's heart-rate variability (HRV) and electrooculography (EOG) [7] signal, which can overcome the system disadvantages mentioned above. Nevertheless, the minute-length scale of HRV and EOG analyses limit the monitoring system to a low-temporal-resolution output.

Recently, numbers of studies in neural engineering are devoted to explore the informative index of scalp EEG activities engaging with the particular cognitive task. With the high-temporal-resolution of the sampling rate and the portability of the hardware, the EEG has been shown as a promising approach to effectively assess the physiological states. Review of the existing studies related to the low performance, fatigue, or drowsiness [8]-[26], the changes in EEG power spectrum are regarded as the robust index for the change of the cognitive state. Beatty et al. [8] demonstrated the phenomenon of increasing occipital theta (4-7 Hz) power when the radar operators were less vigilant. Huang et al. [9] demonstrated tonic EEG power increase in low-frequency bands in the occipital cortex during high-error periods in a continuous visual tracking task, and they also showed similar tonic EEG power increase in low-frequency bands in the

occipital cortex in simulated driving experiments [10]. In addition, Lin et al. [11] have shown the high correlation between $\alpha$-(8-11 Hz) and $\theta$-(4-7 Hz) band power and driving error, which is defined as the mean deviation from lane center in each moving window in the virtual-reality (VR) environment. Besides, the research [12] showed that changes in EEG spectra in the $\theta$- and $\alpha$-band reflect changes in the drowsy state and memory performance. Other studies also showed that the EEG power spectra in the $\theta$- [13] and/or $\alpha$-band [14] are associated with drowsiness, and EEG power spectrum has largely linearly related to subject's driving performance. According to these fundamental findings, several algorithms and systems are proposed [11], [15]-[22]. Our research [11], [15]-[19] have demonstrated an automatic drowsy state prediction system with EEG power spectra by constructing a linear regression model. In [17], an independent component analysis-based (ICA-based) Fuzzy Neural Networks was proposed based on the independent sources instead of the scalp EEG activities. Moreover, the comparison of three neural networks based monitoring system was shown in [23]. The performance could reach a low prediction error across subjects while using the occipital component. Subasi et al. [20], Kiymik et al., [21] and Vuckovic et al. [22] also successfully demonstrated an automatic recognition algorithm to classify alertness level with the combination of EEG power bands among 1-30 Hz. However, most of the proposed models above are a subject-dependent system, i.e., the parameters of the system are not a generalization solution for each individual. Consequently, the performance might be unreliable when different users applied the proposed model shown above.

## 1.3. Research Objectives

Based on the discoveries in the researches mentioned above, the objective of this dissertation is to proposes a generalized EEG-based Self-organizing Neural Fuzzy Inference Network (SONFIN) system to monitor the occipital $\theta$- and $\alpha$-band power and further predict the driver's reaction time (RT) to an unexpected event. The main goal of this proposed system is to provide an practically implementable cross-subject predictor practically to build a common model that can be also applied to another user whose EEG signals are neither acquired first nor used for system model construction to still maintain his/her driving performance.

Two kinds of drowsiness prediction models, the subject-dependent and generalized cross–subject ones, were investigated. The system performances of SONFIN are compared with three benchmark systems including the Multi-Layer Perceptron Neural Network (MLPNN), the Radial Basis Function Neural Network (RBFNN) and Support Vector Regression (SVR) with Radial Basis kernel. The system performance evaluation was accomplished by calculating the values of Pearson Product-Moment Correlation Coefficient (PPMCC) and Root-Mean-of-Square-Error (RMSE) between recorded and estimated RTs. Firstly, ten-fold statistical validation approach was applied to subject-dependant drowsiness prediction to test if proposed framework is feasible to work or not. The acquired EEG signals were fed into the applied four predictors, and experimental results showed that the prediction performance of each applied predictor is high and stable in each subject-dependent session. Then, the generalized cross-subject drowsiness prediction system was applied to evaluate if such generalized system can predict the moment of driver based on other subjects' EEG signals. Hence, we applied leave one subject out cross validation way to evaluate the prediction performance in the cross-subject session. Experimental results indicate that the proposed neural fuzzy system performs

better prediction performance than other systems in correlation analysis and prediction error especially for the cross-subject model, which means the proposed system in this dissertation can not only overcome the individual difference problem occurred by collecting EEG signals from different subjects but also be applied to the real-world applications. It advantages the development of in-vehicle protocol to the real-life applications for the publics.

## 1.4. Organization of the Thesis

This dissertation is organized as follows. Chapter 2 describes the experimental environment that includes the virtual reality-based dynamic driving environment, electroencephalogram (EEG) signal acquisition system, and event-related lane departure experiment. Chapter 3 explores the flowchart of data analysis procedures for subject-dependent and cross-subject drowsiness prediction that include Independent Component Analysis (ICA), power spectra analysis, drowsiness prediction model introduction and system performance estimation approaches. Chapter 4 investigates and discusses the experimental benchmark result among four different drowsiness prediction models. Finally, the major contribution of this work is given in Chapter 5.

# II  Materials and Methods

## 2.1. Virtual Reality (VR)-based Dynamic Driving Simulator

The experiments in this study used a VR-based highway-driving environment, as shown in Figure 1, which was developed from the VR-based dynamic platform with its supported emulation software, WorldToolKit (WTK) library and application programmer's interface (API) [27]. The detailed highway-driving environment scene development procedure with the VR-based dynamic platform was illustrated in Figure 2. Firstly, models of various objects (such as cars, roads and trees etc.) for the scene were created including the native parameters, e.g., the relative positions between objects, attitudes, and so on. Then, the dynamic models among these virtual objects were developed to complete the simulated highway scene of full functionality with the aid of the high-level C-based API program.

This simulator was also developed in our previous studies [17], [18], [28]-[31] to investigate the changes of the driver's drowsy state during long-term monotonous driving at a fix speed of 100 km/hr. The experimental environment includes a 3-D surrounding view projected by seven projectors, and a real car mounted on a six-degree of freedom Stewart platform [22]-[25], as Figure 1(a) and 1(b) shown, respectively. The vestibular cues, or motion cues, were stimulated by the motion platform driven by these six hydraulic linear actuators.

Even driving in the real world on a smooth road, any vehicle deceleration and acceleration will never been avoided. Therefore, the strong stimulus capability of Stewart platform can generate accelerations and deceleration in many ways, such as longitudinal, lateral, and vertical directions of a vehicle as well as sling, roll, and deflective angular accelerations etc. For example, to simulate a deceleration situation when driving in a vehicle, the driver would

experience some strength to push him/her against the seat belt, and then the platform would simultaneously slant forward to simulate the deceleration force caused by the change of the gravity in opposite direction. Similarly, the platform would slant backward to simulate an acceleration force situation. All scenes move depending on the displacement of the car and the subjects maneuvering of the wheel during the driving experiments, making drivers feel like they are driving a real car on a real road, and such (or comparable) technique has been used widely in driving simulation studies [32], [33].
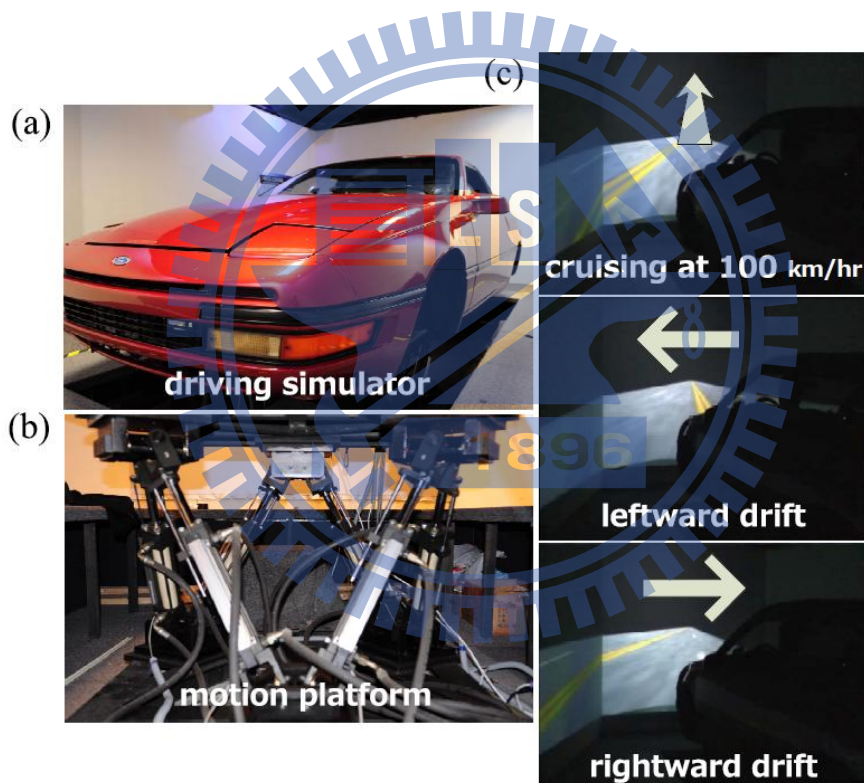


Figure 1. VR-based Highway Driving Environment. (a) Driving simulator, (b) six degree-of-freedom motion platform, and (c) illustration of driving task, adapted from [9].
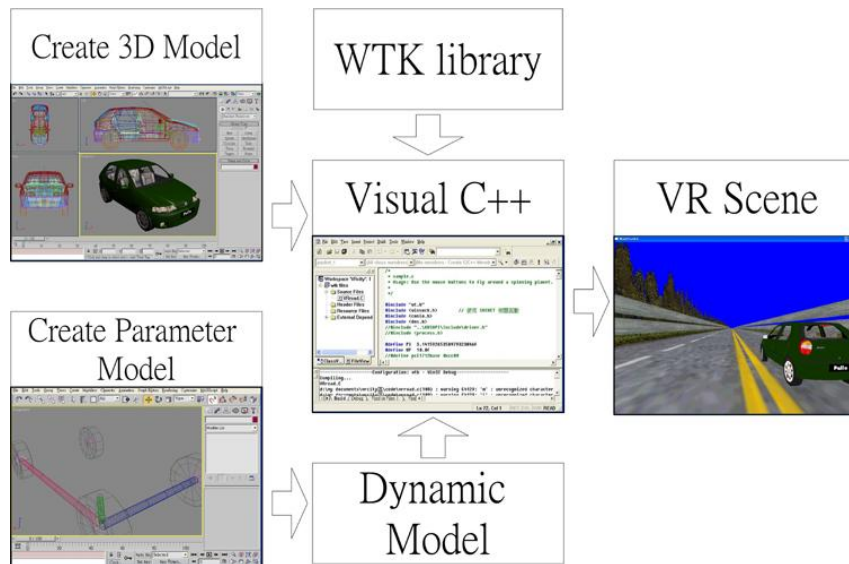
Figure 2.   VR-based   highway-driving   environment   scene   developed procedures. The interactive VR simulated scene was integrated with the dynamic models and the 3D shapes objects that are created and linked to the WTK library.

## 2.2.  Event-related Lane-Departure Experiment

This study implemented the event-related lane-departure paradigm [10] on the driving simulator. The simulator automatically and randomly drifts the car away from the center of the cruising lane as shown on Figure 1(c). The subjects were instructed to keep the car in the third lane using the steering wheel whenever the occurrence of a lane-departure event. During an hour-long experiment, this unexciting and monotonous task easily makes drivers fall asleep. Each lane-departure event (or "trial") captured the acquired EEG data, deviation distance, and time latency for analysis. Three important time points (see Figure 3(a) and Figure 4) in this experiment were recorded to determine the driving trajectory [10]: (1) deviation onset (Dev-on) – the time at which the car starts to drift away from the cruising lane, (2) response onset (Rps-on) – the time at which the subject starts responding to the car-drifting event, and (3) response offset (Rps-off) – the time at which the car returns to the center of the third lane. The lane-departure event repeated 5-10 s after the "response offset of the

8

preceding lane-departure event." In Figure 3 (b) and 3(c), the EEG data recorded 1-s before the "deviation onset" was served as the driver's physiological state inside the brain, and the time duration from "deviation onset" to "response onset" was defined as the RT to represent the state of driver's arousal. When subjects were alert, their RT to the random drift was short, resulting in a small deviation from the center of the lane. When the subjects were drowsy, the RT and resulting lane deviation was long. Based on this relationship between EEG and RT, we attempt to design a monitor system to process a 1-s EEG data continuously and to predict the RT for real-world applications.
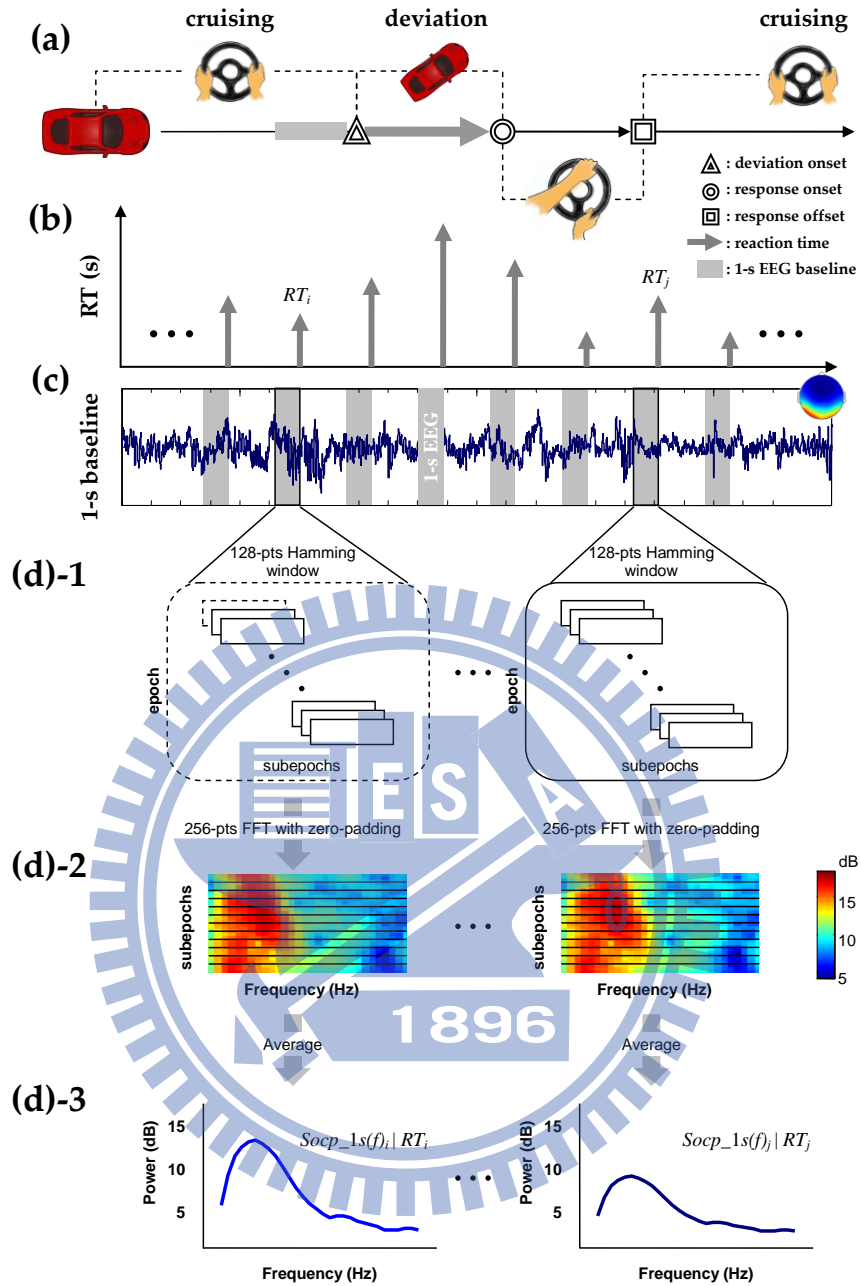
Figure 3.     (a) Event-related lane departure paradigm, (b) recorded RT for all trials, (c) 1-s epoch EEG data of the occipital activation before the deviation onset (the 1-s EEG before Dev-on part during the cruising period), and (d) signal processing procedures of the spectral feature extraction including 128-pts Hamming window, 256-pts FFT, and zero-padding for each 1-s epoch. The output is a paired data set including the spectral power and the corresponding RT.
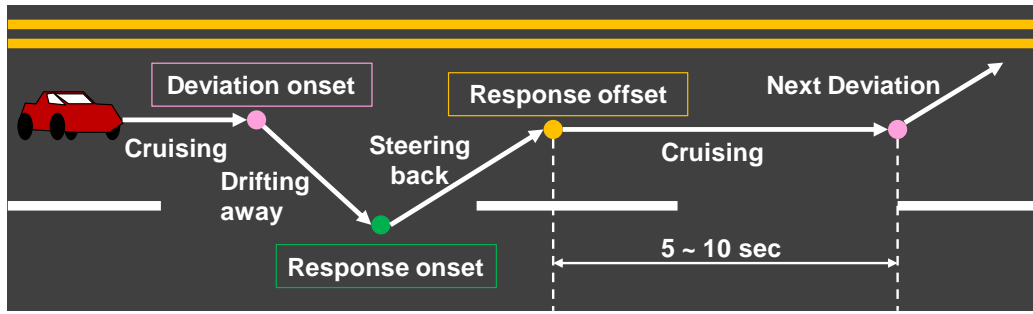
Figure 4.    Detailed illustration of event-related lane departure experiment, which is permitted for recreation by [34], [35]. The time duration taken from Deviation onset to Response onset is defined as Reaction Time (RT) to represent the state of driver's arousal.

## 2.3. Subjects and EEG Data Recording

The six volunteer subjects (aged 20 to 40 years) participated in the VR-based highway-driving experiments. All subjects involved in this study had good driving skills and were trained with the VR-based highway-driving for one day extra for familiarization before completing the testing section. Previous study [26] showed that people often become drowsy after one hour of continuous driving after lunch. These results indicate that drowsiness is not necessarily caused by long-hours driving. Hence, to maximize the chance of obtaining valuable data for this study, all the experiments were conducted in the early afternoon after lunch.

On the first day, participants were instructed regarding the general procedures of the driving task. In addition, the participants completed an informed consent form. They began a 15- to 45-min practice session to learn how to keep the car in the center of the third cruising lane using the steering wheel. Participants were allowed to unlimited practice.

On the test day, the participants were wired with an EEG electrode cap connected to a physiology signals amplifier, as shown in Figure 5(a) and 5(b) respectively, to acquire the EEG signals for analysis. The EEG data acquisition process used 33 sintered Ag/AgCl EEG/EOG electrodes with a unipolar

reference at right earlobe and 2 ECG channels with a bipolar connection placed on the chest. All the 30 unipolar EEG/EOG electrodes were placed according to a modified International 10-20 system illustrated in Figure 5(c), and referred to the right ear lobe. Before data acquisition, the contact impedance between EEG electrodes and cortex was calibrated at less than 5KΩ. A NeuroScan NuAmps Express system (Compumedics Ltd., VIC, Australia) simultaneously recorded the EEG/EOG/ECG data, lane deviations, and the RT. The EEG data was recorded with 16-bit quantization at a sampling rate of 500 Hz. Subsequent EEG data processing procedures employed 250Hz down sampling to decrease the calculation load.
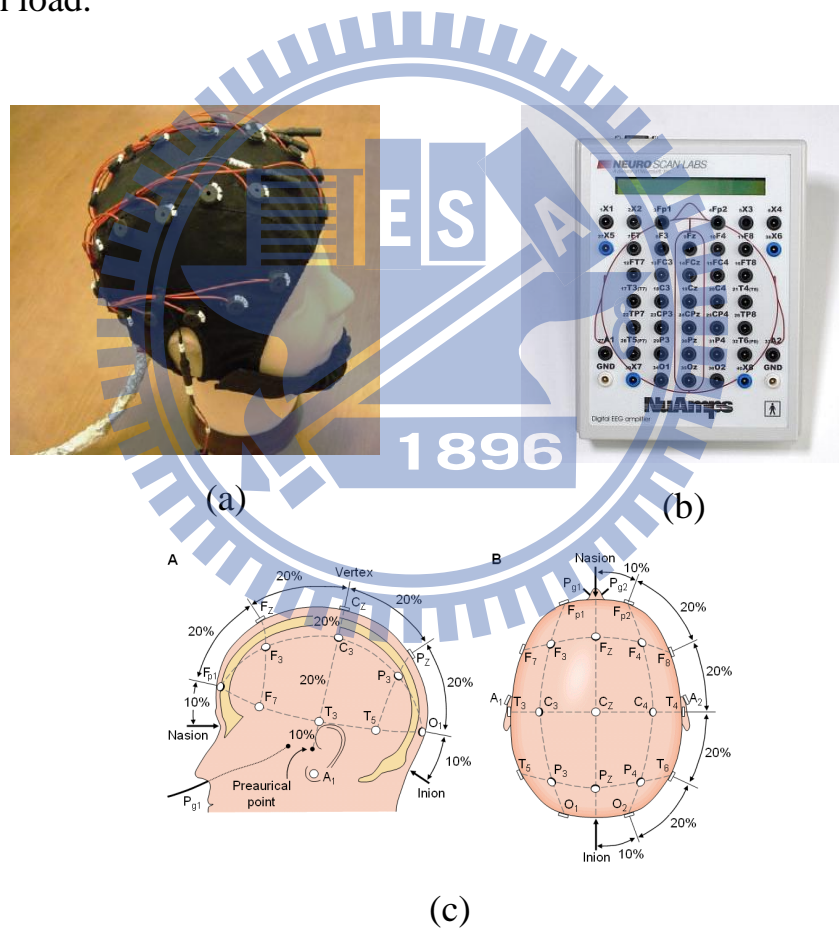


Figure 5.    (a) The 30 channel EEG electrode cap, (b) EEG signal amplifier, and (c) The international 10-20 system view from (A) left side and (B) top side of the head. A = Ear lobe, C = central, Pg = nasopharyngeal, P = parietal, F = frontal, Fp = frontal polar, O = occipital.

# III Data Analysis

In this study, the EEG data analysis and signal processing were implemented by scripts running in MATLAB (R2007a) and the EEGLAB Toolbox (ver. 5.03) was developed by the Swartz Center for Computational Neruoscience, the University of California San Diego (UCSD) [36]. The flowchart of data processing procedures was illustrated in Figure 6 that consists of Independent Component Analysis (ICA), power spectra analysis (see Figure 3(d)), feature extraction, drowsiness predictor model and correlation coefficient analysis and root mean square error (RMSE) for system performance estimation.
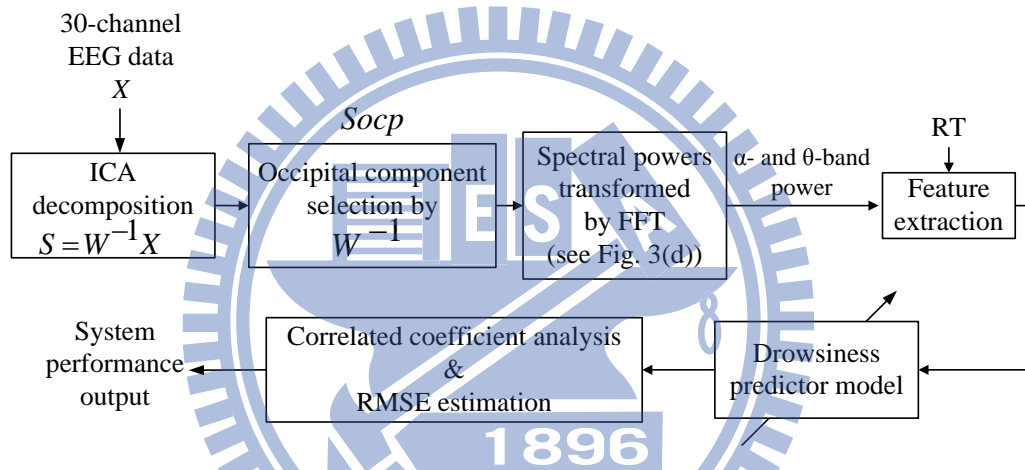


Figure 6.     Flowchart of the proposed drowsiness predictor, and the system performance is verified by correlation coefficient analysis and RMSE of the recorded RT and predicted RT.

## 3.1. Independent Component Analysis

The blind source separation (BSS) problem [37], [38] deserves to be solved in the EEG signal, which is usually contaminated by various artifacts including eye movement and indoor power-line noise [39], [40]. One of the popular methods was applied ICA with the algorithms, such as Infomax [41], FastICA [42] and JADE [43], to find the linear projections that maximizes the mutual independences of estimated components.

The general representation of ICA model can be simply denoted as

$S = W^{-1}X$, where $S = [S_1; S_2; \because S_n]$ presents the $n$ independent sources, $W^{-1}$ is the back-projection weighting matrix, and $X = [X_1; X_2; \because X_n]^T$ is the $n$ observed signals. The purpose of ICA algorithm is to find out the back-projection weighting matrix, $W^{-1}$, which can be rendered as a 2-D scalp topographies with $n$ independent components [44]-[49] as the Figure 7(a) shown, where the weightings distribute around the occipital area is selected as the component of interest, to have a maximum statistically independency of the separated components, $S$. Then, the occipital component [8]-[13], $S_{ocp}$, i.e., 5th scalp map in Figure 7(a), was selected by the weighting distribution of the scalp topography that is rendered from $W^{-1}$[44] as the region of interest for power spectra analysis and feature extraction. The scalp topographies shown in Figure 7(b) are the occipital component selected from six subjects used in this study. The input data to the prediction systems was the $\theta$-band and $\alpha$-band powers of the "occipital component" instead of "occipital channel" after processing ICA, so that the number of the occipital-like component should be one, and the number of features is 9 (4~12 Hz) that will be illustrated more detailed in next section.

## 3.2. Power Spectra Analysis and Feature Extraction

As shown in Figure 7(b), the selected IC, $S_{ocp}$, related to occipital component were taken for power spectra analysis. The power spectra analysis flowchart was illustrated in Figure 3(d). In the first step of the spectral transformation, each 1-s length epoch (250 data points) was divided into several 128-point sub-epochs by Hamming windows. Then, we perform 256-point FFT with zero-padding for each subepoch to obtain the power spectral density. Finally, the average of spectral powers of subepochs was used for the spectral representation of this 1-s length occipital activation. Here, only the spectral

powers of the $\theta$-band (4-7 Hz) and $\alpha$-band (8-12 Hz), which is reported as the significant index for the driving error [11], with the corresponding RT were used as the dataset pair to establish the prediction model.



(a)      (b)
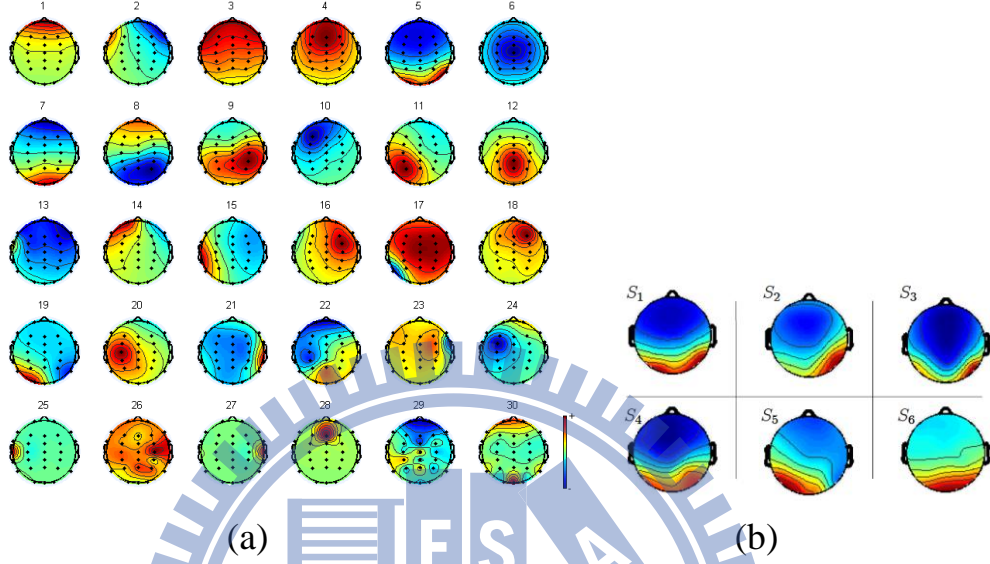
Figure 7.     (a) The scalp map projection of each independent component, where the 5-th scalp map is indentified as the occipital source, and the 5-th sequence of data points is the corresponding component activation. (b) The scalp topographies of the occipital component of six subjects used in this study.

### 3.3. Performance Estimation

To estimate the performance among different predictors, the Pearson Product-Moment Correlation Coefficient (PPMCC) and Root Mean of Square Error (RMSE) were applied in this study.

In this study, the PPMCC, denoted by $r$, between the estimated RTs and recorded RTs was obtained by Eq.(1).

$$r = \frac{\sum\limits_{i=1}^{n}\left(RT_i - \overline{RT}\right)\left(eRT_i - \overline{eRT}\right)}{\sqrt{\sum\limits_{i=1}^{n}\left(RT_i - \overline{RT}\right)^2}\sqrt{\sum\limits_{i=1}^{n}\left(eRT_i - \overline{eRT}\right)^2}}, \tag{1}$$

where $n$ is the number of trials. The $\overline{RT}$ and $\overline{eRT}$ are the average of

recorded RTs and the estimated RTs, respectively. If *r* is high, it can be claimed that two variables have a strong linear relationship and the performance of the predictor is better [12], [18], [19].

The RMSE was another popular and useful index for assessing the performance of the predictor [50]. The RMSE could be estimated as the following:

$$RMSE = \frac{\sqrt{\sum_{i=1}^{n}(RT_i - eRT_i)^2}}{n}, \tag{2}$$

where a smaller RMSE presents a better prediction for the proposed model.

## 3.4. Drowsiness Prediction Models

This study adopts four models for drowsiness prediction: (1) SVR, (2) MLPNN, (3) RBFNN, and (4) SONFIN. Because MLPNN and RBFNN are easy to be over-fitted when the training data contain lots of noises, especially for multi-hidden layers MLPNN, SVR, as known a popular regression model, was also selected for comparisons in this study. Here, all of the proposed approaches predict an unseen RT while confronting an unexpected event in terms of the spectral features of the occipital activation. The following section briefly describes the structure of each predictor.

### 3.4.1. Support Vector Regression

The support vector machine (SVM) is a popular approach for solving the problem of multidimensional function estimation and has been applied to various fields such as classification and regression. When SVM is employed dedicatedly for solving the problems of function approximation and regression estimation, it was denoted as the support vector regression (SVR). Figure 8(a) shows the graphical overview for all steps. The SVR is a complicated and heavy-computation implementation of prediction algorithm based on structuring risk minimization principles to obtain a good generalization capability [51], [52].

For $\varepsilon$-SVR, it is formulated as minimization of the Eq.(3) as the following:

$$\min \quad \frac{1}{2}\|\omega\|^2 + C\sum_i^n(\zeta_i + \zeta_i^*), \tag{3}$$

$$\text{subject to} \begin{cases} y_i - f(x_i,\omega) \le \varepsilon + \zeta_i^* \\ f(x_i,\omega) - y_i \le \varepsilon + \zeta_i \\ \zeta_i^*, \zeta_i \ge 0, i = 1,\dots,n \end{cases}$$

In this study, a library of LIBSVM [53] was used for SVR model construction with the radial basis function applied as its kernel function.

### 3.4.2. Multi-Layer Perceptron Neural Network

The MLPNN is the most commonly used neural-network architecture because of its capability to learn and generalize relatively small training-set requirements, fast operation, and ease of implementation [54], [55]. The MLPNN structure includes one input layer, one output layer, and a couple of hidden layers, as Figure 8(b) shows.

For the $n$-layer, $j$-PE (processing element) output, $y_j^n$ can be written as

$$y_j^n = f(net_j^n), \quad net_j^n = \sum_i w_{ji}^n y_i^{n-1} - b_j^n; \tag{4}$$

where $f(.)$ is the activation function, $w_{ji}$ is the weight from $i$-PE to $j$-PE and $b_j$ denotes the bias value for $net_j$. The MLPNN estimates the weights to minimize the cost function using a back propagation-learning algorithm:

$$E = \frac{1}{2}(d_k - y_k)^2 \tag{5}$$

The Gaussian activation function in Eq.(6) applies to all hidden layers, while the output layer uses a linear activation function:

$$f(x) = \frac{1}{1 + e^{-ax}} \tag{6}$$

This study employs a 5-layer MLPNN with [10 6 5] processing elements (PEs) of hidden layers and 8-layer MLPNN with [10 6 5 4 3 2] PEs of hidden

layers for subject-dependent and generalized cross-subject drowsiness prediction, respectively.

### 3.4.3. Radial Basis Function Neural Network

The radial basis function nerual network (RBFNN) is designed for (nonlinear) function approximation problem with a high-dimension space. The RBFNN provides a best fitting curve of the training data, and its implementation is much simpler than the perceptron approach while retaining the major property of universal approximation of functions [56]. The RBFNN is a 3-layer feed forward neural network structure that consists of an input layer, a single hidden layer with a nonlinear (Gaussian) RBF activation function and a linear output layer, as Figure 8(c) shows.

The output $y_{out}$ can be written as

$$y_{out} = \varphi(x) = \sum_{k=1}^{M} w_k \cdot e^{-\frac{\|x-c_k\|^2}{2(\sigma_k)^2}},$$  (7)

where $w_k$ is the linear combinational weight, $c_k$ is the center of the Gaussian RBF and $\sigma_k$ is its variance. The Orthogonal Least-Squares (OLS) and gradient descent learning algorithms [57]-[59] were employed to minimize the error cost function

$$E(t) = \frac{1}{2}(y(t)_{out} - y_t)^2 = (\sum_{k=1}^{M} w_k(t) \cdot e^{-\frac{\|x-c_k\|^2}{2(\sigma_k)^2}} - y_t)^2$$  (8)

The RBFNN employed 30-40 and 300-500 neurons for subject-dependent drowsiness prediction and generalized subject-independent drowsiness prediction, respectively.

### 3.4.4. Self-Organizing Neural Fuzzy System

The SONFIN [60] combines the nodes with a finite "fan-in" of connections represented by weight values from other nodes, and a "fan-out" of connections

to other nodes, and its architecture is illustrated in Figure 8(d). The integration function $f$ combines information, activation, or evidence from other nodes, and is denoted as

$$net\text{-}input = f\left[u_1^k, u_2^k ... u_p^k, w_1^k, w_2^k ... w_p^k\right], \tag{9}$$

where $u_1^k, u_2^k, \cdots, u_p^k$ are inputs to this node, and $w_1^k, w_2^k, \cdots, w_p^k$ are the associated linking weights. The superscript $\{k\}$ in this equation indicates the layer number. The output for each node is an activation function value of its net input, $output = a(f)$, where $a(.)$ represents the activation function.

The functions of the nodes in each of the five layers of the SONFIN structure are briefly described as follow.

*Layer1*: Transmit inputs to the next node directly, without computation.

$$f = u_i^{(1)}, \ a^{(1)} = f. \tag{10}$$

*Layer2*: Calculate the output of Layer 1 into a fuzzy set.

$$f\left[u_i^{(2)}\right] = \frac{\left[u_i^{(2)} - m_{ij}\right]^2}{\sigma_{ij}^2}, \ a^{(2)} = f. \tag{11}$$

*Layer3*: Perform a fuzzy rule with an AND operation.

$$f\left[u_i^{(3)}\right] = \Pi u_i^{(3)} = e^{-[D_i(x-m_i)]^T[D_i(x-m_i)]}, \ a^{(3)} = f. \tag{12}$$

*Layer4*: Normalize the firing strength calculated in Layer 3.

$$f\left[u_i^{(4)}\right] = \sum_i u_i^{(4)}, \ a^{(4)}(f) = \frac{u_i^{(4)}}{f}. \tag{13}$$

*Layer5*: Integrate all the actions from Layer 5 to defuzzify the results. Each node in this layer corresponds to one output variable.

$$f\left[u_i^{(5)}\right] = \sum_i w_i u_i^{(5)}, \ a^{(5)}(f) = f. \tag{14}$$

The average rule numbers derived for subject-dependent drowsiness prediction and generalized cross-subject drowsiness prediction was less than 10.
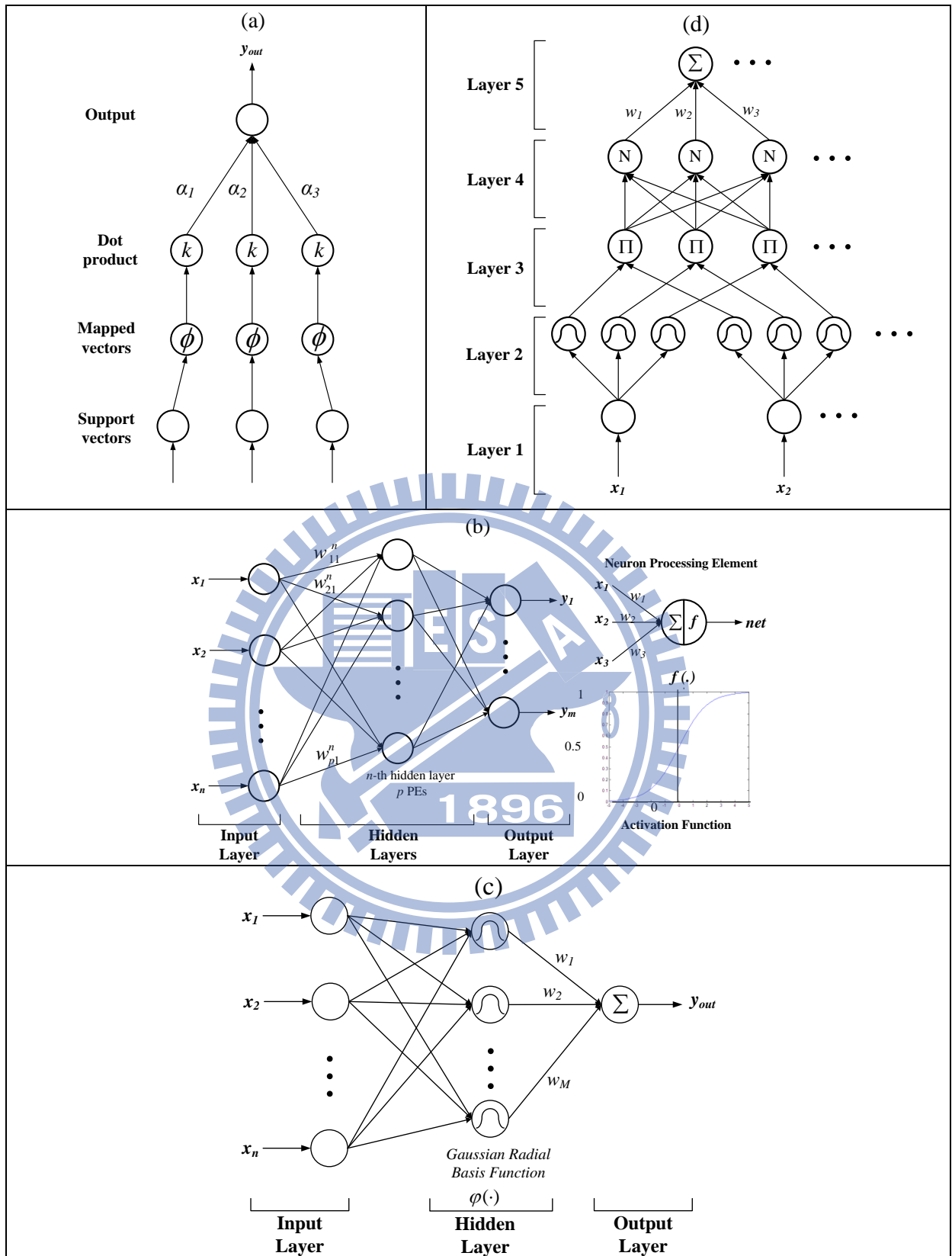
Figure 8.     Prediction models that include the structures of (a) SVR, (b)
MLPNN, (c) RBFNN and (d) five-layer SONFIN.

# IV Experimental Results and Discussion

In this study, a total of six normal healthy subjects participated in the VR-based highway-driving experiments described in Section 2.1. The observing driving events of each subject are consisted of 224 to 335 lane-departure events and the EEG data length for subject 1 to 6 used for ICA decomposition are 44.7 min, 44.7 min, 30.4 min, 29.9 min, 31.5 min and 31.5 min. The occipital components from six subjects were selected the region of interest for establishing the prediction model. In total, we collected about 1594 trial samples as shown in Table 1. The observing data are fed into FFT to transform into EEG power spectra, which are served as the inputs to the SVR, MLPNN, RBFNN and SONFIN predictors. This study applied two validation approaches to verify the performance and robustness of these predictors. The subject-dependent drowsiness prediction using ten-fold cross-validation was first utilized to evaluate the average single-subject performance. In this evaluation, 90% of the trials for each subject were used for training, while the remaining ten-percent of the trials were used for testing. The other validation approach is to evaluate the generalized cross-subject drowsiness prediction performance which was developed to be compared with the performance of the subject-dependent models. In the cross-subject drowsiness prediction regime, the EEG power spectra from randomly selected five subjects are used for training, and the remaining subject was used for testing samples.

Table 1. Observing Lane-Departure Event Number for Each Subject

| Subject | 1 | 2 | 3 | 4 | 5 | 6 | Total |
|---------|-----|-----|-----|-----|-----|-----|-------|
| Trials | 335 | 335 | 228 | 224 | 236 | 236 | 1,594 |

## 4.1. Subject-dependent Drowsiness Prediction

This drowsiness-prediction procedure is depicted in Figure 9. From statistical point of view, each subject completed a 10-round ten-fold cross-validation, in which 90% of the trials were randomly selected as the training set and the reminding 10% of the trials as testing set.
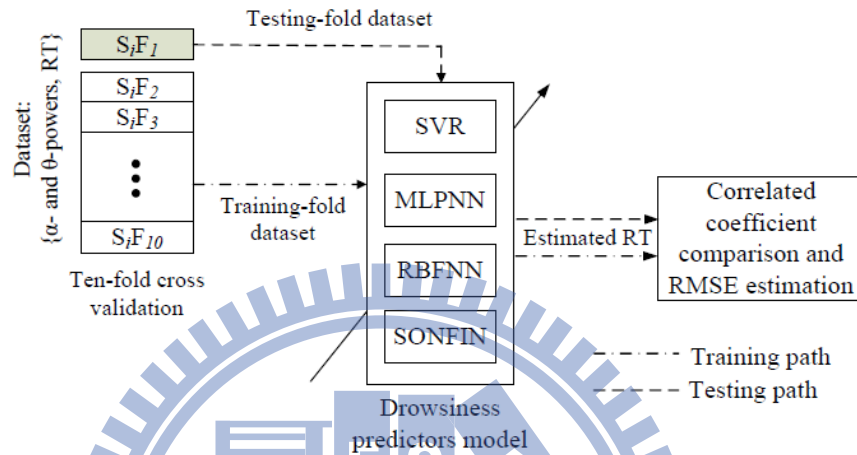


Figure 9.     Subject-dependent drowsiness predictor ten-fold cross-validation analysis structure, where $S_iF_j$ means the $j$-th fold of the $i$-th subject.

### 4.1.1. Boxplots of PPMCC and RMSE

Boxplot is a useful plot for column data analysis from statistical point of view, and it can be simply implemented using a native command in Matlab. In a boxplot, there are three lines for the boxes at the lower quartile, median, and upper quartile values, and two additional lines presents the maximum and minimum values for this vector. Take vector A with values from 0.1 to 1 with a step of 0.1 for example, its boxplot was depicted below in Figure 10. Line "a" and line "e" present the maximum and minimum values for vector A, i.e., 1 and 0.1, respectively. Line "c" is the median value for vector A, i.e., 0.55, while line "b" and line "d" presents the upper and lower quartile values, i.e., 0.8 and 0.3, respectively.

The averages of PPMCC and RMSE between the actual and estimated RTs are shown on Table 2 and Table 3, respectively. The PPMCC on the training and

testing sets obtained by SVR, MLPNN, RBFNN, and SONFIN are 96.8%, 96.6%, 95.4%, 96.7% and 95.2%, 96.2%, 94.8%, 97.2%, respectively The RMSE of training and testing data obtained by SVR, MLPNN, RBFNN, and SONFIN are 0.088 s, 0.089 s, 0.074 s, 0.071 s and 0.130 s, 0.084 s, 0.103 s, 0.076 s.
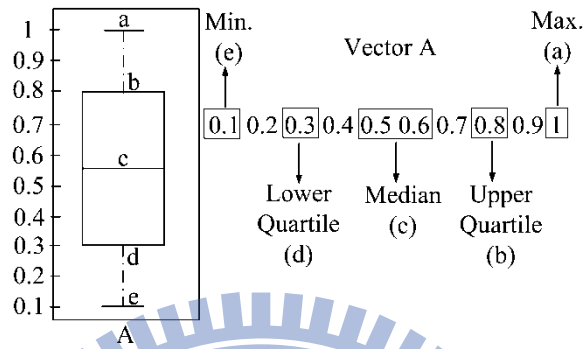


Figure 10.　Boxplot example for vector A = [0.1 0.2 … 1]

Figure 11 depicts the boxplot of the PPMCC of subject-dependent drowsiness prediction with 10-fold cross-validation using SVR, MLPNN, RBFNN and SONFIN. Take Subject 1 for example, the median, upper and lower quartile, maximum and minimum PPMCC for subject-dependent drowsy state predictor with SONFIN are 96.0%, 95.6% and 97.2%, 98.0% and 90.2%, respectively.
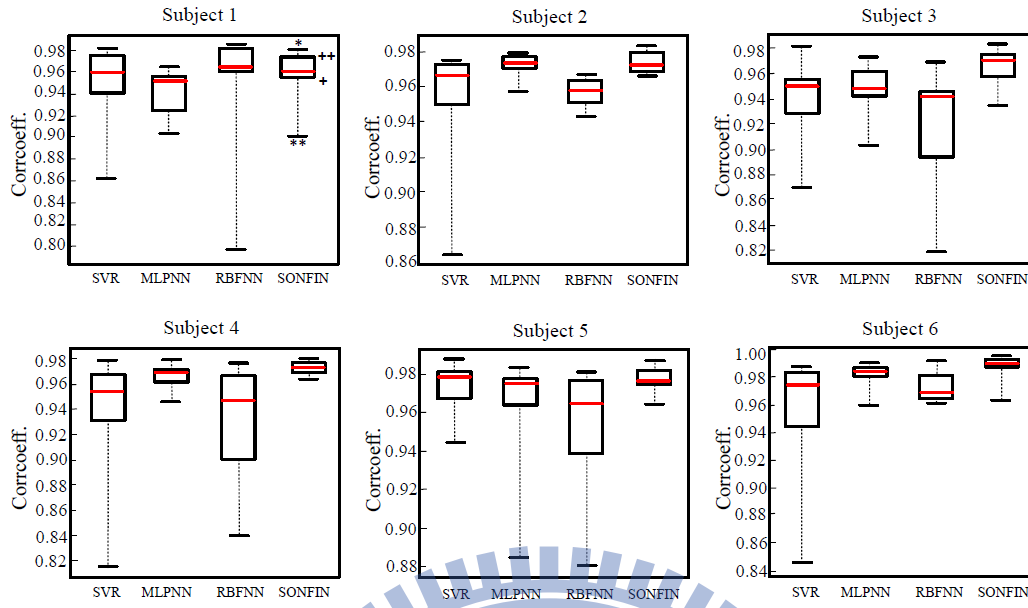
Figure 11. Correlation coefficient boxplot comparison of subject's drowsy state testing evaluation for subject-dependent drowsiness prediction experiment with SVR, MLPNN, RBFNN and SONFIN. The boxes have three lines to present the values for lower quartile (+), median (red line), and upper quartile (++) for column data. Two addition lines at both ends of the whisker indicate the maximum (*) and minimum (**) value of a column data.

Table 2. Correlation coefficients Comparisons for
Subject-Dependent Drowsiness Prediction

| Subject | | 1 | 2 | 3 | 4 | 5 | 6 | Average (%) |
|---------|----------|-------|-------|-------|-------|-------|-------|-------------|
| SVR | Training | 96.1% | 95.5% | 97.3% | 97.2% | 97.1% | 97.5% | 96.8±2.1 |
| | Testing | 95.2% | 95.5% | 94.0% | 93.7% | 97.3% | 95.7% | 95.2±1.5 |
| MLPNN | Training | 94.6% | 97.1% | 95.7% | 97.0% | 96.9% | 98.3% | 96.6±3.9 |
| | Testing | 94.2% | 97.1% | 94.7% | 96.7% | 96.5% | 98.2% | 96.2±0.4 |
| RBFNN | Training | 95.6% | 95.3% | 92.8% | 95.8% | 95.9% | 96.8% | 95.4±1.8 |
| | Testing | 95.1% | 95.7% | 91.8% | 93.6% | 95.4% | 97.3% | 94.8±0.5 |
| SONFIN | Training | 95.6% | 96.8% | 96.6% | 97.0% | 97.4% | 98.3% | 96.7±1.5 |
| | Testing | 95.7% | 97.4% | 96.6% | 97.3% | 97.7% | 98.8% | 97.2±1.6 |

Table 3. RMSE Comparisons for Subject-Dependent Drowsiness Prediction

| Subject | | 1 | 2 | 3 | 4 | 5 | 6 | Average (s) |
|---|---|---|---|---|---|---|---|---|
| SVR | Training | 0.084 | 0.083 | 0.093 | 0.087 | 0.088 | 0.093 | 0.088±0.038 |
| | Testing | 0.111 | 0.104 | 0.164 | 0.175 | 0.119 | 0.155 | 0.13±0.038 |
| MLPNN | Training | 0.075 | 0.054 | 0.095 | 0.095 | 0.071 | 0.056 | 0.089±0.025 |
| | Testing | 0.083 | 0.059 | 0.103 | 0.109 | 0.083 | 0.065 | 0.084±0.034 |
| RBFNN | Training | 0.067 | 0.070 | 0.125 | 0.112 | 0.088 | 0.077 | 0.074±0.030 |
| | Testing | 0.073 | 0.076 | 0.133 | 0.143 | 0.108 | 0.088 | 0.103±0.043 |
| SONFIN | Training | 0.068 | 0.057 | 0.085 | 0.094 | 0.069 | 0.055 | 0.071±0.020 |
| | Testing | 0.071 | 0.059 | 0.088 | 0.100 | 0.082 | 0.055 | 0.076±0.022 |

### 4.1.2. Experimental Result Examples

Some experimental results of testing data evaluation examples with subject-dependent drowsiness prediction infrastructure for Subject 1 to Subject 6 using SVR, MLPNN, RBFNN and SONFIN were depicted from Figure 12 to Figure 17, respectively.

Figure 12 shows some evaluation result examples of testing data for Subject 1 with subject-dependent drowsiness prediction infrastructure using (a) SVR ($r = 0.9525$), (b) MLPNN ($r = 0.9596$), (c) RBFNN ($r = 0.9353$) and (d) SONFIN ($r = 0.9832$). The red dashed line and blue dash-dot line present the golden testing data and estimated evaluation result respectively. The correlation coefficients of training data validation for SVR, MLPNN, RBFNN and SONFIN in the sample results of Subject 1 are 95.3%, 98.1%, 96.6% and 98.6% respectively.
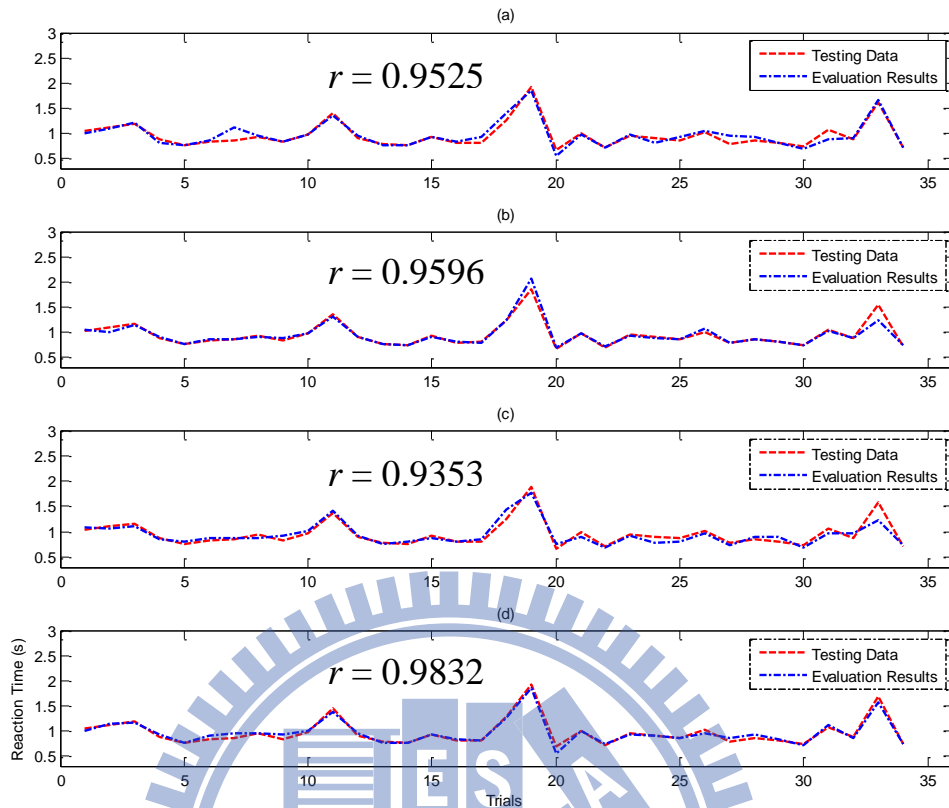
Figure 12. Evaluation result examples of testing data for Subject 1 with subject-dependent drowsiness prediction infrastructure using (a) SVR ($r = 0.9525$), (b) MLPNN ($r = 0.9596$), (c) RBFNN ($r = 0.9353$) and (d) SONFIN ($r = 0.9832$). The red dashed line and blue dash-dot line present the golden testing data and estimated evaluation result respectively.

Figure 13 are some evaluation result examples of testing data for Subject 2 with subject-dependent drowsiness prediction experiment using (a) SVR ($r = 0.9317$), (b) MLPNN ($r = 0.9553$), (c) RBFNN ($r = 0.9464$) and (d) SONFIN ($r = 0.9775$). The red dashed line and blue dash-dot line present the golden testing data and estimated evaluation result respectively. The correlation coefficients of training data validation for SVR, MLPNN, RBFNN and SONFIN in the sample results of Subject 2 are 93.2%, 94.2%, 94.4% and 96.2% respectively.
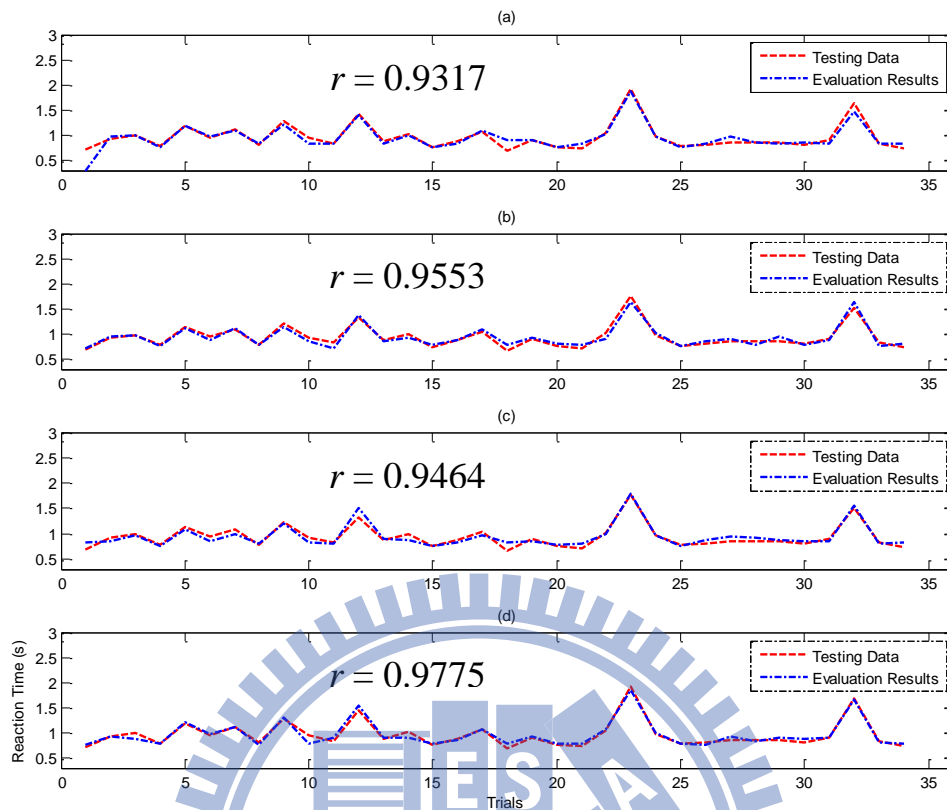
Figure 13. Evaluation result examples of testing data evaluation for Subject 2 with subject-dependent drowsiness prediction infrastructure using (a) SVR ($r =$ 0.9317), (b) MLPNN ($r =$ 0.9553), (c) RBFNN ($r =$ 0.9464) and (d) SONFIN ($r =$ 0.9775). The red dashed line and blue dash-dot line present the golden testing data and estimated evaluation result respectively.

Figure 14 depicts some evaluation result examples of testing data for Subject 3 with subject-dependent drowsiness prediction infrastructure using (a) SVR ($r =$ 0.9483), (b) MLPNN ($r =$ 0.9783), (c) RBFNN ($r =$ 0.9493) and (d) SONFIN ($r =$ 0.9784). The red dashed line and blue dash-dot line present the golden testing data and estimated evaluation result respectively. The correlation coefficients of training data validation for SVR, MLPNN, RBFNN and SONFIN in the sample results of Subject 3 are 94.3%, 98.2%, 95.5% and 96.4% respectively.
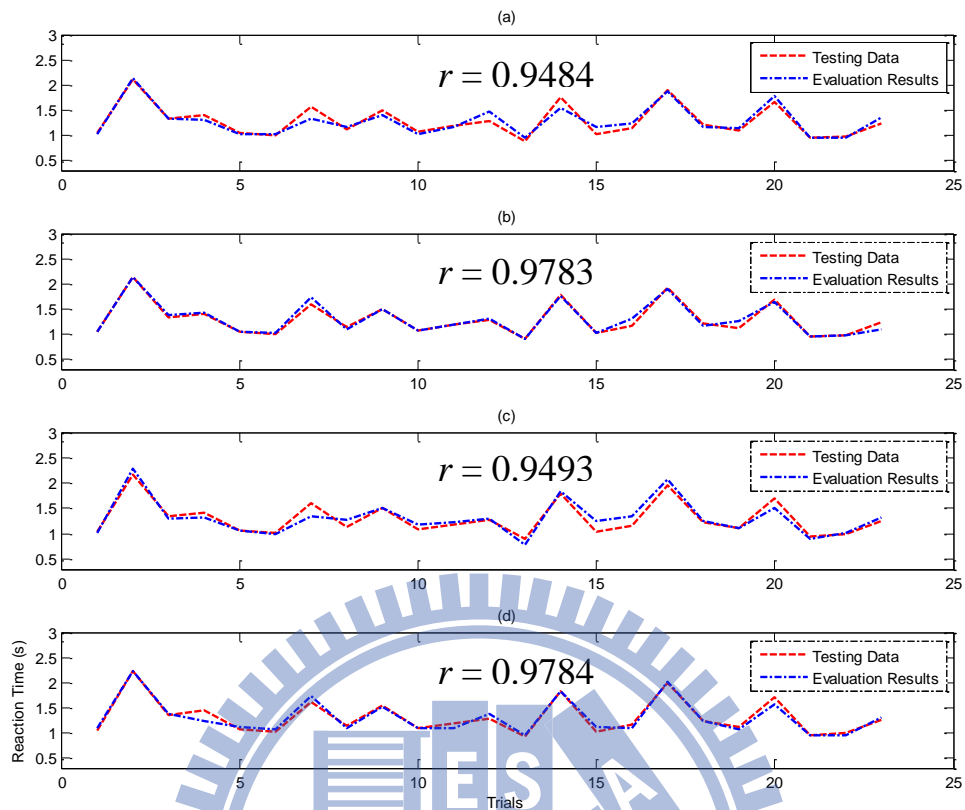
Figure 14.  Evaluation result examples of testing data for Subject 3 with subject-dependent drowsiness prediction infrastructure using (a) SVR ($r$ = 0.9483), (b) MLPNN ($r$ = 0.9783), (c) RBFNN ($r$ = 0.9493) and (d) SONFIN ($r$ = 0.9784). The red dashed line and blue dash-dot line present the golden testing data and estimated evaluation result respectively.

Figure 15 are some evaluation result examples of testing data for Subject 4 with subject-dependent drowsiness prediction infrastructure using (a) SVR ($r$ = 0.9439), (b) MLPNN ($r$ = 0.9542), (c) RBFNN ($r$ = 0.9380) and (d) SONFIN ($r$ = 0.9870). The red dashed line and blue dash-dot line present the golden testing data and estimated evaluation result respectively. The correlation coefficients of training data validation for SVR, MLPNN, RBFNN and SONFIN in the sample results of Subject 4 are 95.3%, 98.7%, 96.8% and 97.5% respectively.
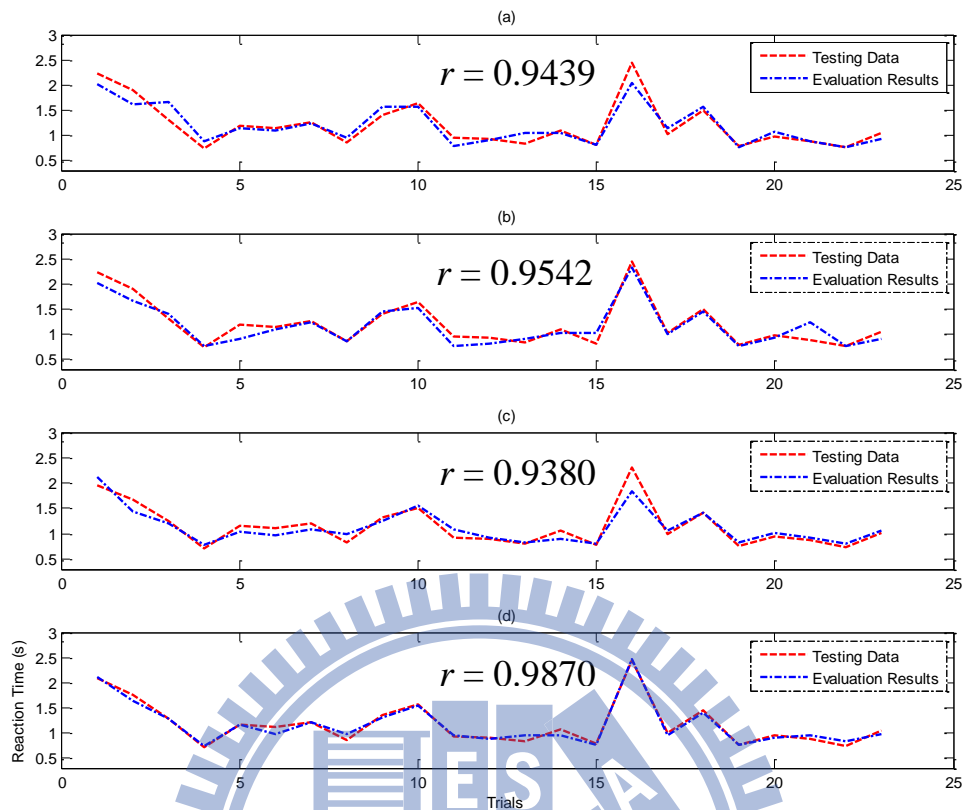
Figure 15. Evaluation result examples of testing data for Subject 4 with subject-dependent drowsiness prediction infrastructure using (a) SVR ($r = 0.9439$), (b) MLPNN ($r = 0.9542$), (c) RBFNN ($r = 0.9380$) and (d) SONFIN ($r = 0.9870$). The red dashed line and blue dash-dot line present the golden testing data and estimated evaluation result respectively.

Figure 16 shows some evaluation result examples of testing data for Subject 5 with subject-dependent drowsiness prediction infrastructure using (a) SVR ($r = 0.9679$), (b) MLPNN ($r = 0.9623$), (c) RBFNN ($r = 0.9462$) and (d) SONFIN ($r = 0.9757$). The red dashed line and blue dash-dot line present the golden testing data and estimated evaluation result respectively. The correlation coefficients of training data validation for SVR, MLPNN, RBFNN and SONFIN in the sample results of Subject 5 are 96.2%, 94.7%, 96.8% and 97.2% respectively.

29
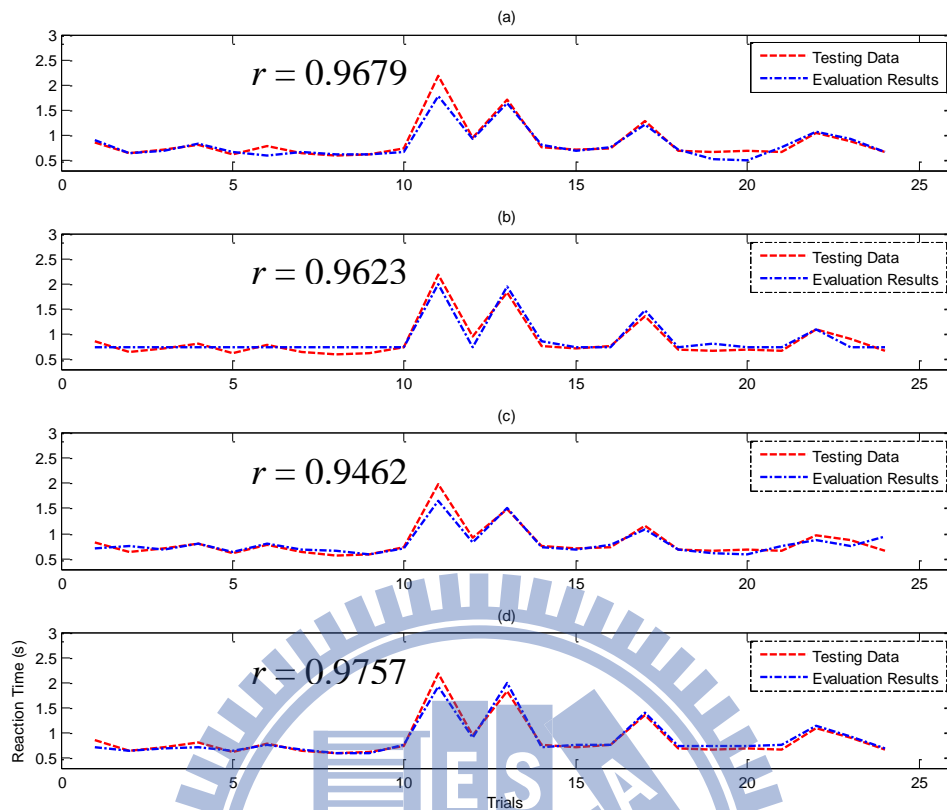
Figure 16. Evaluation result examples of testing data for Subject 5 with subject-dependent drowsiness prediction infrastructure using (a) SVR ($r$ = 0.9679), (b) MLPNN ($r$ = 0.9623), (c) RBFNN ($r$ = 0.9462) and (d) SONFIN ($r$ = 0.9757). The red dashed line and blue dash-dot line present the golden testing data and estimated evaluation result respectively.

Figure 17 illustrates some evaluation result examples of testing data for Subject 6 with subject-dependent drowsiness prediction infrastructure using (a) SVR ($r$ = 0.9752), (b) MLPNN ($r$ = 0.9579), (c) RBFNN ($r$ = 0.9610) and (d) SONFIN ($r$ = 0.9851). The red dashed line and blue dash-dot line present the golden testing data and estimated evaluation result respectively. The correlation coefficients of training data validation for SVR, MLPNN, RBFNN and SONFIN in the sample results of Subject 6 are 95.4%, 95.9%, 98.1% and 97.8% respectively.

30
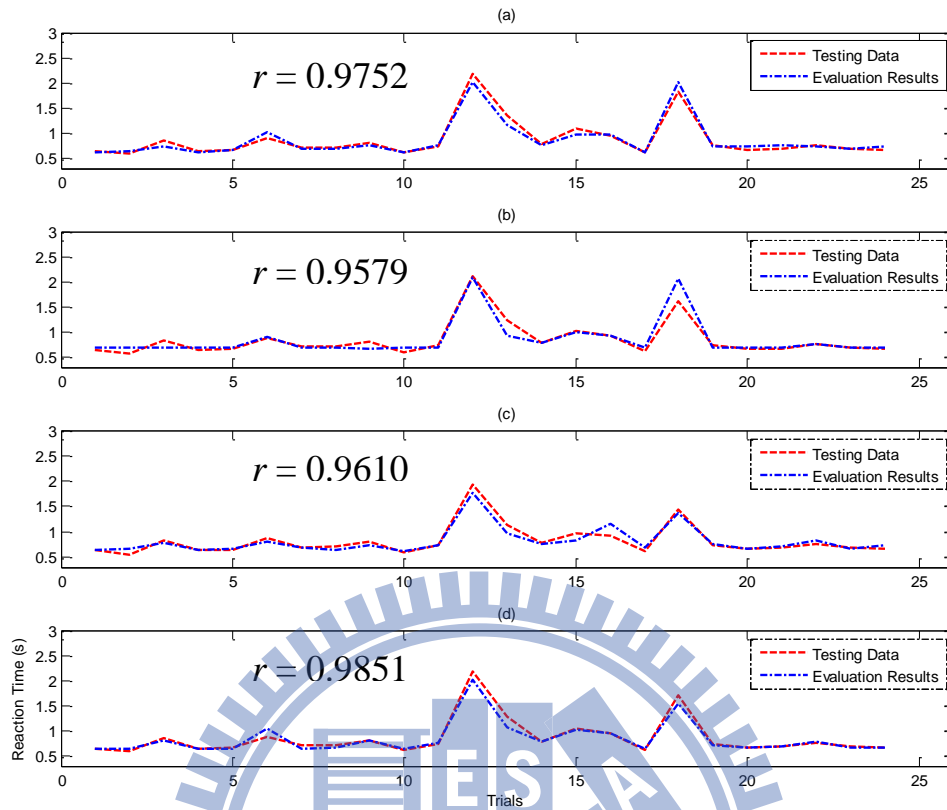
Figure 17. Evaluation result examples of testing data for Subject 6 with subject-dependent drowsiness prediction infrastructure using (a) SVR ($r = 0.9752$), (b) MLPNN ($r = 0.9579$), (c) RBFNN ($r = 0.9610$) and (d) SONFIN ($r = 0.9851$). The red dashed line and blue dash-dot line present the golden testing data and estimated evaluation result respectively.

### 4.1.3. Derived Parameters for SONFIN

The constructed parameters, such as rules numbers, mean values ($m_{ij}$) and variances ($\sigma^2_{ij}$) of membership functions (MF) and weights ($w_i$) for the testing data evaluation examples taken in the previous section with the subject-dependent drowsiness prediction using SONFIN will be comprehensively described in this section.

The RT estimation rule numbers generated by SONFIN for subject-dependent experimental testing evaluation samples of Subject 1-6 are 11, 11, 12, 10, 12 and 8, as listed in Table 4, respectively. The MFs for Subject1-6

were depicted in Figure 18-23, while the corresponded mean values ($m_{ij}$), variance ($\sigma^2_{ij}$) and weights ($w_i$) were summarized in Table 5-10 accordingly.

Table 4. Rules Numbers For Sampled Testing Data Evaluation Subjects Derived by Subject-Dependent Drowsiness Prediction with SONFIN

| Subject | 1 | 2 | 3 | 4 | 5 | 6 |
|---------|----|----|----|----|----|---|
| Rules   | 11 | 11 | 12 | 10 | 12 | 8 |
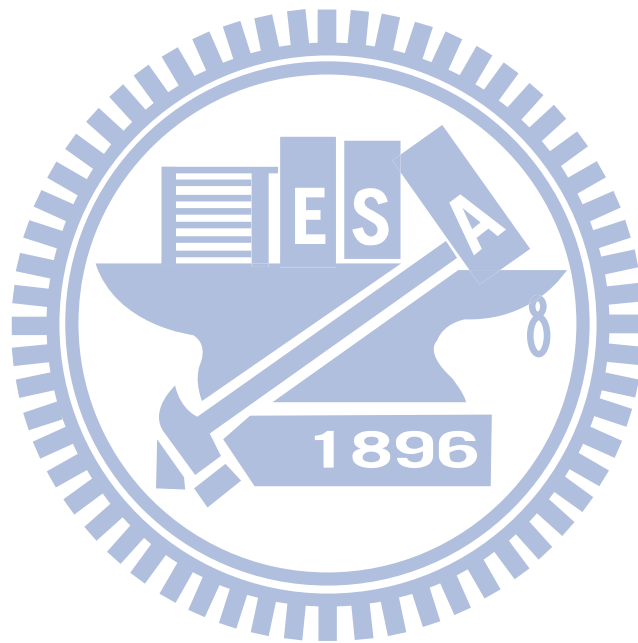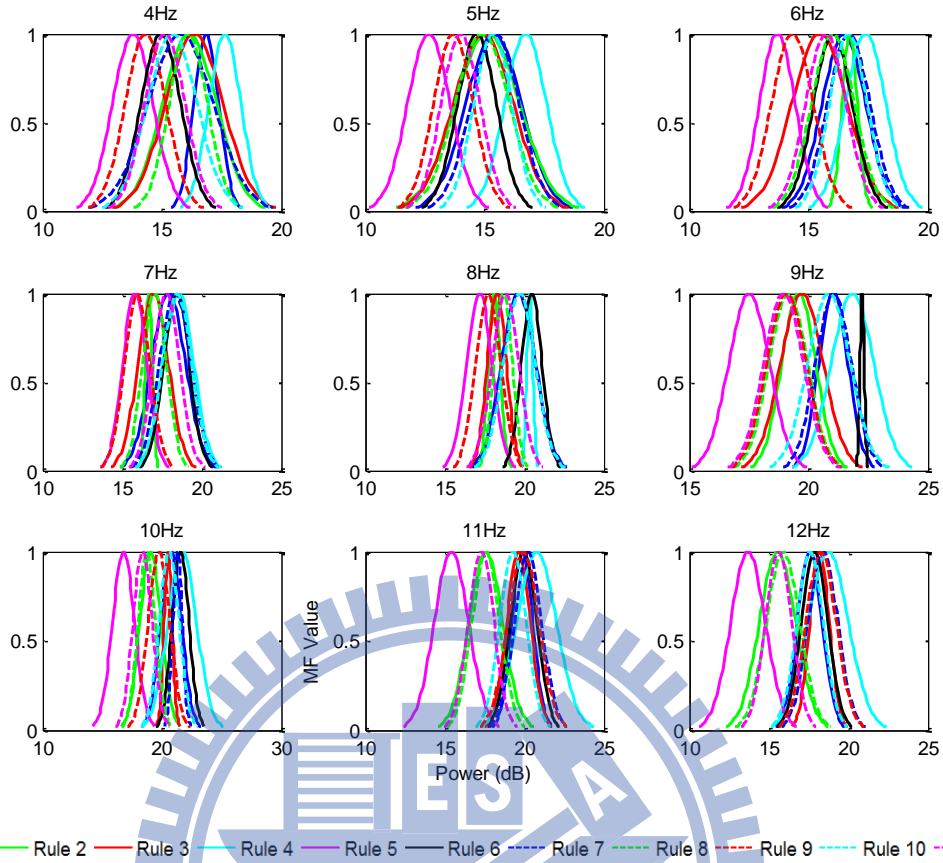
Figure 18. Constructed Membership Functions for Sampled Subject 1 with Subject-Dependent Drowsiness Prediction using SONFIN

Table 5. Constructed Mean Values, Variances and Weights for Sampled Subject 1 with Subject-Dependent Drowsiness Prediction using SONFIN

| Rules | Mean and Variance($m_{ij}$, $\sigma^2_{ij}$) | | | | | | | | | Weight ($w_i$) |
|---|---|---|---|---|---|---|---|---|---|---|
| | 4Hz | 5Hz | 6Hz | 7Hz | 8Hz | 9Hz | 10Hz | 11Hz | 12Hz | |
| 1 | (16.86,0.74) | (15.39,1.65) | (16.47,1.29) | (17.91,1.52) | (19.63,1.53) | (21.04,0.87) | (20.77,1.23) | (19.88,0.94) | (17.58,1.10) | 1.84 |
| 2 | (16.15,1.60) | (15.12,1.92) | (16.72,0.46) | (16.67,0.31) | (18.12,0.53) | (19.59,1.01) | (19.05,1.26) | (17.59,1.50) | (15.54,1.62) | 1.01 |
| 3 | (16.36,1.70) | (14.95,1.77) | (15.46,1.65) | (16.96,1.34) | (18.28,0.85) | (19.72,1.27) | (20.52,0.49) | (19.64,1.06) | (18.18,0.87) | 1.09 |
| 4 | (17.64,0.95) | (16.72,1.24) | (17.39,1.20) | (18.56,1.34) | (20.35,0.27) | (21.84,1.27) | (21.70,1.71) | (20.78,1.78) | (18.73,1.82) | 1.86 |
| 5 | (13.78,1.20) | (12.67,1.26) | (13.69,1.07) | (15.80,1.07) | (17.18,1.16) | (17.50,1.20) | (16.79,1.32) | (15.42,1.53) | (13.69,1.54) | 0.74 |
| 6 | (14.95,1.17) | (14.68,1.17) | (16.02,1.15) | (18.42,1.15) | (20.47,0.92) | (22.24,0.13) | (21.56,1.01) | (19.95,1.15) | (17.88,1.16) | -0.48 |
| 7 | (15.79,1.94) | (15.44,1.43) | (16.68,1.26) | (18.33,1.40) | (19.67,1.47) | (21.05,1.06) | (21.31,0.56) | (20.23,1.23) | (18.40,1.32) | 1.08 |
| 8 | (16.10,1.14) | (14.90,1.61) | (16.02,1.28) | (17.04,1.07) | (18.68,0.80) | (19.15,1.15) | (18.72,1.03) | (17.59,1.24) | (15.89,1.49) | 1.00 |
| 9 | (14.31,1.21) | (13.69,1.18) | (14.32,1.24) | (15.95,1.14) | (17.74,1.12) | (19.07,1.17) | (19.75,1.29) | (19.94,1.38) | (18.28,1.35) | 0.77 |
| 10 | (15.43,1.48) | (15.35,1.12) | (16.67,1.12) | (18.46,1.31) | (19.70,1.43) | (20.85,1.26) | (20.62,1.18) | (19.32,1.18) | (17.58,1.20) | 0.84 |
| 11 | (15.13,1.20) | (14.00,1.15) | (15.73,1.20) | (17.80,1.20) | (18.80,1.20) | (18.96,1.18) | (18.37,1.13) | (17.28,1.16) | (15.61,1.18) | 0.50 |
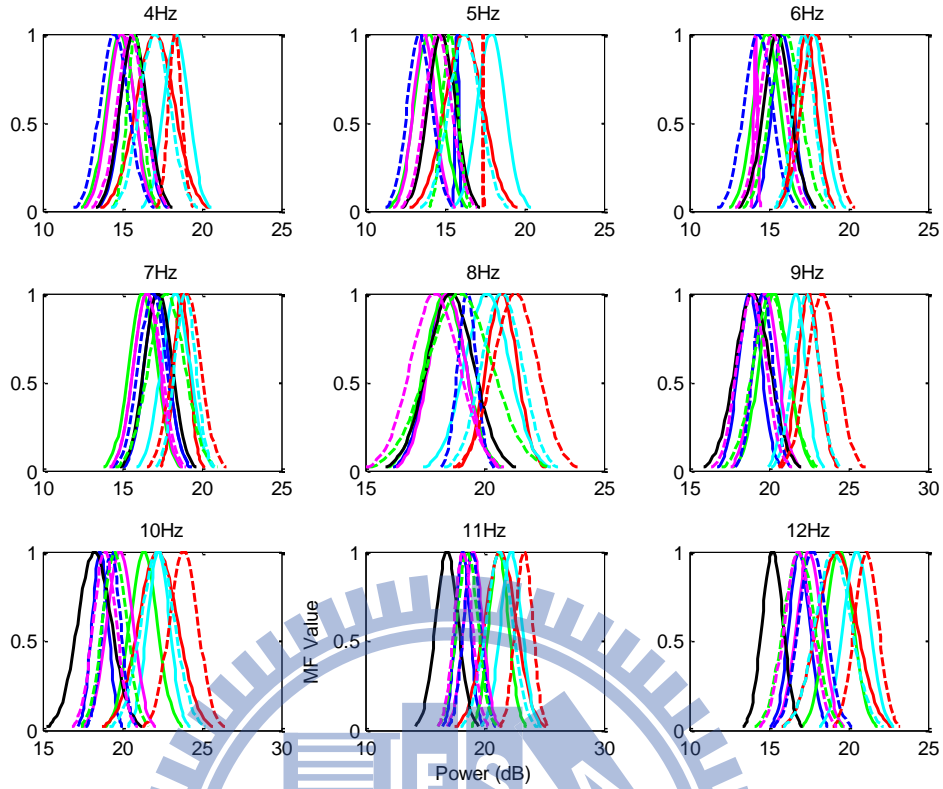
Figure 19. Constructed Membership Functions for Sampled Subject 2 with Subject-Dependent Drowsiness Prediction using SONFIN

Table 6. Constructed Mean Values, Variances and Weights for Sampled Subject 2 with Subject-Dependent Drowsiness Prediction using SONFIN

| Rules | Mean and Variance($m_{ij}$, $\sigma^2_{ij}$) | | | | | | | | | Weight ($w_i$) |
|---|---|---|---|---|---|---|---|---|---|---|
| | 4Hz | 5Hz | 6Hz | 7Hz | 8Hz | 9Hz | 10Hz | 11Hz | 12Hz | |
| 1 | (15.68,1.09) | (15.77,0.15) | (15.87,0.97) | (17.18,1.07) | (18.41,1.13) | (18.81,1.02) | (18.61,0.72) | (18.19,0.87) | (16.91,0.92) | -0.19 |
| 2 | (14.88,1.24) | (13.98,1.25) | (14.88,1.17) | (16.30,1.23) | (18.35,1.21) | (20.31,1.30) | (21.35,1.23) | (21.19,1.18) | (19.44,1.21) | 0.77 |
| 3 | (17.08,1.71) | (16.20,1.69) | (17.35,0.92) | (18.74,0.69) | (20.72,0.92) | (22.48,0.95) | (22.25,1.75) | (21.33,1.90) | (19.27,1.75) | 1.46 |
| 4 | (18.40,1.10) | (17.93,1.24) | (17.78,1.04) | (18.36,1.24) | (20.11,1.34) | (21.68,0.88) | (22.28,0.99) | (22.24,1.27) | (20.53,1.17) | 1.89 |
| 5 | (14.93,1.16) | (13.71,0.97) | (14.17,0.15) | (16.54,1.14) | (18.44,1.09) | (19.78,1.11) | (19.85,1.15) | (19.05,1.12) | (17.53,1.13) | 0.91 |
| 6 | (15.75,1.19) | (14.79,1.22) | (15.52,1.22) | (17.26,1.20) | (18.58,1.38) | (18.97,1.54) | (18.27,1.50) | (16.86,1.35) | (15.24,0.94) | 1.00 |
| 7 | (14.51,1.27) | (13.41,1.08) | (14.32,1.26) | (16.92,1.25) | (19.27,0.56) | (19.63,0.88) | (19.33,0.80) | (18.96,1.01) | (17.73,1.24) | 0.94 |
| 8 | (15.81,0.70) | (15.33,0.67) | (16.05,1.36) | (17.79,1.59) | (18.96,1.90) | (20.11,1.52) | (19.53,1.08) | (18.56,1.25) | (16.90,1.39) | 0.90 |
| 9 | (18.32,0.59) | (17.45,0.00) | (17.93,1.27) | (19.04,1.26) | (21.30,1.31) | (23.35,1.35) | (23.87,1.28) | (23.31,1.03) | (21.13,1.07) | 1.40 |
| 10 | (17.05,1.36) | (16.24,1.40) | (17.18,0.92) | (18.97,0.94) | (20.72,1.19) | (22.35,1.11) | (22.24,1.50) | (21.24,1.61) | (19.06,1.60) | 0.81 |
| 11 | (15.53,1.22) | (14.59,1.21) | (15.24,1.19) | (16.60,1.19) | (17.92,1.44) | (18.92,1.26) | (18.91,1.03) | (18.21,1.08) | (16.84,1.23) | 0.77 |
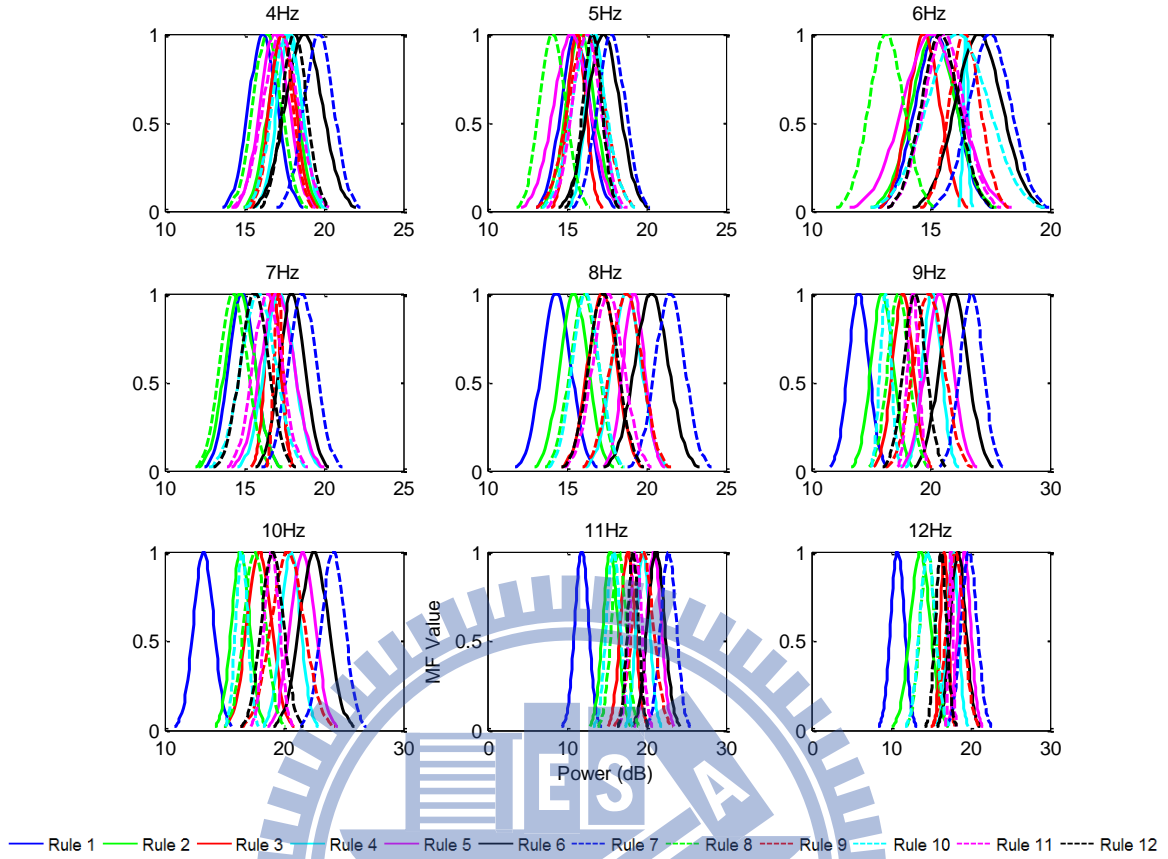
Figure 20. Constructed Membership Functions for Sampled Subject 3 with Subject-Dependent Drowsiness Prediction using SONFIN

Table 7. Constructed Mean Values, Variances and Weights for Sampled Subject 3 with Subject-Dependent Drowsiness Prediction using SONFIN

| Rules | Mean and Variance($m_{ij}$, $\sigma^2_{ij}$) | | | | | | | | | Weight ($w_i$) |
|---|---|---|---|---|---|---|---|---|---|---|
| | 4Hz | 5Hz | 6Hz | 7Hz | 8Hz | 9Hz | 10Hz | 11Hz | 12Hz | |
| 1 | (16.18,1.27) | (15.54,1.25) | (15.21,1.21) | (14.89,1.19) | (14.34,1.29) | (13.96,1.22) | (13.26,1.20) | (11.88,1.23) | (10.84,1.22) | 0.94 |
| 2 | (17.41,1.24) | (15.86,1.27) | (15.12,1.31) | (14.73,1.32) | (15.45,1.24) | (15.94,1.30) | (16.37,1.08) | (15.48,1.32) | (13.69,1.77) | 1.06 |
| 3 | (17.41,1.13) | (15.63,0.79) | (14.73,0.94) | (16.81,0.68) | (17.24,1.28) | (17.67,1.23) | (17.94,1.45) | (17.67,1.28) | (16.71,0.69) | 1.60 |
| 4 | (17.85,1.09) | (16.77,0.83) | (16.47,0.15) | (17.20,1.32) | (18.77,1.30) | (20.11,1.11) | (20.57,1.17) | (19.61,1.17) | (17.78,0.99) | 1.70 |
| 5 | (16.91,1.29) | (15.30,1.59) | (15.03,1.70) | (17.09,1.46) | (19.21,0.96) | (20.72,1.61) | (21.56,1.47) | (20.97,1.28) | (19.26,1.14) | 1.37 |
| 6 | (18.76,1.64) | (17.31,1.43) | (17.02,1.39) | (18.01,1.15) | (20.33,1.50) | (21.95,1.69) | (22.51,1.70) | (21.22,1.53) | (18.46,1.36) | 2.06 |
| 7 | (19.70,1.32) | (17.79,1.24) | (17.49,1.24) | (18.65,1.26) | (21.49,1.32) | (23.44,1.36) | (24.13,1.39) | (22.80,1.39) | (19.84,1.42) | 2.23 |
| 8 | (16.45,1.26) | (14.13,1.17) | (13.14,1.04) | (14.32,1.21) | (16.09,1.24) | (17.31,1.26) | (17.55,1.28) | (16.54,1.30) | (14.61,1.34) | 1.23 |
| 9 | (17.36,1.01) | (16.23,1.59) | (16.43,0.92) | (17.16,0.40) | (18.74,1.39) | (19.87,1.81) | (20.32,1.95) | (19.57,1.85) | (18.10,1.51) | 1.88 |
| 10 | (17.67,1.30) | (16.37,1.48) | (16.14,1.82) | (15.89,1.55) | (16.22,1.19) | (16.23,0.65) | (16.47,0.71) | (15.87,1.24) | (14.60,1.41) | 1.11 |
| 11 | (17.29,1.56) | (16.25,1.26) | (15.55,1.20) | (16.46,1.28) | (17.60,1.38) | (18.53,0.66) | (18.99,0.90) | (18.65,1.09) | (17.57,0.36) | 1.49 |
| 12 | (18.16,1.10) | (16.60,0.85) | (15.40,1.12) | (15.66,1.28) | (17.30,1.30) | (18.68,1.32) | (19.03,1.31) | (18.33,0.96) | (16.31,0.99) | 1.09 |
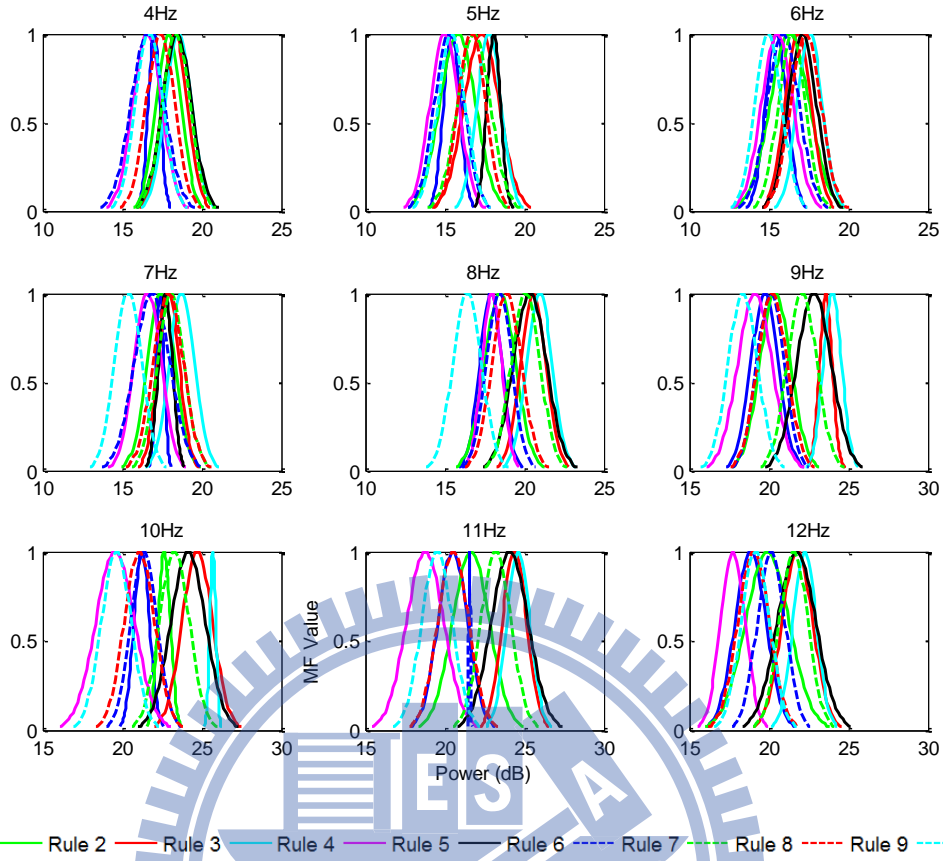
Figure 21. Constructed Membership Functions for Sampled Subject 4 with Subject-Dependent Drowsiness Prediction using SONFIN

Table 8. Constructed Mean Values, Variances and Weights for Sampled Subject 4 with Subject-Dependent Drowsiness Prediction using SONFIN

| Rules | Mean and Variance($m_{ij}$, $\sigma^2_{ij}$) | | | | | | | | | Weight ($w_i$) |
|---|---|---|---|---|---|---|---|---|---|---|
| | 4Hz | 5Hz | 6Hz | 7Hz | 8Hz | 9Hz | 10Hz | 11Hz | 12Hz | |
| 1 | (17.01,0.53) | (15.43,0.72) | (15.47,0.95) | (17.38,0.36) | (17.90,1.00) | (19.74,1.23) | (21.23,0.70) | (20.51,1.33) | (18.85,1.39) | 1.19 |
| 2 | (17.92,1.11) | (15.82,1.58) | (16.31,1.74) | (17.45,1.24) | (18.47,1.40) | (20.40,1.38) | (22.63,0.56) | (21.65,1.65) | (19.90,1.95) | 1.22 |
| 3 | (18.32,1.12) | (17.31,1.57) | (16.84,1.15) | (17.92,0.96) | (20.56,1.13) | (23.58,0.57) | (24.72,1.37) | (24.39,1.10) | (21.79,1.38) | 1.62 |
| 4 | (18.53,1.19) | (17.78,1.09) | (17.57,1.12) | (18.75,1.14) | (20.96,1.14) | (24.00,0.83) | (25.70,0.27) | (24.63,1.03) | (22.25,1.04) | -0.54 |
| 5 | (16.58,1.29) | (14.98,1.29) | (15.53,1.41) | (16.59,1.23) | (17.96,0.87) | (19.12,1.53) | (19.56,1.74) | (18.77,1.67) | (17.74,1.10) | 0.98 |
| 6 | (18.45,1.30) | (18.07,0.61) | (17.11,1.26) | (17.72,0.62) | (20.36,1.48) | (22.84,1.54) | (24.15,1.56) | (24.09,1.65) | (21.75,1.71) | 2.77 |
| 7 | (16.60,1.49) | (15.28,1.31) | (15.90,1.41) | (16.88,1.59) | (18.41,1.16) | (20.10,1.20) | (21.36,1.16) | (21.56,0.07) | (20.14,1.24) | 1.00 |
| 8 | (18.38,1.24) | (16.84,1.45) | (16.45,1.22) | (18.06,1.22) | (20.08,1.29) | (22.09,1.32) | (23.28,1.34) | (23.22,1.35) | (21.57,1.27) | 1.28 |
| 9 | (17.41,1.27) | (16.70,1.22) | (17.32,1.34) | (17.90,1.34) | (18.90,1.31) | (20.21,1.33) | (21.09,1.36) | (20.53,1.39) | (19.04,1.41) | 0.88 |
| 10 | (16.70,1.21) | (15.42,1.23) | (14.97,1.20) | (15.38,1.22) | (16.41,1.28) | (18.36,1.31) | (19.64,1.34) | (19.51,1.37) | (19.16,1.28) | 0.71 |
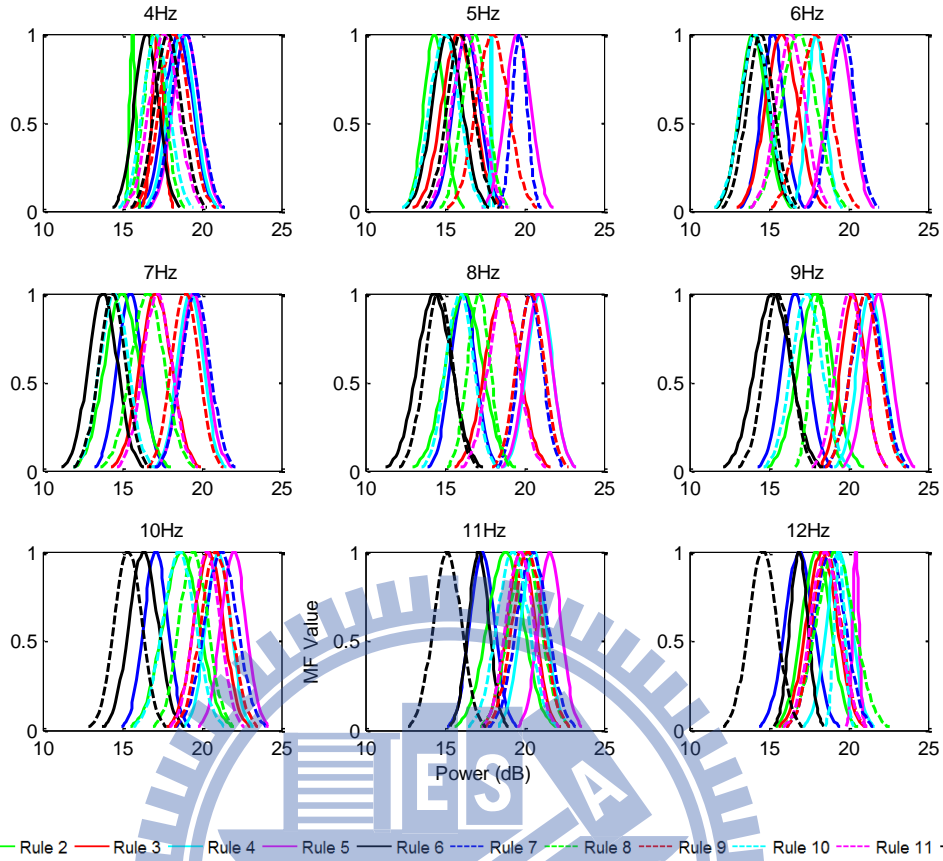
Figure 22. Constructed Membership Functions for Sampled Subject 5 with Subject-Dependent Drowsiness Prediction using SONFIN

Table 9. Constructed Mean Values, Variances and Weights for Sampled Subject 5 with Subject-Dependent Drowsiness Prediction using SONFIN

| Rules | Mean and Variance($m_{ij}$, $\sigma^2_{ij}$) | | | | | | | | | Weight ($w_i$) |
|---|---|---|---|---|---|---|---|---|---|---|
| | 4Hz | 5Hz | 6Hz | 7Hz | 8Hz | 9Hz | 10Hz | 11Hz | 12Hz | |
| 1 | (18.53,1.26) | (16.38,1.17) | (15.25,1.02) | (15.49,1.13) | (16.16,1.13) | (16.62,1.17) | (17.11,1.07) | (17.36,1.09) | (16.91,1.27) | 0.63 |
| 2 | (15.65,0.25) | (14.33,0.93) | (14.02,1.21) | (14.98,1.53) | (16.21,1.62) | (17.92,1.53) | (18.72,1.62) | (18.82,1.60) | (17.98,1.29) | 0.92 |
| 3 | (17.24,0.50) | (15.83,1.42) | (15.79,1.42) | (17.11,1.41) | (18.61,1.52) | (20.29,1.08) | (20.44,1.31) | (19.79,1.24) | (18.33,1.37) | 1.32 |
| 4 | (18.76,1.17) | (17.92,0.07) | (17.98,0.80) | (19.30,1.14) | (20.97,1.14) | (21.38,1.13) | (21.04,1.10) | (20.57,1.13) | (19.40,1.12) | -0.20 |
| 5 | (19.02,1.19) | (19.60,1.13) | (19.43,1.11) | (19.52,1.18) | (20.89,1.18) | (21.89,1.15) | (22.01,1.12) | (21.61,1.02) | (20.47,0.29) | -0.48 |
| 6 | (16.53,1.07) | (15.16,1.33) | (14.12,1.25) | (13.79,1.29) | (14.34,1.53) | (15.25,1.58) | (16.34,1.29) | (17.14,0.92) | (16.89,0.79) | 0.75 |
| 7 | (18.99,1.24) | (19.70,0.67) | (19.65,1.13) | (19.62,1.27) | (20.38,1.07) | (21.16,1.35) | (21.22,1.45) | (20.50,1.38) | (18.83,1.39) | 2.02 |
| 8 | (17.04,0.97) | (16.88,1.11) | (16.88,1.57) | (16.61,1.49) | (17.14,1.00) | (18.16,0.77) | (19.49,1.28) | (20.04,1.43) | (19.18,1.70) | 0.76 |
| 9 | (18.27,1.31) | (17.98,1.43) | (17.90,1.40) | (18.96,1.22) | (20.39,1.19) | (21.06,1.28) | (20.90,1.34) | (20.22,1.35) | (18.62,1.26) | 1.39 |
| 10 | (17.10,1.19) | (14.98,1.33) | (14.12,1.30) | (14.49,1.27) | (15.95,1.22) | (17.39,1.37) | (18.59,1.45) | (19.28,1.43) | (19.43,0.46) | 0.71 |
| 11 | (17.62,1.28) | (16.39,1.31) | (16.37,1.28) | (17.21,1.28) | (18.70,1.34) | (20.09,1.20) | (20.34,1.19) | (19.73,1.22) | (18.54,1.31) | 0.68 |
| 12 | (17.90,1.21) | (15.99,1.22) | (14.47,1.22) | (14.38,1.21) | (14.61,1.25) | (15.55,1.23) | (15.37,1.23) | (15.16,1.24) | (14.63,1.26) | 0.60 |
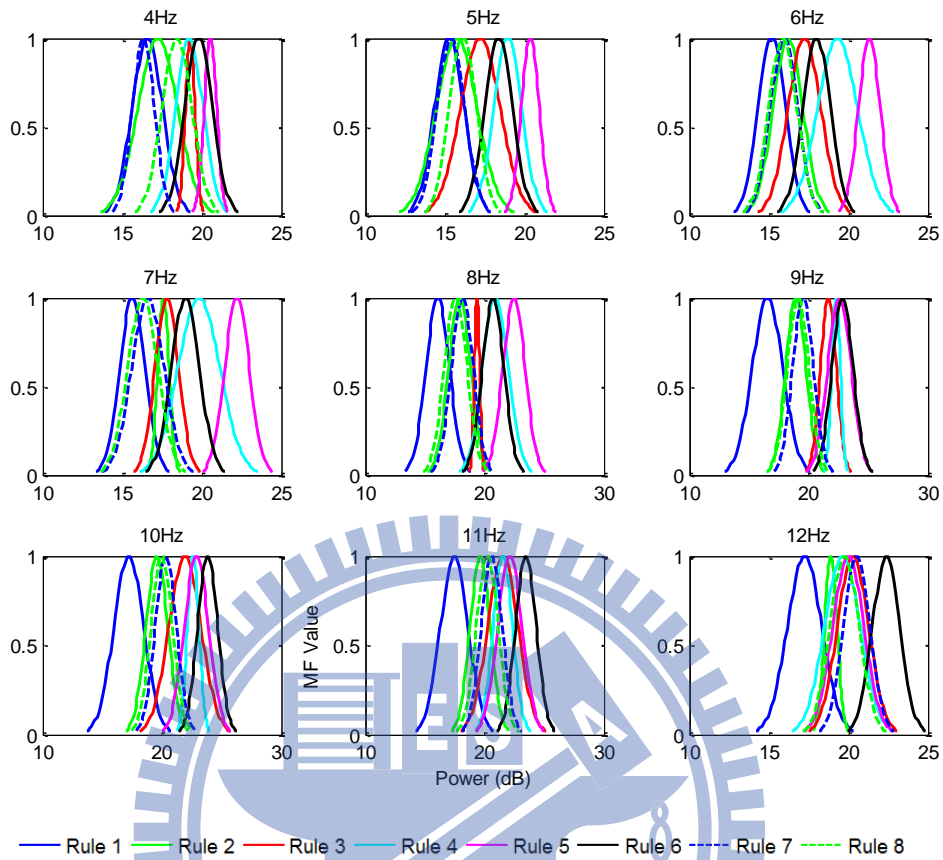
Figure 23.　Constructed Membership Functions for Sampled Subject 6 with
Subject-Dependent Drowsiness Prediction using SONFIN

Table 10.　Constructed Mean Values, Variances and Weights for Sampled
Subject 6 with Subject-Dependent Drowsiness Prediction using SONFIN

| Rules | Mean and Variance($m_{ij}$, $\sigma^2{}_{ij}$) | | | | | | | | | Weight ($w_i$) |
|---|---|---|---|---|---|---|---|---|---|---|
| | 4Hz | 5Hz | 6Hz | 7Hz | 8Hz | 9Hz | 10Hz | 11Hz | 12Hz | |
| 1 | (16.59,1.36) | (15.29,1.32) | (15.19,1.21) | (15.66,1.17) | (16.08,1.39) | (16.56,1.81) | (17.22,1.77) | (17.47,1.65) | (17.25,1.53) | 0.65 |
| 2 | (17.23,1.78) | (15.75,1.82) | (16.20,1.33) | (17.60,0.51) | (17.91,1.32) | (18.93,1.21) | (19.58,1.30) | (19.64,1.21) | (18.90,0.56) | 0.86 |
| 3 | (19.28,0.43) | (17.23,1.77) | (17.24,1.47) | (17.81,1.04) | (19.37,0.31) | (21.65,0.94) | (21.93,1.90) | (21.54,1.80) | (20.29,1.39) | 1.03 |
| 4 | (19.22,1.23) | (18.96,1.25) | (19.32,1.79) | (19.83,1.86) | (20.91,1.53) | (22.29,0.52) | (22.62,0.69) | (21.53,1.16) | (19.63,1.59) | 1.54 |
| 5 | (20.55,0.56) | (20.38,0.81) | (21.32,0.98) | (22.22,1.10) | (22.48,1.32) | (22.58,1.40) | (22.90,1.44) | (22.13,1.45) | (19.99,1.39) | 2.02 |
| 6 | (19.81,1.24) | (18.39,1.25) | (18.01,1.23) | (18.98,1.25) | (20.73,1.28) | (22.85,1.26) | (23.84,1.20) | (23.47,1.23) | (22.38,1.22) | 0.95 |
| 7 | (16.34,0.99) | (15.40,1.25) | (15.97,1.22) | (16.61,1.44) | (18.14,1.31) | (19.54,1.24) | (20.33,1.26) | (20.60,1.26) | (20.52,1.19) | 0.79 |
| 8 | (18.45,1.34) | (16.13,1.22) | (15.88,1.26) | (16.30,1.35) | (17.58,1.36) | (19.12,1.29) | (19.98,1.27) | (20.24,1.30) | (19.76,1.30) | 0.66 |

### 4.1.4. Section Discussion

The performances of all four predictors are comparable in subject-dependent drowsiness prediction, and SONFIN has a better PPMCC and a smaller RMSE value on testing data in this experiment ($r = 97.2\%$ and RMSE $= 0.076$). However, subject-dependent prediction system is not applicable in real world to be generalized for other users. Developer must record user's EEG data in advance and only the recorded user can achieve that high performance ($r > 95\%$). Therefore, a generalized cross-subject drowsiness prediction system shall be constructed, and the proposed infrastructure will be detailed investigated in next section.

### 4.2. Generalized Cross-subject Drowsiness Prediction

The procedure of generalized cross-subject drowsiness predictor analysis is depicted in Figure 24. The EEG data from five subjects were used as the training data, and the remaining subject was reserved as the testing pattern.
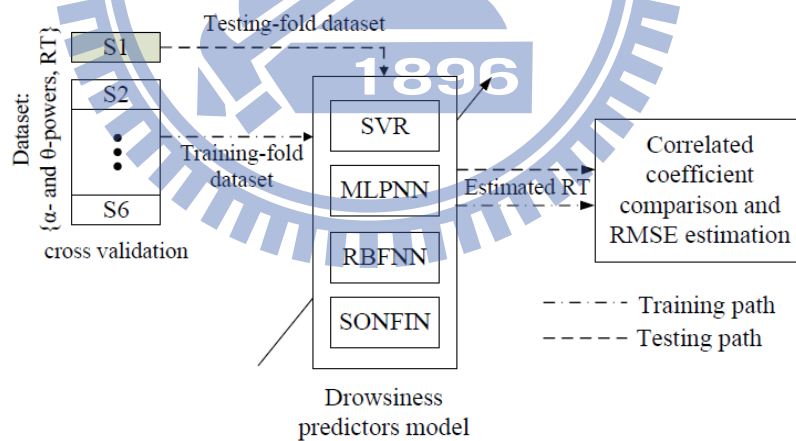


Figure 24. Generalized cross-subject drowsiness predictor analysis structure, where $S_i$ means the $i$-th subject.

### 4.2.1. Boxplots of PPMCC and RMSE

Table 11-12 summarize the averages of PPMCC and RMSE performance in comparison with the actual and estimated RTs. The PPMCC on the training and

testing sets using obtained by SVR, MLPNN, RBFNN, and SONFIN are 98.0%, 96.8%, 99.3%, 98.4% and 61.6%, 61.3%, 47.9%, 78.3%, respectively. The RMSE values for training and testing evaluation with SVR, MLPNN, RBFNN, and SONFIN are 0.06 s, 0.04 s, 0.01 s, 0.06 s and 0.37 s, 0.42 s, 1.01 s, 0.36 s, respectively.

Table 11.    Correlation coefficients Comparisons for
Generalized Cross-Subject Drowsiness Prediction

| Subject | | 1 | 2 | 3 | 4 | 5 | 6 | Average (%) |
|---|---|---|---|---|---|---|---|---|
| SVR | Training | 96.5% | 99.1% | 95.5% | 98.8% | 98.9% | 99.0% | 98.0±1.4 |
| | Testing | 58.0% | 65.3% | 66.4% | 51.4% | 62.2% | 66.5% | 61.6±8.6 |
| MLPNN | Training | 95.4% | 99.4% | 98.9% | 91.6% | 98.5% | 97.0% | 96.8±9.7 |
| | Testing | 56.5% | 66.5% | 58.2% | 61.2% | 63.8% | 61.6% | 61.3±12.2 |
| RBFNN | Training | 96.4% | 99.6% | 98.7% | 98.7% | 95.4% | 96.7% | 97.3±1.8 |
| | Testing | 68.3% | 48.5% | 62.6% | 74.2% | 17.1% | 16.5% | 47.9±23.6 |
| SONFIN | Training | 98.5% | 99.1% | 97.9% | 97.6% | 98.2% | 99.0% | 98.4±1.3 |
| | Testing | 78.1% | 81.7% | 74.6% | 82.7% | 76.0% | 76.4% | 78.3±5.7 |

Table 12.    RMSE Comparisons for
Generalized Cross-Subject Drowsiness Prediction

| Subject | | 1 | 2 | 3 | 4 | 5 | 6 | Average (s) |
|---|---|---|---|---|---|---|---|---|
| SVR | Training | 0.092 | 0.046 | 0.089 | 0.049 | 0.048 | 0.047 | 0.060±0.030 |
| | Testing | 0.222 | 0.309 | 0.454 | 0.267 | 0.540 | 0.337 | 0.370±0.110 |
| MLPNN | Training | 0.069 | 0.025 | 0.024 | 0.060 | 0.033 | 0.041 | 0.040±0.070 |
| | Testing | 0.229 | 0.448 | 0.578 | 0.366 | 0.443 | 0.430 | 0.420±0.150 |
| RBFNN | Training | 0.006 | 0.006 | 0.006 | 0.003 | 0.005 | 0.004 | 0.010±0.002 |
| | Testing | 0.417 | 0.467 | 0.798 | 3.361 | 0.496 | 0.507 | 1.010±1.070 |
| SONFIN | Training | 0.058 | 0.048 | 0.060 | 0.063 | 0.060 | 0.046 | 0.060±0.020 |
| | Testing | 0.153 | 0.318 | 0.537 | 0.371 | 0.321 | 0.488 | 0.360±0.140 |

Figure 25 shows the boxplot of the PPMCC for cross-subject drowsiness prediction using SVR, MLPNN, RBFNN, and SONFIN. Take Subject 1 for example, the median, upper and lower quartile, maximum and minimum PPMCC for cross-subject drowsy state predictor with SONFIN are 77.0%, 82.9% and 74.6%, 84.0% and 74.5%, respectively.
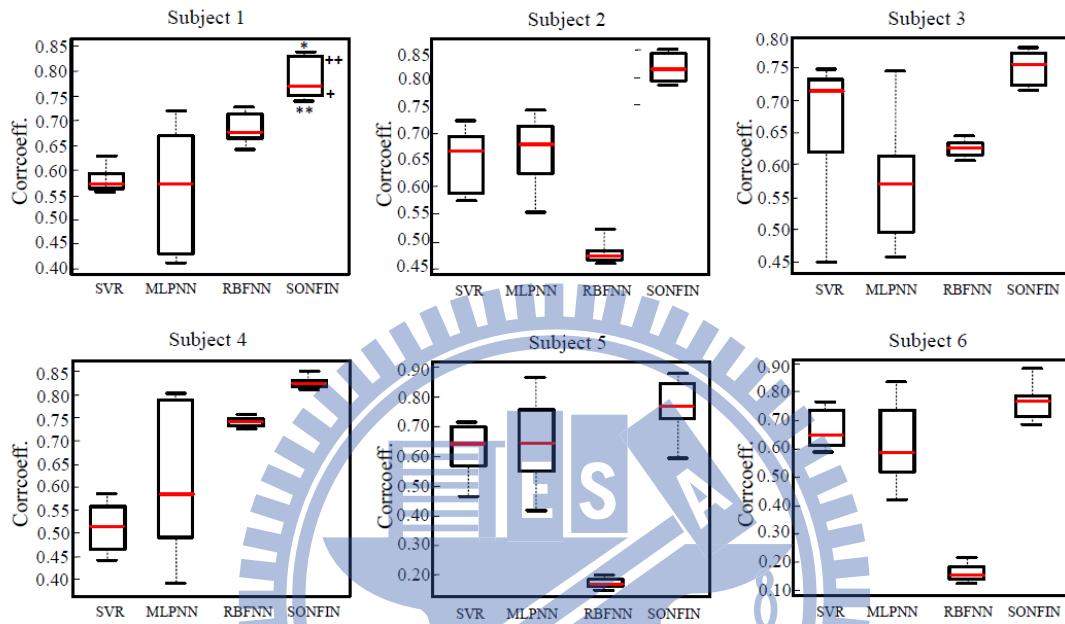


Figure 25.   Correlation coefficient boxplot comparison of subject's drowsy state testing evaluation for generalized cross-subject drowsiness prediction experiment with SVR, MLPNN, RBFNN and SONFIN. The boxes have three lines to present the values for lower quartile (+), median (red line), and upper quartile (++) for column data. Two addition lines at both ends of the whisker indicate the maximum (*) and minimum (**) value of a column data.

### 4.2.2. Experimental Result Examples

Some experimental results of testing data evaluation with cross-subject drowsiness prediction experiment for Subject 1 to Subject 6 that use SVR, MLPNN, RBFNN and SONFIN were depicted from Figure 26 to Figure 31 respectively.

Figure 26 shows some estimated RT evaluation result samples of testing

data for Subject 1 with cross-subject drowsiness prediction infrastructure using (a) SVR ($r = 0.5615$), (b) MLPNN ($r = 0.5178$), (c) RBFNN ($r = 0.6625$) and (d) SONFIN ($r = 0.8352$). The red dashed line and blue dash-dot line present the golden testing data and estimated evaluation result respectively. The correlation coefficients of training data validation for SVR, MLPNN, RBFNN and SONFIN in the sample results of Subject 1 are 96.5%, 95.4%, 96.4% and 96.5% respectively.

Figure 27 shows some estimated RT evaluation result samples of testing data for Subject 2 with cross-subject drowsiness prediction infrastructure using (a) SVR ($r = 0.7232$), (b) MLPNN ($r = 0.6989$), (c) RBFNN ($r = 0.5230$) and (d) SONFIN ($r = 0.8650$)The red dashed line and blue dash-dot line present the golden testing data and estimated evaluation result respectively. The correlation coefficients of training data validation for SVR, MLPNN, RBFNN and SONFIN in the sample results of Subject 2 are 98.1%, 97.9%, 98.6% and 97.8% respectively.

Figure 28 shows some estimated RT evaluation result samples of testing data for Subject 3 with cross-subject drowsiness prediction infrastructure using (a) SVR ($r = 0.6882$), (b) MLPNN ($r = 0.6841$), (c) RBFNN ($r = 0.6553$) and (d) SONFIN ($r = 0.7934$). The red dashed line and blue dash-dot line present the golden testing data and estimated evaluation result respectively. The correlation coefficients of training data validation for SVR, MLPNN, RBFNN and SONFIN in the sample results of Subject 3 are 95.5%, 98.9%, 98.7% and 97.9% respectively.

Figure 29 shows some estimated RT evaluation result samples of testing data for Subject 4 with cross-subject drowsiness prediction infrastructure using (a) SVR ($r = 0.5998$), (b) MLPNN ($r = 0.6790$), (c) RBFNN ($r = 0.7737$) and (d) SONFIN ($r = 0.8510$). The red dashed line and blue dash-dot line present the golden testing data and estimated evaluation result respectively. The correlation

coefficients of training data validation for SVR, MLPNN, RBFNN and SONFIN in the sample results of Subject 4 are 98.8%, 92.5%, 98.7% and 97.6% respectively.

Figure 30 shows some estimated RT evaluation result samples of testing data for Subject 5 with cross-subject drowsiness prediction infrastructure using (a) SVR ($r = 0.6345$), (b) MLPNN ($r = 0.7370$), (c) RBFNN ($r = 0.2033$) and (d) SONFIN ($r = 0.8843$). The red dashed line and blue dash-dot line present the golden testing data and estimated evaluation result respectively. The correlation coefficients of training data validation for SVR, MLPNN, RBFNN and SONFIN in the sample results of Subject 5 are 97.9%, 98.5%, 96.4% and 98.2% respectively.

Figure 31 shows some estimated RT evaluation result samples of testing data for Subject 6 with cross-subject drowsiness prediction infrastructure using (a) SVR ($r = 0.6573$), (b) MLPNN ($r = 0.7219$), (c) RBFNN ($r = 0.2573$) and (d) SONFIN ($r = 0.8789$). The red dashed line and blue dash-dot line present the golden testing data and estimated evaluation result respectively. The correlation coefficients of training data validation for SVR, MLPNN, RBFNN and SONFIN in the sample results of Subject 6 are 96.9%, 97.0%, 96.7% and 97.9% respectively.
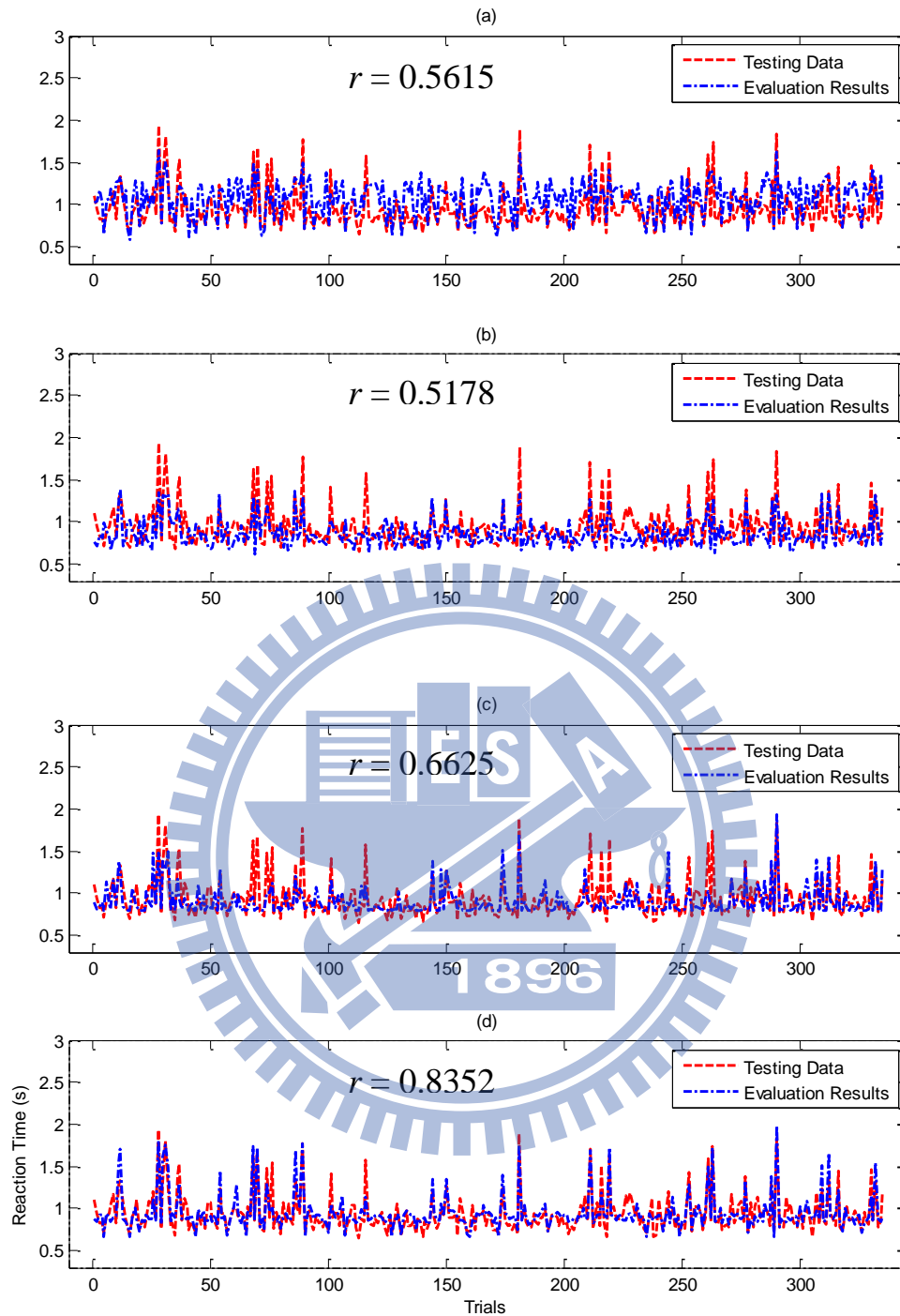
Figure 26. Evaluation result examples of testing data for subject1 with cross-subject drowsiness prediction infrastructure using (a) SVR ($r = 0.5615$), (b) MLPNN ($r = 0.5178$), (c) RBFNN ($r = 0.6625$) and (d) SONFIN ($r = 0.8352$). The red dashed line and blue dash-dot line present the golden testing data and estimated evaluation result respectively.
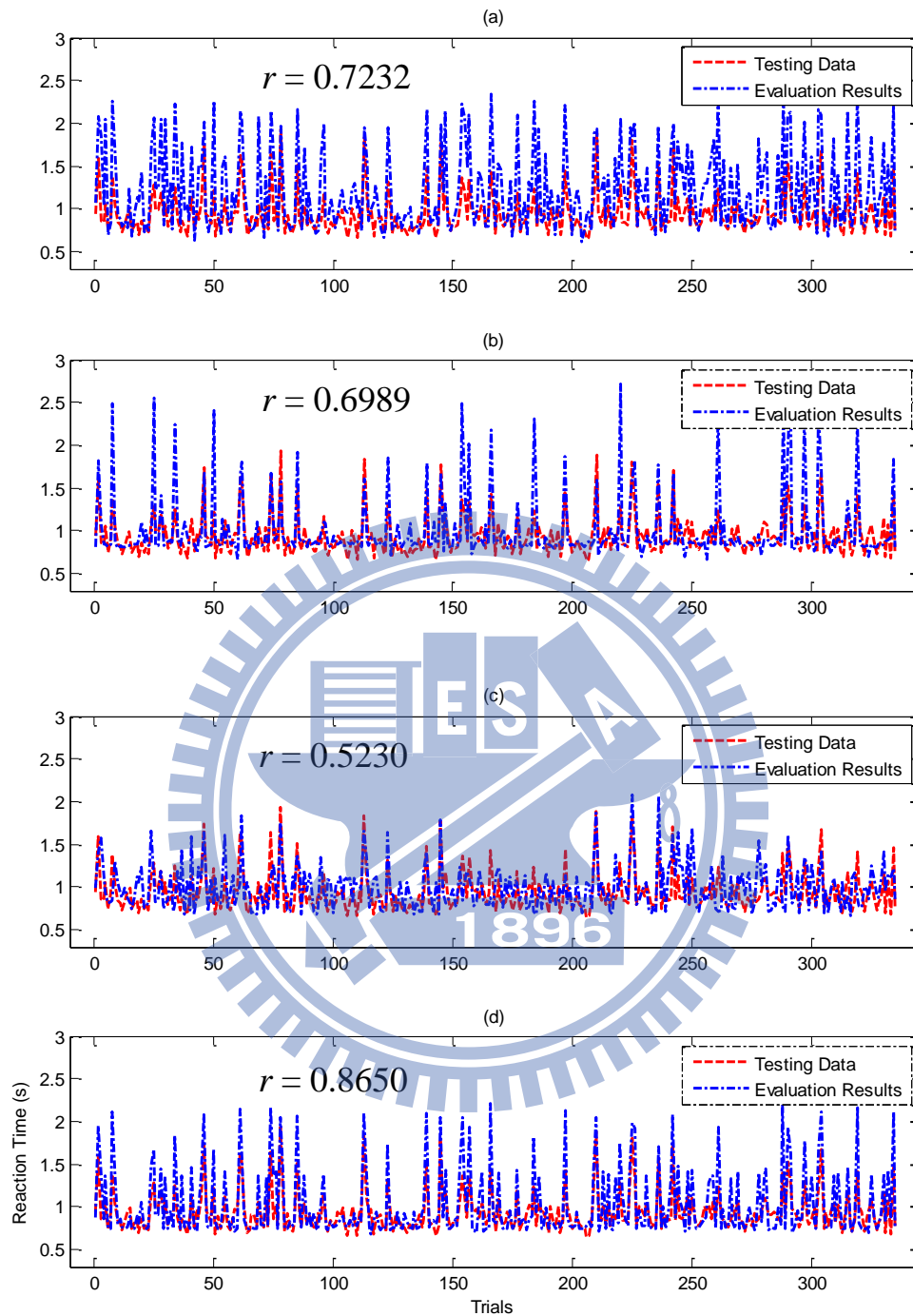
Figure 27.  Evaluation result examples of testing data for subject 2 with cross-subject drowsiness prediction infrastructure using (a) SVR ($r = 0.7232$), (b) MLPNN ($r = 0.6989$), (c) RBFNN ($r = 0.5230$) and (d) SONFIN ($r = 0.8650$). The red dashed line and blue dash-dot line present the golden testing data and estimated evaluation result respectively.
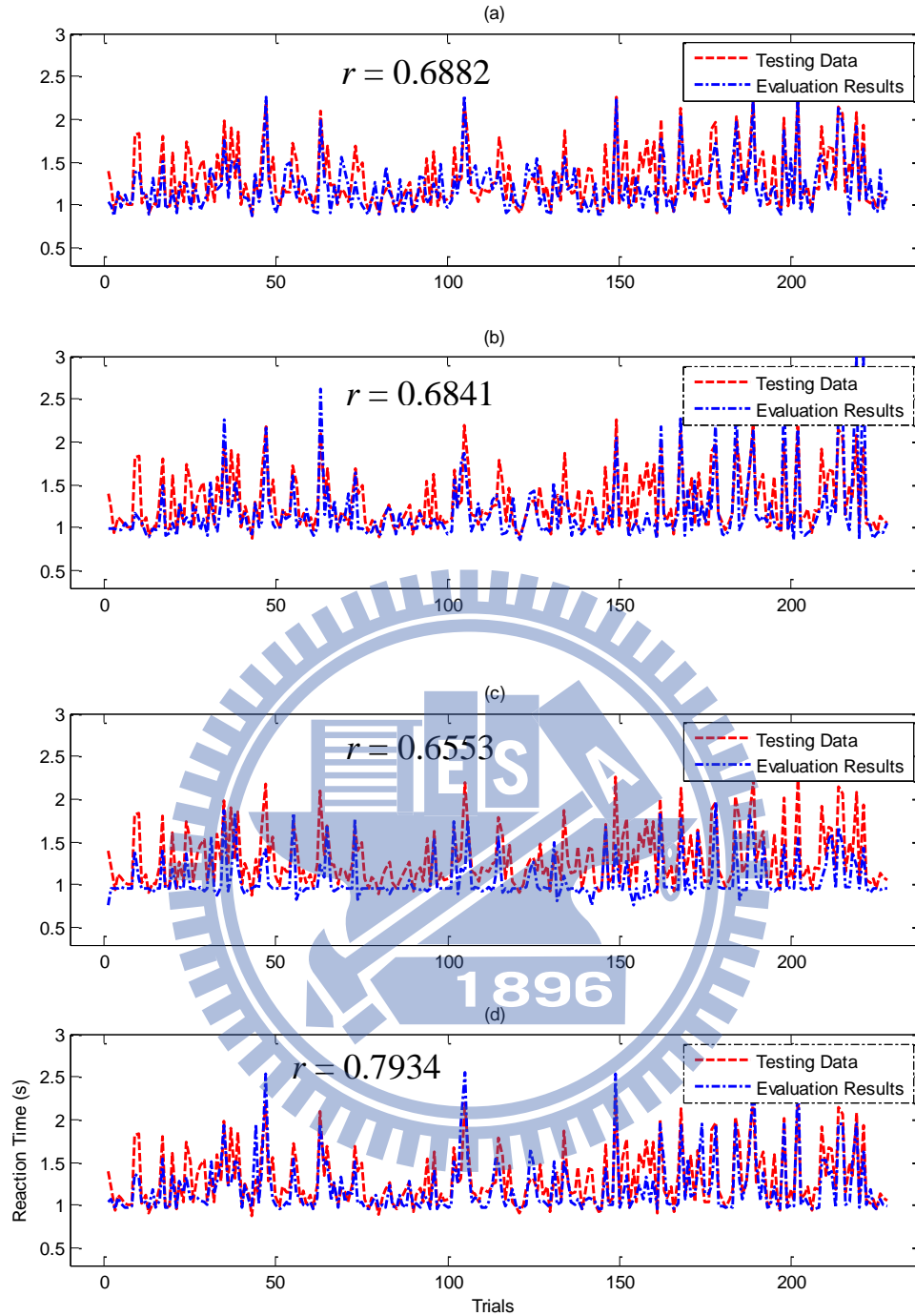
Figure 28.    Evaluation result examples of testing data for subject 3 with cross-subject drowsiness prediction infrastructure using (a) SVR ($r = 0.6882$), (b) MLPNN ($r = 0.6841$), (c) RBFNN ($r = 0.6553$) and (d) SONFIN ($r = 0.7934$). The red dashed line and blue dash-dot line present the golden testing data and estimated evaluation result respectively.
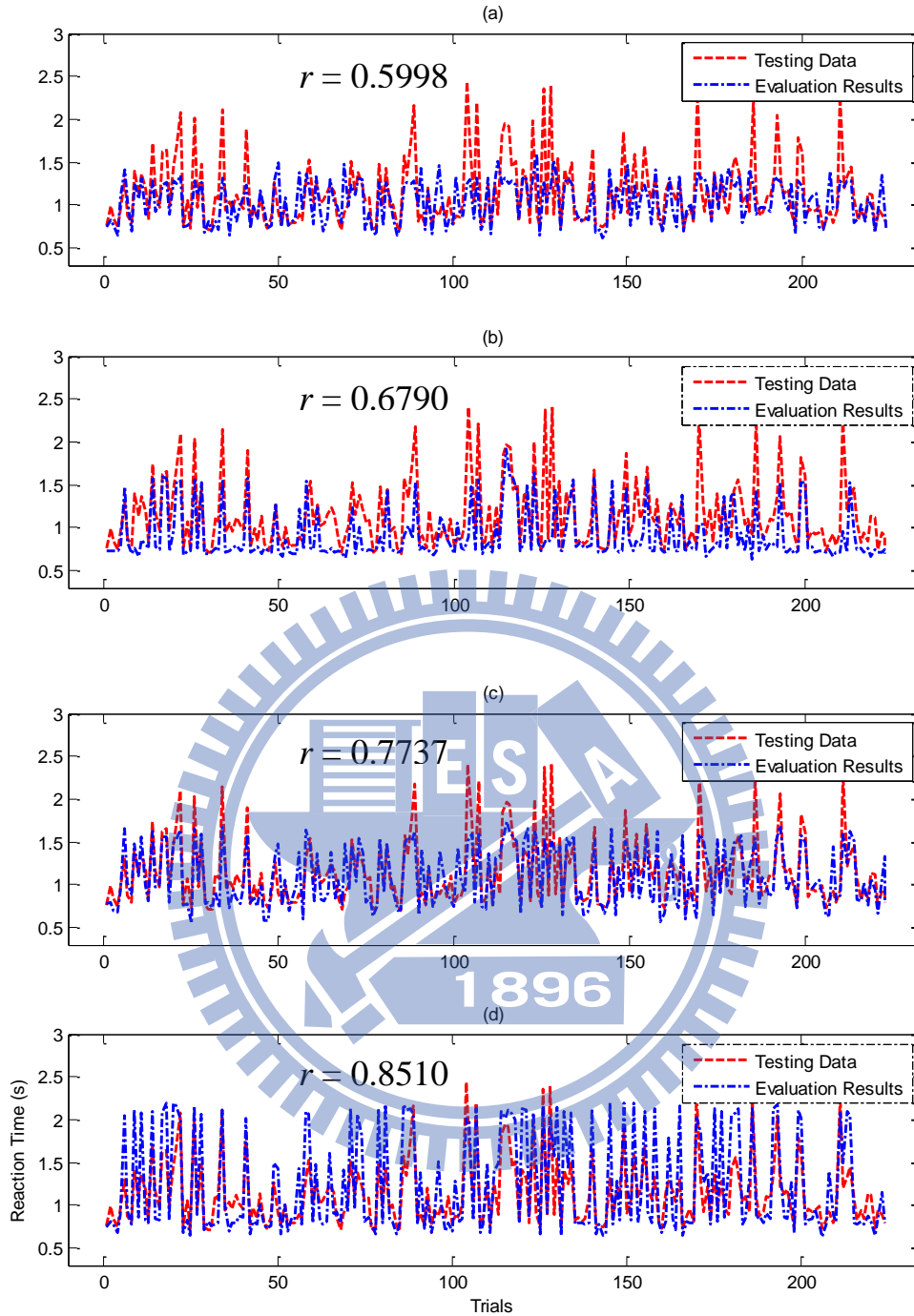
Figure 29.   Evaluation result examples of testing data for subject 4 with cross-subject drowsiness prediction infrastructure using (a) SVR ($r = 0.5998$), (b) MLPNN ($r = 0.6790$), (c) RBFNN ($r = 0.7737$) and (d) SONFIN ($r = 0.8510$). The red dashed line and blue dash-dot line present the golden testing data and estimated evaluation result respectively.
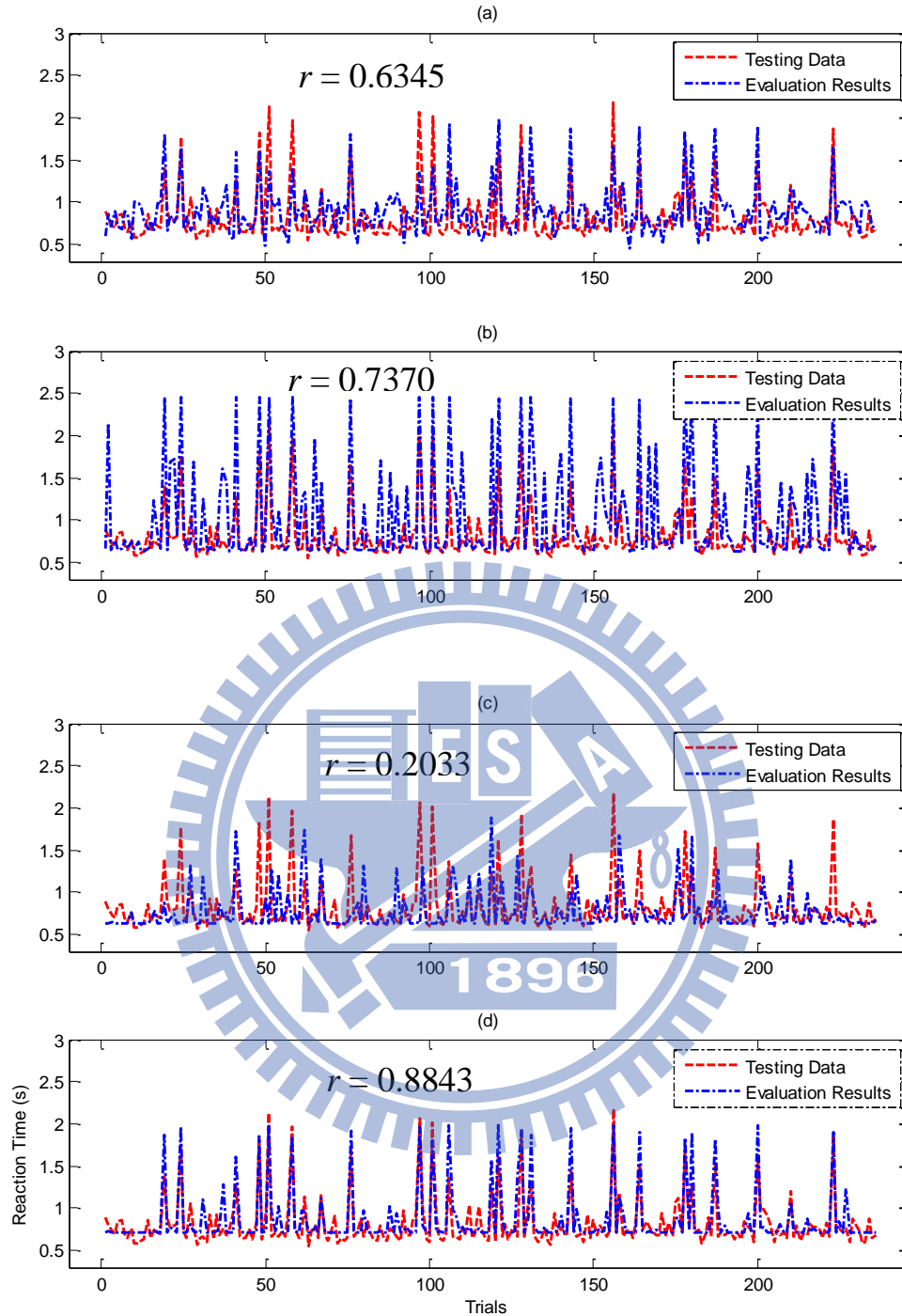
Figure 30.   Evaluation result examples of testing data for subject 5 with cross-subject drowsiness prediction infrastructure using (a) SVR ($r = 0.6345$), (b) MLPNN ($r = 0.7370$), (c) RBFNN ($r = 0.2033$) and (d) SONFIN ($r = 0.8843$). The red dashed line and blue dash-dot line present the golden testing data and estimated evaluation result respectively.
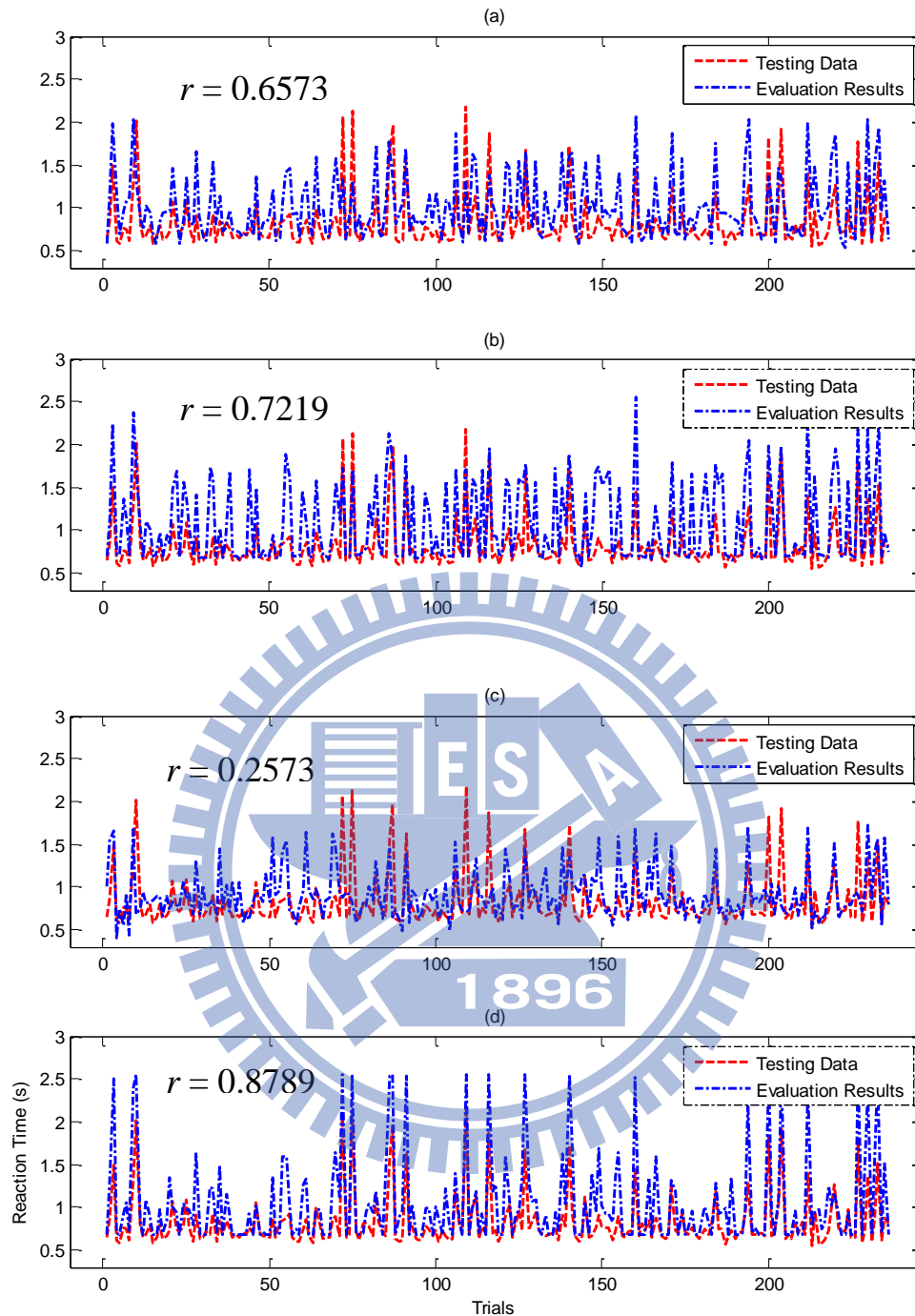
Figure 31.    Evaluation result examples of testing data for subject 6 with cross-subject drowsiness prediction infrastructure using (a) SVR ($r = 0.6573$), (b) MLPNN ($r = 0.7219$), (c) RBFNN ($r = 0.2573$) and (d) SONFIN ($r = 0.8789$). The red dashed line and blue dash-dot line present the golden testing data and estimated evaluation result respectively.

## 4.2.3. Derived Parameters for SONFIN

The constructed parameters, such as rules numbers, mean values and variances of membership functions (MF) and weights for the testing data evaluation examples taken in the previous section with the generalized cross-subject drowsiness prediction using SONFIN will be comprehensively described in this section.

The RT estimation rule numbers generated by SONFIN for the generalized cross-subject experimental testing evaluation samples of Subject 1-6 are 11, 11, 12, 10, 12 and 8, as listed in Table 13, respectively. The MFs for Subject1-6 were depicted in Figure 32-37, while the corresponded mean values ($m_{ij}$), variance ($\sigma^2_{ij}$) and weights ($w_i$) were summarized in Table 14-19 accordingly.

Table 13.    Rules Numbers For Sampled Testing Data Evaluation Subjects Derived by Cross-Subject Drowsiness Prediction with SONFIN

| Subject | 1 | 2 | 3 | 4 | 5 | 6 |
|---------|---|---|---|---|---|---|
| Rules | 8 | 9 | 8 | 10 | 10 | 14 |
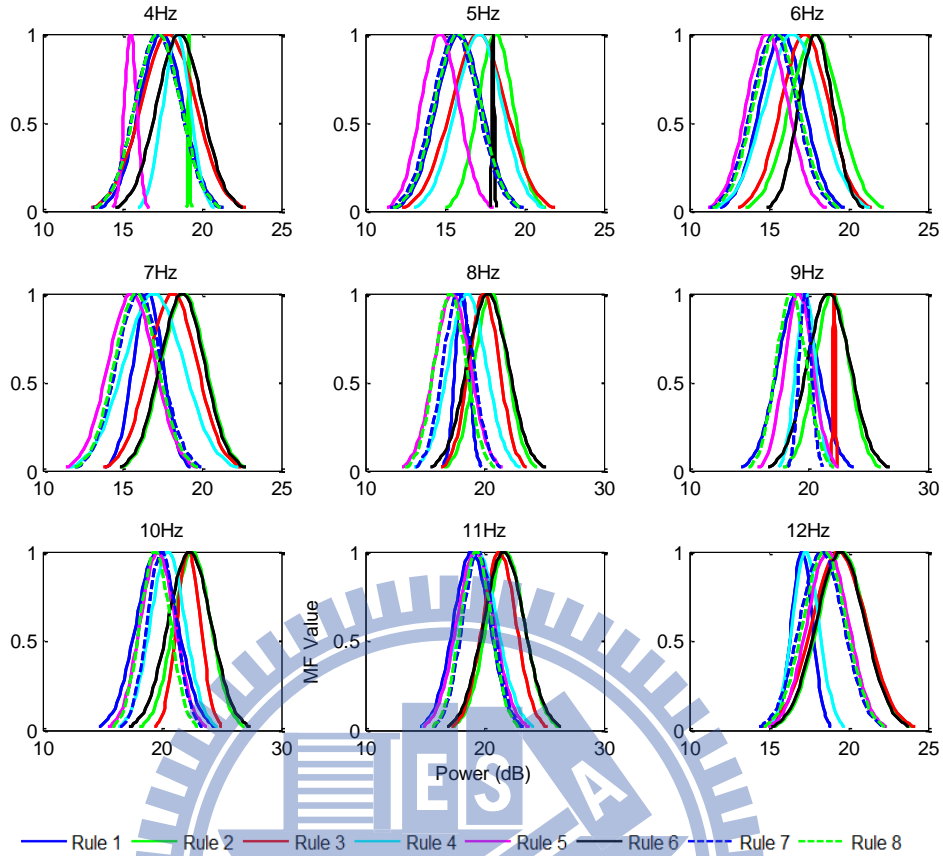
Figure 32.  Constructed Membership Functions for Sampled Subject 1 with Subject-Dependent Drowsiness Prediction using SONFIN

Table 14.  Constructed Mean Values, Variances and Weights for Sampled Subject 1 with Cross-Subject Drowsiness Prediction using SONFIN

| Rules | Mean and Variance($m_{ij}$, $\sigma^2_{ij}$) | | | | | | | | | Weight ($w_i$) |
|---|---|---|---|---|---|---|---|---|---|---|
| | 4Hz | 5Hz | 6Hz | 7Hz | 8Hz | 9Hz | 10Hz | 11Hz | 12Hz | |
| 1 | (17.47,1.94) | (15.90,2.00) | (15.83,1.96) | (16.63,1.34) | (18.11,0.82) | (19.07,2.37) | (19.59,2.47) | (18.92,2.17) | (17.08,0.93) | 1.14 |
| 2 | (19.20,0.08) | (18.19,1.58) | (17.88,2.19) | (18.87,1.97) | (20.54,1.94) | (21.96,2.03) | (22.54,2.20) | (21.77,2.24) | (19.60,2.17) | 2.89 |
| 3 | (17.90,2.42) | (17.13,2.41) | (17.26,2.12) | (18.19,2.16) | (19.97,1.79) | (22.14,0.14) | (22.24,1.42) | (21.25,2.00) | (19.41,2.41) | 1.98 |
| 4 | (18.42,1.21) | (17.15,2.06) | (16.49,2.46) | (16.99,2.66) | (18.55,2.24) | (19.74,1.15) | (20.49,2.08) | (19.42,2.37) | (17.34,1.20) | 1.78 |
| 5 | (15.53,0.55) | (14.70,1.68) | (14.90,1.86) | (15.59,2.07) | (17.28,2.12) | (19.16,1.69) | (19.65,2.06) | (19.25,2.23) | (18.70,1.86) | 0.85 |
| 6 | (18.60,2.02) | (18.04,0.10) | (17.94,1.52) | (18.78,1.98) | (20.28,2.42) | (21.68,2.54) | (22.32,2.55) | (21.62,2.41) | (19.51,2.18) | 2.19 |
| 7 | (17.23,2.01) | (15.66,2.04) | (15.32,2.00) | (16.05,2.00) | (17.79,1.80) | (19.71,0.74) | (19.98,1.73) | (19.46,1.88) | (18.32,1.97) | 0.87 |
| 8 | (17.26,2.01) | (15.82,2.02) | (15.47,2.01) | (15.89,1.95) | (17.14,1.88) | (18.54,1.79) | (19.43,1.80) | (19.29,1.84) | (18.51,1.93) | 0.66 |
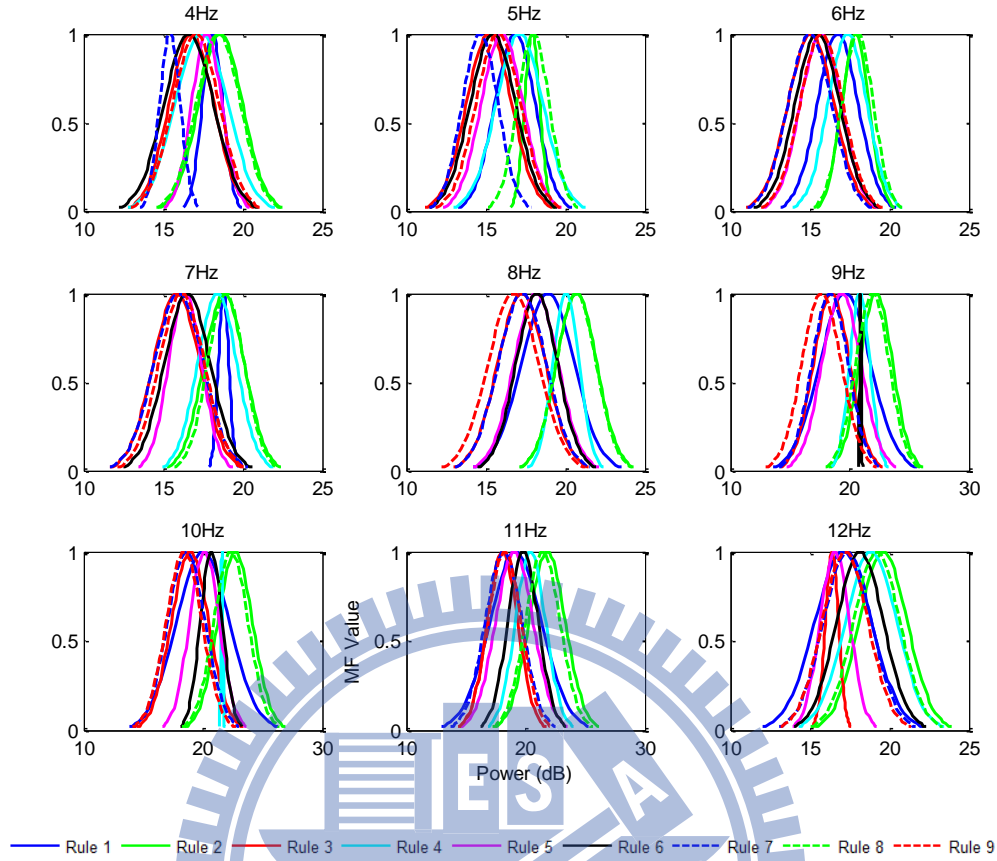
Figure 33.   Constructed Membership Functions for Sampled Subject 2 with Subject-Dependent Drowsiness Prediction using SONFIN

Table 15.   Constructed Mean Values, Variances and Weights for Sampled Subject 2 with Cross-Subject Drowsiness Prediction using SONFIN

| Rules | Mean and Variance($m_{ij}$, $\sigma^2_{ij}$) | | | | | | | | | Weight ($w_i$) |
|---|---|---|---|---|---|---|---|---|---|---|
| | 4Hz | 5Hz | 6Hz | 7Hz | 8Hz | 9Hz | 10Hz | 11Hz | 12Hz | |
| 1 | (18.10,0.92) | (16.84,1.78) | (16.75,1.81) | (18.81,0.48) | (18.90,2.33) | (19.63,3.03) | (20.02,3.12) | (19.17,3.09) | (17.09,2.51) | 1.82 |
| 2 | (18.61,1.95) | (17.92,0.69) | (17.86,1.22) | (18.84,1.81) | (20.72,1.80) | (22.22,1.96) | (22.70,2.09) | (21.81,2.18) | (19.61,2.15) | 2.72 |
| 3 | (16.78,1.99) | (15.21,2.02) | (15.07,2.04) | (15.85,2.09) | (17.26,2.12) | (18.49,2.16) | (18.92,2.22) | (18.08,1.82) | (16.38,0.60) | 1.22 |
| 4 | (17.40,2.32) | (17.12,2.08) | (17.37,1.74) | (18.41,1.75) | (20.04,1.20) | (20.85,1.21) | (21.60,0.12) | (20.41,1.80) | (18.84,2.30) | 1.46 |
| 5 | (17.75,1.35) | (16.02,1.86) | (15.68,1.82) | (16.38,1.49) | (18.15,1.97) | (19.33,2.32) | (20.12,1.78) | (19.06,2.25) | (16.57,1.32) | 1.41 |
| 6 | (16.61,2.20) | (15.45,2.02) | (15.47,1.99) | (16.52,2.04) | (18.21,1.85) | (20.90,0.09) | (20.71,1.31) | (19.80,1.81) | (18.15,2.09) | 1.05 |
| 7 | (15.43,0.93) | (14.64,1.60) | (15.00,1.96) | (15.98,2.18) | (17.30,2.14) | (18.36,2.15) | (18.61,2.23) | (18.16,2.19) | (17.36,2.15) | 0.86 |
| 8 | (18.48,1.96) | (17.99,1.43) | (18.00,1.40) | (18.95,1.64) | (20.68,1.76) | (21.92,1.98) | (22.36,2.03) | (21.44,2.08) | (19.20,2.07) | 1.45 |
| 9 | (17.06,2.06) | (15.79,1.99) | (15.73,1.92) | (16.16,2.01) | (16.74,2.27) | (17.65,2.33) | (18.43,2.14) | (18.27,1.96) | (17.22,2.05) | 0.58 |
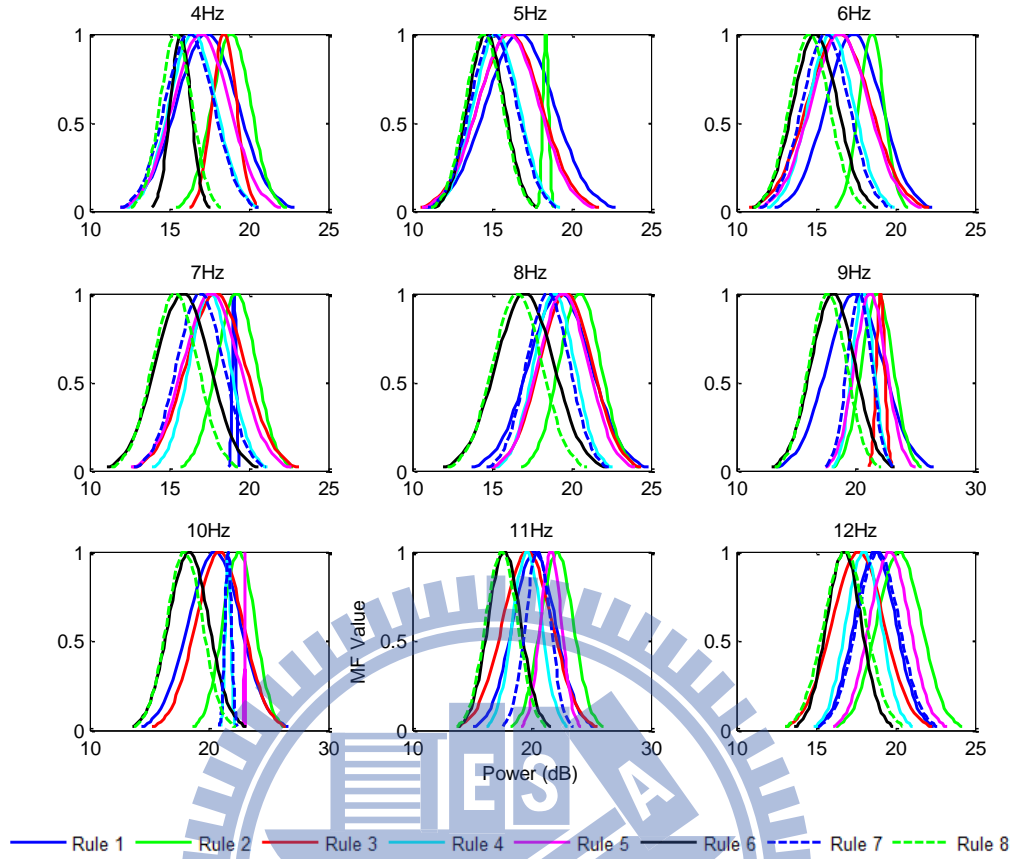
Figure 34. Constructed Membership Functions for Sampled Subject 3 with Subject-Dependent Drowsiness Prediction using SONFIN

Table 16. Constructed Mean Values, Variances and Weights for Sampled Subject 3 with Cross-Subject Drowsiness Prediction using SONFIN

| Rules | Mean and Variance($m_{ij}$, $\sigma^2_{ij}$) | | | | | | | | | Weight ($w_i$) |
|---|---|---|---|---|---|---|---|---|---|---|
| | 4Hz | 5Hz | 6Hz | 7Hz | 8Hz | 9Hz | 10Hz | 11Hz | 12Hz | |
| 1 | (17.38,2.74) | (16.76,3.03) | (17.38,2.48) | (19.09,0.17) | (19.28,2.78) | (19.95,3.31) | (20.48,3.09) | (20.22,2.53) | (18.72,1.86) | 2.07 |
| 2 | (18.90,1.73) | (18.39,0.26) | (18.50,1.15) | (19.21,1.77) | (20.54,1.86) | (21.82,1.87) | (22.52,1.92) | (22.14,1.94) | (20.24,2.00) | 2.04 |
| 3 | (18.46,1.09) | (16.14,2.82) | (16.45,2.82) | (17.93,2.60) | (19.68,2.34) | (22.09,0.49) | (20.88,2.80) | (19.64,2.93) | (17.67,2.32) | 1.45 |
| 4 | (16.48,2.09) | (15.29,2.02) | (15.96,2.02) | (17.54,1.81) | (18.92,1.83) | (20.62,1.29) | (21.60,0.32) | (19.62,1.72) | (18.00,1.56) | 1.21 |
| 5 | (17.01,2.52) | (16.06,2.72) | (16.50,2.57) | (17.64,2.50) | (19.48,2.24) | (21.23,1.89) | (22.97,0.11) | (21.64,1.26) | (19.63,1.79) | 1.57 |
| 6 | (15.72,0.91) | (14.65,1.64) | (14.96,1.99) | (15.86,2.38) | (17.09,2.57) | (18.10,2.58) | (18.31,2.39) | (17.72,1.94) | (16.77,1.55) | 0.95 |
| 7 | (16.27,2.17) | (15.11,2.05) | (15.62,2.07) | (16.95,2.07) | (18.54,1.91) | (20.32,1.45) | (21.62,0.38) | (20.53,1.49) | (18.90,1.89) | 0.99 |
| 8 | (15.43,1.42) | (14.51,1.66) | (14.61,1.78) | (15.38,2.01) | (16.61,2.19) | (17.66,2.22) | (17.96,2.12) | (17.50,1.90) | (16.83,1.88) | 0.46 |
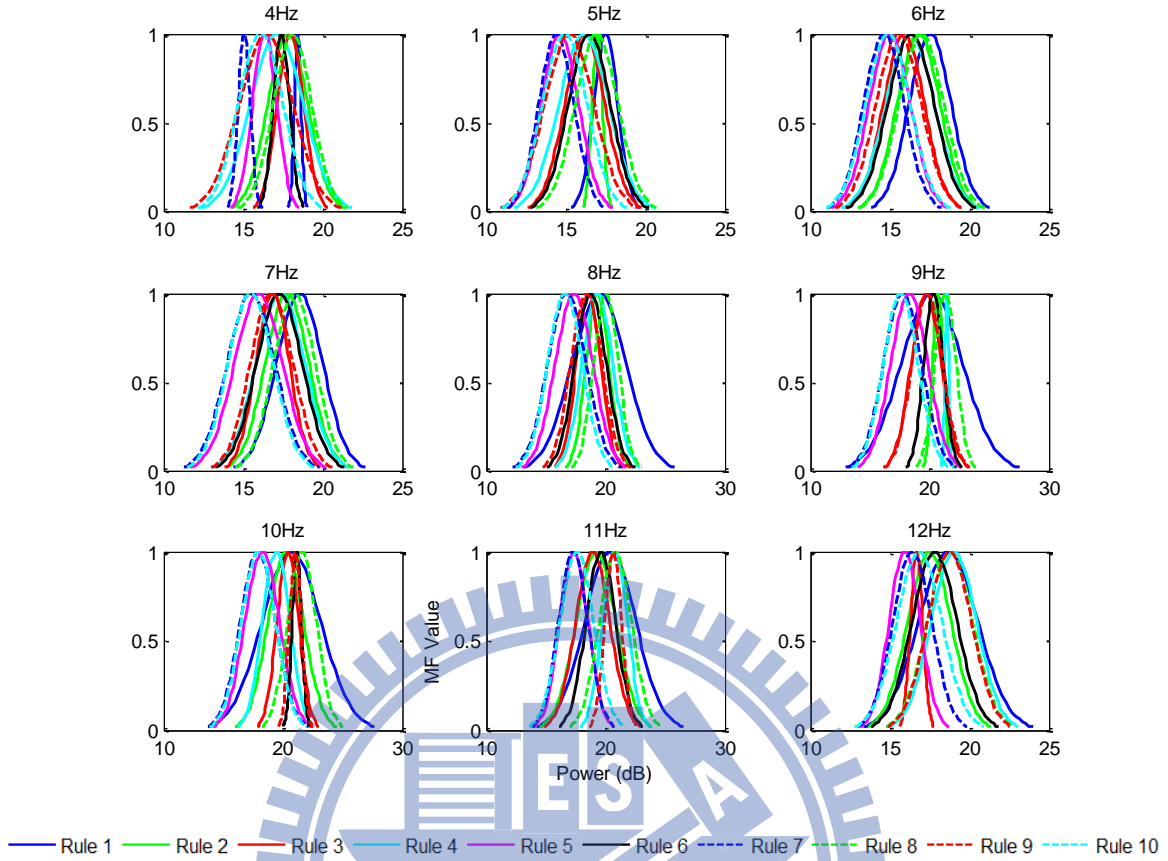
Figure 35. Constructed Membership Functions for Sampled Subject 4 with Subject-Dependent Drowsiness Prediction using SONFIN

Table 17. Constructed Mean Values, Variances and Weights for Sampled Subject 4 with Cross-Subject Drowsiness Prediction using SONFIN

| Rules | Mean and Variance($m_{ij}$, $\sigma^2_{ij}$) | | | | | | | | | Weight ($w_i$) |
|---|---|---|---|---|---|---|---|---|---|---|
| | 4Hz | 5Hz | 6Hz | 7Hz | 8Hz | 9Hz | 10Hz | 11Hz | 12Hz | |
| 1 | (18.42,0.30) | (17.52,1.07) | (17.53,1.87) | (18.55,2.06) | (19.46,3.18) | (20.20,3.65) | (20.71,3.51) | (20.39,3.06) | (18.67,2.65) | 2.72 |
| 2 | (17.79,1.77) | (16.98,0.46) | (16.81,1.91) | (17.76,1.93) | (19.33,1.36) | (20.69,0.64) | (20.24,2.12) | (19.20,2.35) | (17.48,1.95) | 1.95 |
| 3 | (17.96,1.19) | (16.20,1.79) | (15.88,1.81) | (16.85,1.50) | (18.58,1.45) | (19.72,1.78) | (20.43,1.30) | (18.93,2.04) | (16.68,0.55) | 1.13 |
| 4 | (17.13,2.36) | (16.14,2.21) | (16.27,2.16) | (17.35,2.17) | (19.33,1.81) | (21.44,0.22) | (19.44,1.61) | (20.79,1.48) | (19.03,2.04) | 1.33 |
| 5 | (16.35,1.08) | (14.64,1.65) | (14.99,1.84) | (15.97,2.14) | (17.36,2.22) | (18.29,2.20) | (18.27,2.07) | (17.35,1.68) | (15.93,1.39) | 1.09 |
| 6 | (17.40,0.73) | (16.48,1.86) | (16.33,2.05) | (17.28,2.03) | (18.75,1.85) | (20.33,1.16) | (21.16,0.56) | (19.61,1.76) | (17.81,2.01) | 1.58 |
| 7 | (15.06,0.54) | (14.41,1.55) | (14.63,1.80) | (15.50,2.12) | (16.77,2.28) | (17.73,2.26) | (17.90,2.10) | (17.28,1.75) | (16.40,1.74) | 0.64 |
| 8 | (18.11,1.71) | (16.94,1.90) | (16.99,1.99) | (18.22,1.86) | (20.04,1.46) | (21.33,1.26) | (21.61,1.71) | (20.83,1.92) | (18.79,2.02) | 1.39 |
| 9 | (16.44,2.39) | (15.23,2.17) | (15.56,2.01) | (16.80,1.90) | (18.40,1.85) | (19.79,1.80) | (21.05,0.72) | (20.65,0.99) | (18.76,1.96) | 0.79 |
| 10 | (16.10,1.98) | (14.94,1.97) | (14.88,1.97) | (15.47,2.02) | (16.60,2.06) | (17.57,2.06) | (17.95,2.04) | (17.60,2.02) | (16.84,2.03) | 0.64 |

Figure 36. Constructed Membership Functions for Sampled Subject 5 with Subject-Dependent Drowsiness Prediction using SONFIN

Table 18. Constructed Mean Values, Variances and Weights for Sampled Subject 5 with Cross-Subject Drowsiness Prediction using SONFIN

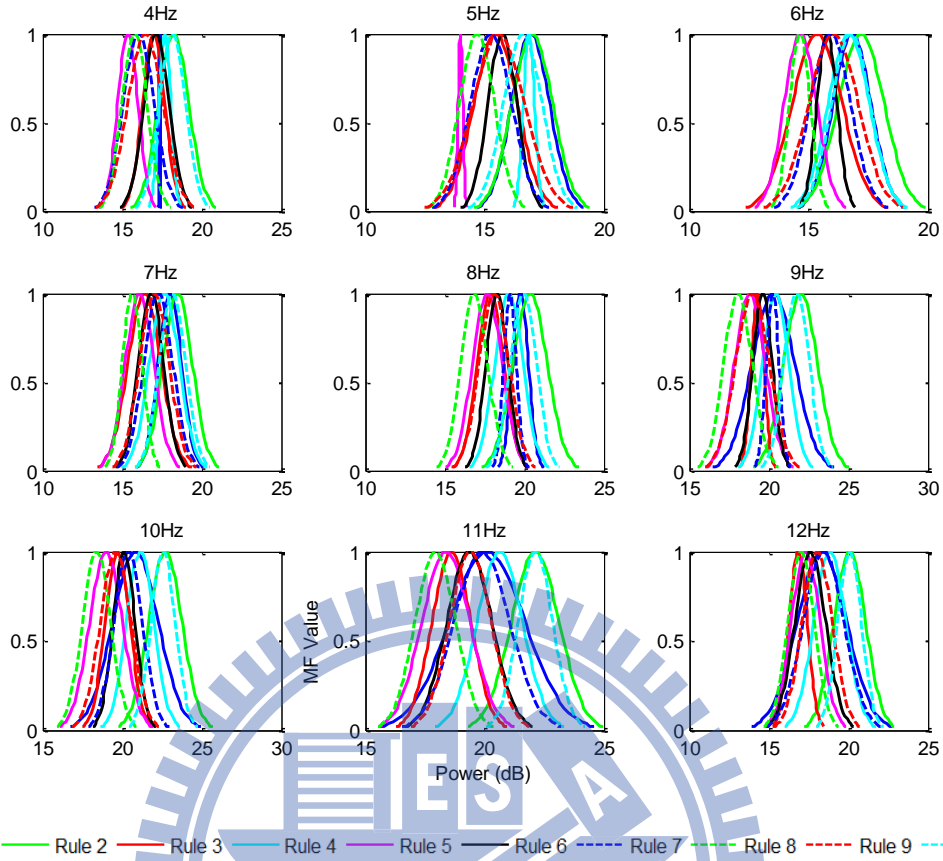| Rules | Mean and Variance($m_{ij}$, $\sigma^2_{ij}$) | | | | | | | | | Weight ($w_i$) |
|---|---|---|---|---|---|---|---|---|---|---|
| | 4Hz | 5Hz | 6Hz | 7Hz | 8Hz | 9Hz | 10Hz | 11Hz | 12Hz | |
| 1 | (17.36,0.05) | (16.93,1.12) | (16.82,1.13) | (18.00,1.04) | (19.76,0.71) | (20.28,1.89) | (20.84,2.03) | (20.11,2.25) | (18.33,2.21) | 1.90 |
| 2 | (18.24,1.35) | (17.00,1.21) | (17.20,1.36) | (18.47,1.32) | (20.37,1.53) | (22.00,1.51) | (22.71,1.48) | (22.13,1.42) | (20.08,1.42) | 2.70 |
| 3 | (16.98,1.00) | (15.47,1.30) | (15.36,1.48) | (16.41,1.47) | (17.86,1.19) | (19.29,0.56) | (19.71,1.09) | (18.61,1.16) | (16.85,0.81) | 1.06 |
| 4 | (17.69,0.53) | (16.86,0.34) | (16.68,1.23) | (17.65,1.33) | (19.03,1.26) | (20.46,1.18) | (21.14,1.23) | (20.64,1.35) | (18.83,1.44) | 1.60 |
| 5 | (15.36,0.90) | (13.99,0.14) | (14.66,0.97) | (16.09,1.27) | (17.68,1.32) | (18.80,1.37) | (18.99,1.46) | (18.38,1.43) | (17.32,1.28) | 0.74 |
| 6 | (17.15,1.14) | (15.75,0.86) | (15.77,0.60) | (16.82,1.12) | (18.27,0.98) | (19.60,0.87) | (20.12,0.98) | (19.36,1.34) | (17.60,1.37) | 1.41 |
| 7 | (16.04,1.38) | (15.28,1.23) | (15.92,1.20) | (17.28,1.29) | (19.11,0.56) | (20.24,0.57) | (20.39,1.27) | (19.89,1.66) | (18.44,1.82) | 0.89 |
| 8 | (15.79,1.13) | (14.68,1.04) | (14.63,0.62) | (15.63,0.88) | (16.88,1.18) | (18.06,1.27) | (18.39,1.26) | (17.94,1.21) | (17.03,1.16) | 0.71 |
| 9 | (16.45,1.57) | (15.59,1.56) | (16.04,1.47) | (17.02,1.33) | (18.10,1.32) | (18.97,1.50) | (19.59,1.37) | (19.41,1.24) | (18.04,1.35) | 0.72 |
| 10 | (18.12,1.18) | (16.61,1.14) | (16.77,1.15) | (18.17,1.16) | (19.93,1.16) | (21.74,1.13) | (22.58,1.08) | (22.14,1.03) | (20.08,1.06) | 0.40 |
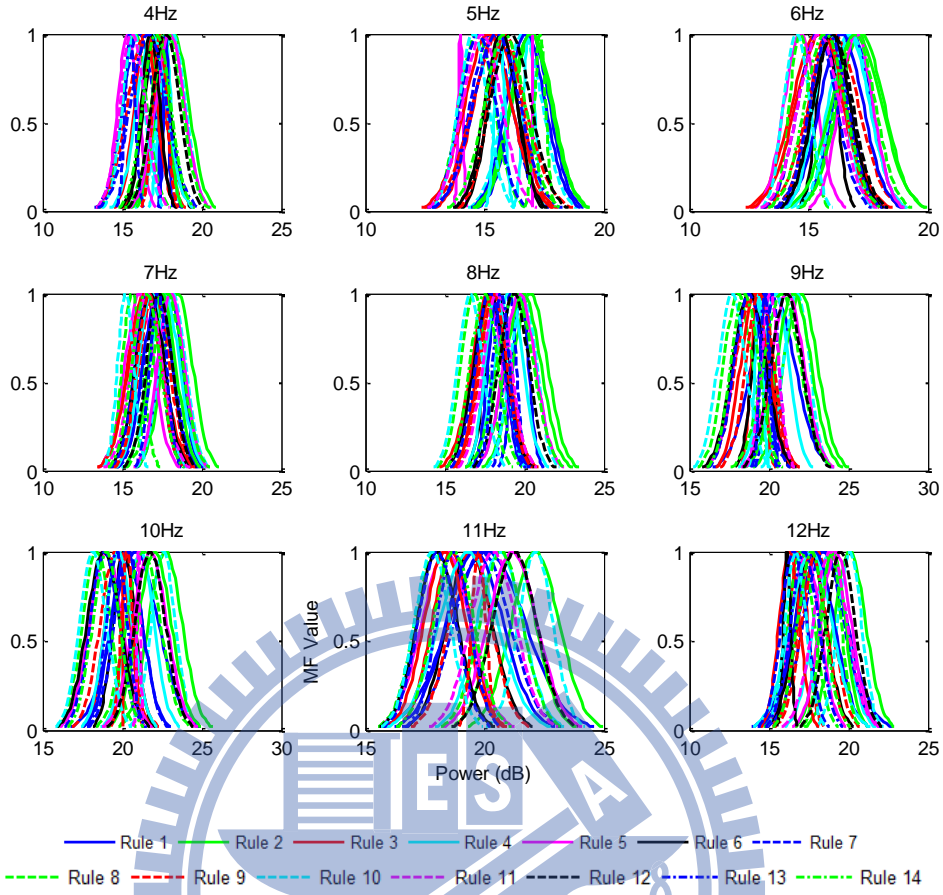
Figure 37. Constructed Membership Functions for Sampled Subject 6 with Subject-Dependent Drowsiness Prediction using SONFIN

Table 19. Constructed Mean Values, Variances and Weights for Sampled Subject 6 with Cross-Subject Drowsiness Prediction using SONFIN

| Rules | Mean and Variance($m_{ij}$, $\sigma^2_{ij}$) | | | | | | | | | Weight ($w_i$) |
|---|---|---|---|---|---|---|---|---|---|---|
| | 4Hz | 5Hz | 6Hz | 7Hz | 8Hz | 9Hz | 10Hz | 11Hz | 12Hz | |
| 1 | (17.75,0.22) | (16.74,1.16) | (16.38,1.28) | (17.23,1.29) | (18.29,0.80) | (19.78,0.47) | (20.28,1.38) | (19.59,1.68) | (17.86,1.74) | 1.72 |
| 2 | (17.36,0.74) | (16.93,1.22) | (17.00,1.49) | (17.51,1.22) | (19.92,1.56) | (21.56,1.55) | (22.03,1.47) | (21.22,1.30) | (18.99,1.15) | 2.54 |
| 3 | (16.48,1.00) | (15.15,1.38) | (15.52,1.49) | (16.52,1.53) | (17.79,1.55) | (19.11,1.25) | (20.06,0.10) | (18.35,1.25) | (16.30,0.91) | 1.10 |
| 4 | (16.86,1.31) | (15.64,0.30) | (15.89,0.94) | (16.85,1.14) | (18.22,0.97) | (19.37,0.33) | (19.79,1.21) | (19.31,1.72) | (17.65,1.84) | 1.37 |
| 5 | (18.00,1.28) | (17.03,0.12) | (17.00,1.00) | (18.05,1.19) | (19.70,1.40) | (21.16,1.48) | (21.75,1.49) | (21.17,1.46) | (19.21,1.36) | 1.76 |
| 6 | (16.79,0.80) | (15.69,0.97) | (15.96,1.09) | (16.74,1.29) | (17.82,1.39) | (18.75,1.47) | (18.83,1.47) | (18.01,1.20) | (16.14,0.32) | 1.01 |
| 7 | (15.50,0.44) | (14.73,1.05) | (15.37,1.15) | (16.62,1.16) | (17.84,1.27) | (18.75,1.31) | (18.90,1.28) | (18.02,1.13) | (16.57,1.14) | 0.92 |
| 8 | (17.84,1.33) | (17.33,0.33) | (16.97,1.18) | (17.86,1.32) | (19.44,1.59) | (20.82,1.61) | (21.33,1.51) | (20.70,1.27) | (18.91,0.91) | 1.65 |
| 9 | (17.37,0.60) | (15.87,1.00) | (15.78,1.08) | (16.70,1.09) | (18.09,1.20) | (19.42,1.24) | (20.31,0.52) | (19.76,0.43) | (17.70,1.24) | 1.17 |
| 10 | (15.71,0.99) | (14.53,0.88) | (14.50,0.76) | (15.22,0.70) | (16.60,1.15) | (17.68,1.24) | (18.19,1.20) | (17.80,1.07) | (16.69,0.93) | 0.68 |
| 11 | (15.65,1.17) | (14.91,1.16) | (15.44,1.23) | (16.56,1.35) | (18.28,1.25) | (20.07,0.78) | (21.03,0.15) | (20.37,1.34) | (18.86,1.52) | 0.76 |
| 12 | (17.73,1.20) | (16.09,1.22) | (16.01,1.17) | (17.34,1.16) | (19.35,1.32) | (21.11,1.39) | (21.76,1.36) | (21.26,1.31) | (19.52,1.29) | 0.91 |
| 13 | (16.66,1.61) | (15.51,1.37) | (15.84,1.12) | (17.27,0.73) | (18.54,0.75) | (19.73,0.40) | (19.66,0.93) | (18.69,1.00) | (17.24,1.23) | 0.85 |
| 14 | (17.17,1.20) | (15.84,1.20) | (15.69,1.20) | (16.51,1.20) | (17.47,1.21) | (18.48,1.21) | (18.98,1.20) | (18.71,1.21) | (17.67,1.23) | 0.67 |

56

### 4.2.4. Section Discussion

Compared to the subject-dependent drowsiness results, the averaged PPMCC between the actual and estimated RTs on testing data with these four predictors maintained sound results.

However, the PPMCC obtained by the generalized cross-subject drowsiness prediction showed a significant performance decline on the test data ($p$-value < 0.038). Only SONFIN still maintained a better PPMCC between actual and estimated RTs at 78.3% than other predictors. Furthermore, the SONFIN produced the lowest RMSE (0.36 s) on the testing data in this experiment. According to safety distance between vehicles reported by CEDR [61] and RSA [62], a rule thumb of 2-s braking distance under dry ground conditions with additional reaction distance of 18.3 m at a 100 km/hr car speed is recommended. The RMSE of proposed cross-subject drowsiness predictor with SONFIN is 0.36 s or 10 m at a 100 km/hr car speed in average, which does not violate the recommended reaction distance requirement of 18.3 m. Therefore, the proposed cross-subject drowsy state predictor with SONFIN showed a promising model for real-life applications.

## 4.3. Discussion

### 4.3.1. Power Distribution Analysis

The relationship between EEG patterns and EEG drowsiness usually varies rapidly and is quite different between individuals. Most machine learning algorithms are designed for doing pattern recognition in identical distributed data, and have less capability for EEG drowsiness level, i.e., RTs, estimation with EEG signals from other individuals. The major concern here is if these six subjects have similar power distribution to make SONFIN can work better than other cross-subject predictors. Firstly, investigations on subject-dependent perdition shows that the performance for all predictors in this study are almost

same high (r > 95%), and the reason is the EEG power distribution is similar within same subject. Hence, if these six subjects have similar EEG power distributions, the performances shall be also high for cross-subject predictors when using MLPNN, RBFNN and SVR. Unfortunately, the results shows only SONFIN can still present a higher performance (r > 78%). Secondary, the power distribution analysis of these six subjects were analyzed and it error bar plot, mean value and standard variance has been depicted and summarized in Figure 38 and Table 20, respectively. Results show that these six subjects have different power distributions and the concern of similar power distributions among these subjects here can be omitted in this study.
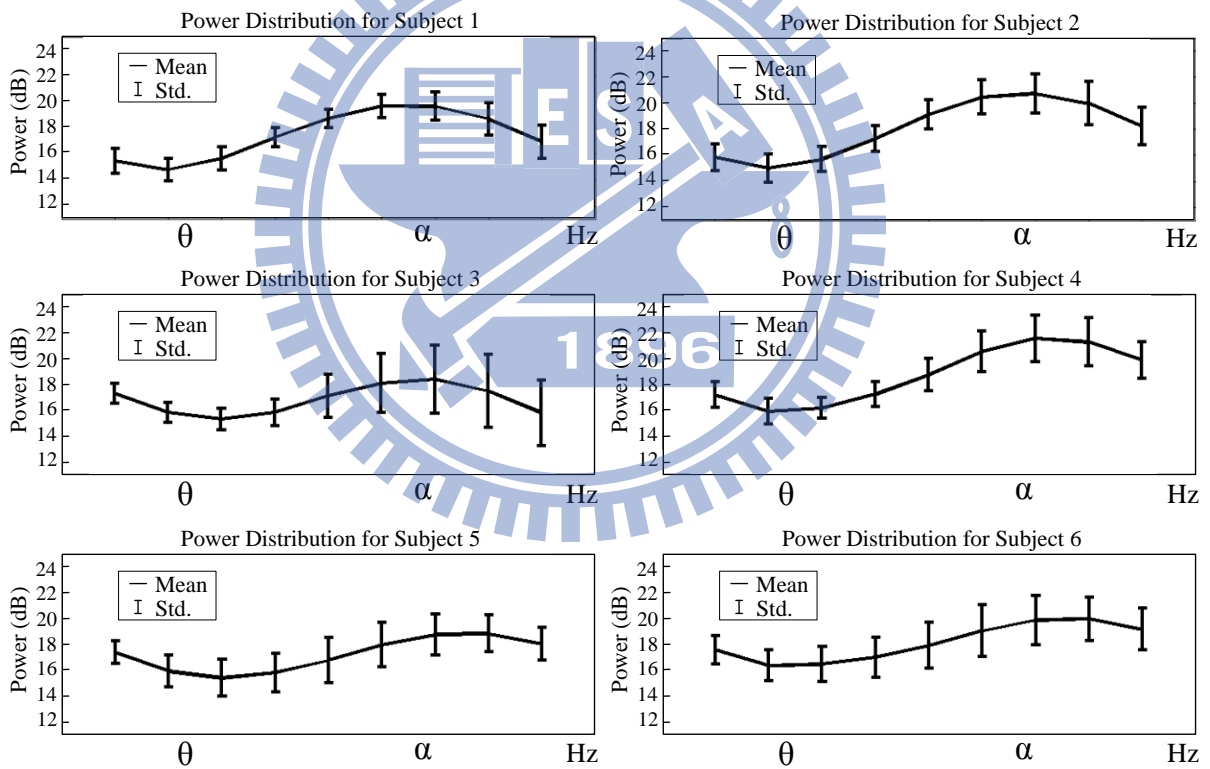


Figure 38.    Power Distribution Analysis for Six Subjects Used in this Study.

Table 20.    Power Mean Value and Variance of Subjects Used in This Study

| Subject | Mean and Variance($m_{ij}, \sigma^2_{ij}$) | | | | | | | | |
|---|---|---|---|---|---|---|---|---|---|
| | 4Hz | 5Hz | 6Hz | 7Hz | 8Hz | 9Hz | 10Hz | 11Hz | 12Hz |
| 1 | (15.45,0.89) | (14.78,0.74) | (15.64,0.76) | (17.27,0.55) | (18.71,0.47) | (19.68,0.79) | (19.65,1.19) | (18.68,1.56) | (16.91,1.64) |
| 2 | (15.83,1.04) | (15.00,1.20) | (15.68,0.94) | (17.27,1.03) | (19.09,1.24) | (20.45,1.72) | (20.72,2.24) | (19.98,2.68) | (18.23,2.13) |
| 3 | (17.34,0.62) | (15.85,0.56) | (15.34,0.66) | (15.87,1.04) | (17.14,2.75) | (18.12,5.12) | (18.42,6.95) | (17.52,7.84) | (15.83,6.51) |
| 4 | (17.22,0.96) | (15.94,1.04) | (16.17,0.64) | (17.25,0.95) | (18.76,1.60) | (20.55,2.46) | (21.59,3.23) | (21.29,3.44) | (19.90,1.95) |
| 5 | (17.43,0.73) | (16.02,1.42) | (15.50,1.93) | (15.90,2.09) | (16.84,2.94) | (18.01,2.87) | (18.81,2.47) | (18.88,1.98) | (18.09,1.52) |
| 6 | (17.61,1.13) | (16.41,1.42) | (16.53,1.74) | (17.05,2.39) | (17.97,3.15) | (19.08,3.89) | (19.91,3.58) | (19.98,2.85) | (19.21,2.51) |

## 4.3.2. Strength Analysis for Generalized Cross-Subject Drowsiness Prediction with SONFIN

The reason for this drastic performance drop in generalized cross-subject drowsiness prediction using SVR, MLPNN, and RBFNN is that EEG data characteristics between distinct subjects usually vary widely. A model constructed by training data from individuals might not be generalized to others. Therefore, it is difficult to predict subject's behavior with others subjects' EEG without more adaptive features like SONFIN can provide. The SVR, MLPNN, and RBFNN provide a good system performance for subject-dependent drowsiness prediction due to the small power variation within the same subject. However, MLPNN, RBFNN and SVR have fixed structure and they have less capability to provide a good system performance for generalized cross-subject drowsiness prediction because EEG power deviation among different subjects are not as similar as same subject may have.

Figure 39-44 demonstrate the RT estimation rules for Subject 1-6 that were automatically generated by generalized cross-subject drowsiness prediction with SONFIN, respectively. The RT estimation rules generated here for Subject 1-6 are 8, 9, 8, 10, 10 and 14 respectively. The red dash line in each RT estimation rules plot is the mean of these rules. Denote the rules triggered over this mean line are Low Performance (LP) rules, while the rules triggered below LP are denoted as High Performance (HP) rules. Two test samples with '□' (LP state)

and '◇' (HP state) sign were fed into this model, and the rules triggered here are mostly by LP rules and HP rules, respectively.

This is the evidence engaging with the previous studies to use $\theta$-band and $\alpha$-band for indexing the arousal state, and furthermore the derived fuzzy rules perform in the same manner with the trend of spectral powers. Experimental results show that adopting a fuzzy algorithm in a neural network can produce a more robust model for estimating task performance of subjects not seen in the training data because of adoptive features that SONFIN can have.

Figure 39.    Testing Data Evaluation Example for Subject 1 with Generalized Cross-Subject Drowsiness Prediction Using RT Estimation Rules Generated by SONFIN.



Figure 40.    Testing Data Evaluation Example for Subject 2 with Generalized Cross-Subject Drowsiness Prediction Using RT Estimation Rules Generated by SONFIN.
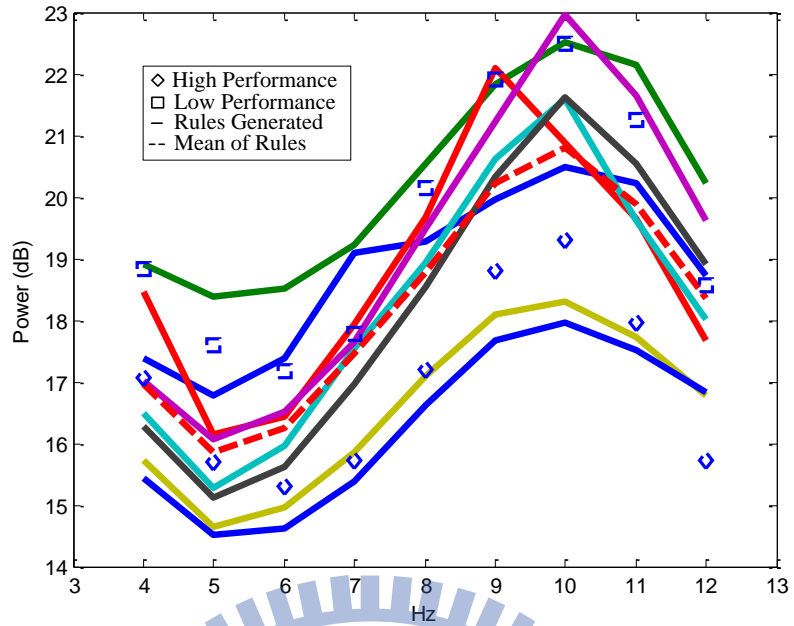
Figure 41.　Testing Data Evaluation Example for Subject 3 with Generalized Cross-Subject Drowsiness Prediction Using RT Estimation Rules Generated by SONFIN.



Figure 42.　Testing Data Evaluation Example for Subject 4 with Generalized Cross-Subject Drowsiness Prediction Using RT Estimation Rules Generated by SONFIN.

Figure 43.  Testing Data Evaluation Example for Subject 5 with Generalized Cross-Subject Drowsiness Prediction Using RT Estimation Rules Generated by SONFIN.



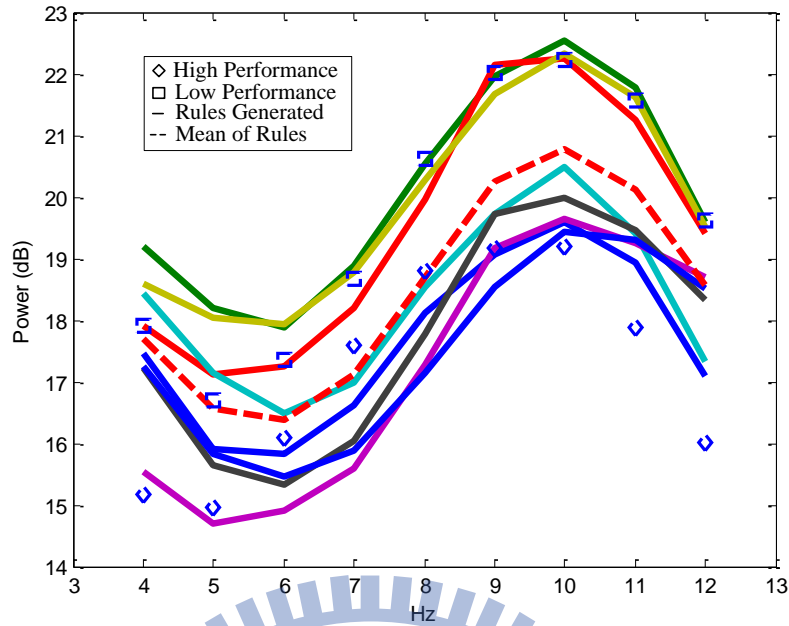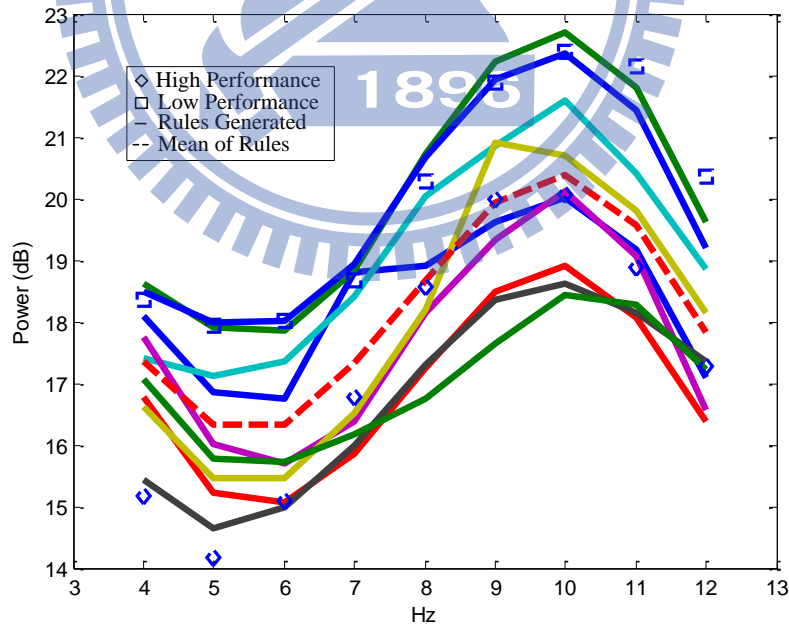Figure 44.  Testing Data Evaluation Example for Subject 6 with Generalized Cross-Subject Drowsiness Prediction Using RT Estimation Rules Generated by SONFIN.

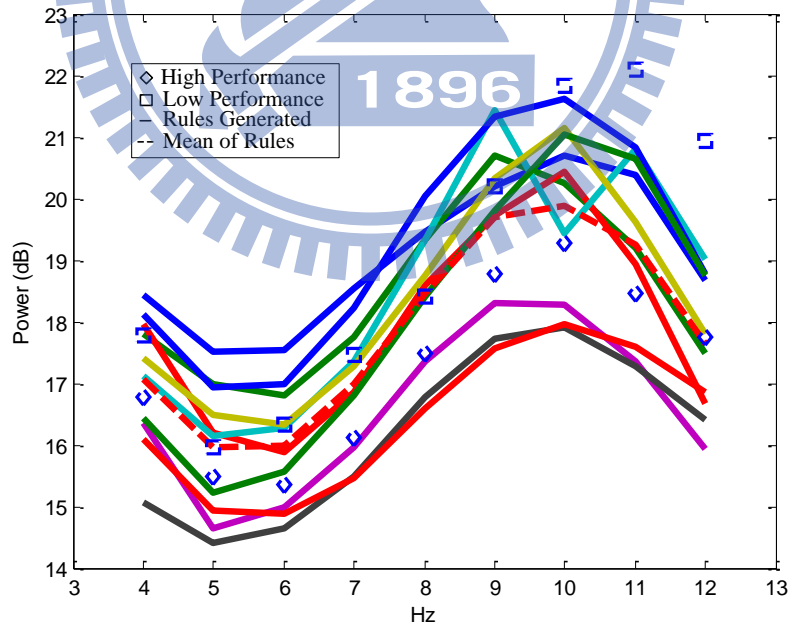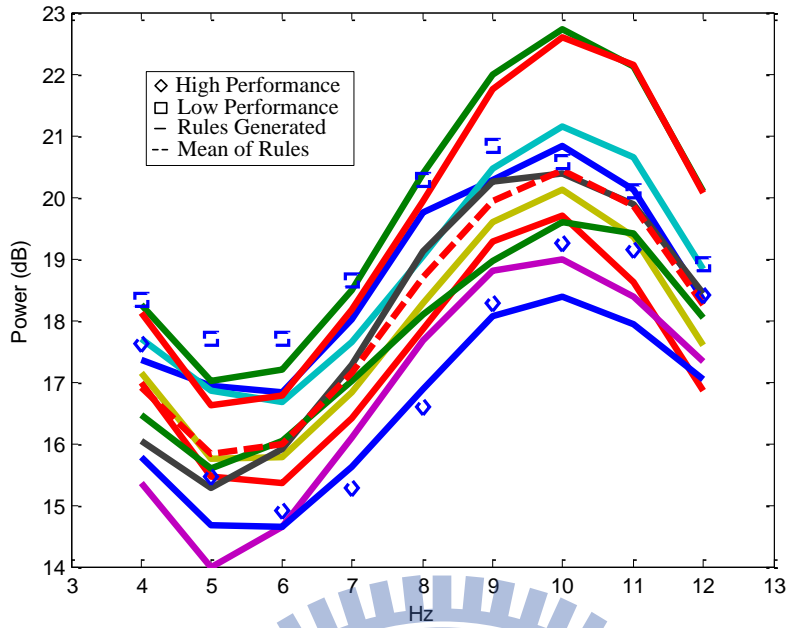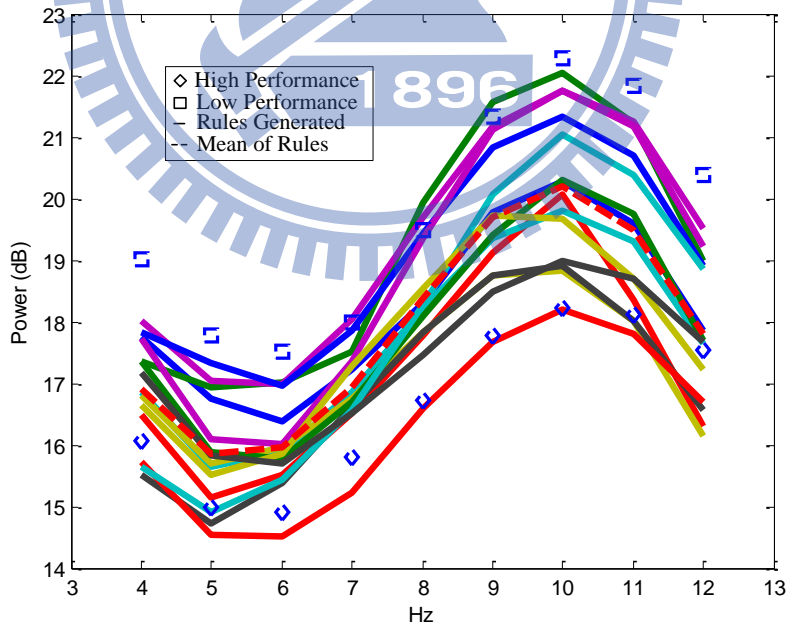# V  Conclusions

The amplitude of an EEG signal fluctuates on the microvolt level, making the EEG signal extremely noise-sensitive and easily influenced by artifacts. In addition, the EEG features between different subjects usually vary widely, making it difficult to apply and generalize results from one individual to another. The proposed EEG signal-processing procedures and SONFIN method in this study overcome these two limitations. Signal-processing methods based on ICA and time-frequency analysis successfully excludes the EEG contaminations and extracts the EEG features related to task performance. For each experiment, 1-s EEG before deviation onset whose $\theta$- and $\alpha$-band power spectra of the activations of the occipital component, along with RTs of trials, were used to build an RT prediction model. This study tests four predictors, SVR, MLPNN, RBFNN, and SONFIN, for drowsiness prediction. Experimental results of this study showed that it is feasible to estimate subject's reaction times based on 1-s EEG power spectra before the onsets of lane-departure events.

In addition, the main contribution of this study is to propose an implementable cross-subject predictor practically to build a common model that can be also applied on another user who does not need to acquire the EEG signals first and can keep maintaining his/her driving performance. Hence, we applied two kinds of validation ways to verify the system performance. One is subject-dependent validation and the other is cross-subject evaluation. In subject-dependant validation, we majorly test the performance of the proposed framework that acquired EEG signals fed into the applied four predictors are feasible to work. Experimental results showed that the prediction performance of each applied predictor is high and stable in each subject-dependent session. Then we would like to propose a generalized system that can predict the moment driver based on other subjects' EEG signals. Hence, we applied leave one subject out cross validation way to evaluate the prediction performance in

the cross-subject session. Experimental results showed that the proposed neural fuzzy system can get the better prediction performance than others. It means that the proposed system of this study not only can overcome the individual difference problem occurred by collecting EEG signals from different subjects, but also we can apply the system in the real-world applications.

A comparison between subject-dependent and cross-subject prediction models showed that the subject's RTs could be better estimated by an individualized RT prediction model. Furthermore, SONFIN outperformed SVR, MLPNN, and RBFNN in terms of PPMCC and RMSE especially for the cross-subject case. This demonstration might lead to a practical system for noninvasive predicting and monitoring subject responses to critical events in real-world applications. However, some notifications and limitations shall be highlighted here before applying proposed system to a practical environment. The proposed SONFIN system shall be applied only to the environments that are not dangerous even if an operation error occurs. It can be implemented just as a passive and assistive alert system to warn the driver if he/she is becoming excessively drowsy and could fall asleep while driving.

# Reference

[1] US National Sleep Foundation, "1.9 Million Drivers Have Fatigue-Related Car Crashes or Near Misses Each Year," Nov., 2009. http://www.sleepfoundation.org/article/press-release/19-million-drivers-have-fatigue-related-car-crashes-or-near-misses-each-year.

[2] K. Kozak, J. Pohl, W. Birk, J. Greenberg, B. Artz, M. Blommer, L. Cathey, and R. Curry, "Evaluation of Lane Departure Warnings for Drowsy Drivers," in Proc. *Human Factors and Ergonomics Society 50th Annual Meeting, San Francisco*, California, USA, 16-20 Oct. 2006, pp. 2400-2404.

[3] M. Rimini-Doering, T. Altmueller, and U. Ladstaetter, "Effects of Lane Departure Warning on Drowsy Drivers' Performance and State in a Simulator," in Proc. *3rd International Driving Symposium on Human Factors in Driver Assessment*, Training and Vehicle Design, Rockport, Maine, USA, 27-30 June 2005, pp. 88-95.

[4] J. C. Popieul, P. Simon, and P. Loslever, "Using Driver's Head Movements Evolution as a Drowsiness Indicator," in Proc *IEEE Intelligent Vehicles Symposium*, 2003, pp. 616-621.

[5] Q. Ji, Z. Zhu, and P. Lan, "Real-Time Nonintrusive Monitoring and Prediction of Driver Fatigue," *IEEE Transactions on Vehicular Technology*, vol. 53, no. 4, pp. 1052-068, July 2004.

[6] D. K. McGregor and J. A. Stern, "Time on Task and Blink Effects on Saccade Duration," *Ergonomics*, vol. 39, no. 4, pp. 649-660, Mar. 1996.

[7] F. Zhang, A. Mishra, A.G. Richardson, and B. Otis, "A Low-Power ECoG/EEG Processing IC With Integrated Multiband Energy Extractor," *IEEE Transactions on Circuits and Systems I*, vol. 58, no. 9, pp. 2069-2082, Sep. 2011.

[8] J. Beatty, A. Greenberg, W. P. Deibler, and J. F. O'hanlon, "Operant

Control of Occipital Theta Rhythm Affects Performance in a Radar Monitoring Task," *Science*, vol. 183, no. 4127, pp. 871-873, Mar. 1974.

[9] R. S. Huang, T. P. Jung, A. Delorme, and S. Makeig, "Tonic and Phasic Electroencephalographic Dynamics During Continuous Compensatory Tracking," *NeuroImage*, vol. 39, no. 4, pp. 1896-1909, Feb. 2008.

[10] R. S. Huang, T. P. Jung, and S. Makeig, "Tonic changes in EEG power spectra during simulated driving," *Lecture Notes in Computer Science*, vol. 5638 LNAI, pp. 394-403, Dec. 2009.

[11] C. T. Lin, R. C. Wu, S. F. Liang, W. H. Chao, Y. J. Chen, and T. P. Jung, "EEG-Based Drowsiness Estimation for Safety Driving Using Independent Component Analysis," *IEEE Transactions on Circuits and Systems I*, vol. 52, no. 12, pp. 2726-2738, 12 Dec. 2005.

[12] W. Klimesch, "EEG alpha and theta oscillations reflect cognitive and memory performance: a review and analysis," *Brain Research Reviews*, vol. 29, no. 2-3, pp. 169-195, 1999.

[13] S. Makeig and T.-P. Jung, "Tonic, phasic, and transient EEG correlates auditory awareness in drowsiness," *Cognitive Brain Research*, vol. 4, no. 1, pp. 15-25, 1996.

[14] M. A. Schier, "Changes in EEG alpha power during simulated driving: a demonstration," *International Journal of Psychophysiology*, vol. 37, no. 2, pp. 155-162, 2000.

[15] C. T. Lin, Y. C. Chen, T. Y. Huang, T. T. Chiu, L. W. Ko, S. F. Liang. H. Y. Hsieh, S. H. Hsu, and J. R. Duann, "Development of Wireless Brain Computer Interface with Embedded Multitask Scheduling and its Application on Real-Time Driver's drowsiness Detection and Warning," *IEEE Transactions on Biomedical Engineering*, vol. 55, no. 5, pp. 1582-1591, May 2008.

[16] C. T. Lin, L. W. Ko, J. C. Chiou, J. R. Duann, R. S. Huang, S. F. Liang. T.

W. Chiu, and T. P. Jung, "Noninvasive Neural Prostheses Using Mobile and Wireless EEG," *Proceedings of the IEEE*, vol. 96, no. 7, pp. 1167-1183, July 2008.

[17] C. T. Lin, L. W. Ko, I. F. Chung, T. Y. Huang, Y. C. Chen, T. P. Jung, and S. F. Liang, "Adaptive EEG-based alertness estimation system by using ICA-based Fuzzy Neural networks," *IEEE Transactions on Circuits and Systems I*: Regular Papers, vol. 53, no. 11, pp. 2469-2476, Nov. 2006.

[18] C.T. Lin, R.C. Wu, T.-P. Jung, S.-F. Liang, and T.Y. Huang, "Estimating driving performance based on EEG spectrum analysis," *EURASIP Journal on Applied Signal Processing*, vol. 2005, no. 19, pp. 3165-3174, 2005.

[19] F. C. Lin, L. W. Ko, S. A. Chen, C. F. Chen, and C. T. Lin, "EEG-based Cognitive State Monitoring and Prediction by Using the Self-Constructing Neural Fuzzy System," *in Proc. 2010 IEEE International Symposium on Circuits and* Systems (ISCAS 2010), Paris, France, 2010.

[20] A. Subasi, "Automatic recognition of alertness level from EEG by using neural network and wavelet coefficients," *Expert Systems with Applications*, vol. 28, no. 4, pp. 701-711, May 2005.

[21] M. K. Kiymik, M. Akin and A. Subasi, "Automatic recognition of alertness level by using wavelet transform and artificial neural network," *Journal of Neuroscience Methods*, vol. 139, no. 2, pp. 231-240, Oct. 2004.

[22] A. Vuckovic, V. Radivojevic, A. C.N. Chen, D. Popovic, "Automatic recognition of alertness and drowsiness from EEG by an artificial neural network," *Medical eng. & Physics*, vol. 24, no. 5, pp. 349-360, Jun. 2002.

[23] D. Stewart, "A platform with six degrees of freedom", *Proceedings of the Institution of Mechanical Engineers*, vol. 180, Part 1, no. 5, pp. 371-386,1965-1966.

[24] K. Liu, J. M. Fitzgerald and F. L. Lewis, "Kinematic analysis of a Stewart platform manipulator," *IEEE Trans. Industrial Electronics*, vol. 40, no. 2,

pp. 282-293, 1993.

[25] C. T. Lin, J. Y. Lin and Y. C. Lin, "A neural fuzzy inference network for the motion analyses of Stewart platform," *International Journal of Fuzzy Systems*, vol. 4, no.2, pp.704-714, 2002.

[26] H. Ueno, M. Kaneda, and M. Tsukino, "Development of drowsiness detection system," *in Proc. Veh. Navigation Inf. Syst. Conf.*, Aug. 1994, pp. 15-20.

[27] Cardoso J. F. and Souloumiac A., "Blind beamforming for non Gaussian signals," *IEE Proceedings F in Radar and Signal Processing*, vol. 140, no. 6, pp. 362-370, Dec. 1993.

[28] Fu-Chang Lin, Li-Wei Ko, Chun-Hsiang Chuang, Tung-Ping Su and Chin-Teng Lin, "Generalized EEG-based Drowsiness Prediction System by Using a Self-Organizing Neural Fuzzy System", *IEEE Transactions on Circuits and Systems I* (Accepted, 17th Dec. 2011).

[29] Chin-Teng Lin, Fu-Chang Lin, Shi-An Chen, Shao-Wei Lu, Te-Chi Chen, Li-Wei Ko, "EEG-based Brain-computer Interface for Smart Living Environmental Auto-adjustment", *Journal of Medical and Biological Engineering*, vol. 30, no. 4, pp.237-245, June 2010.

[30] Shi-An Chen, Fu-Chang Lin, Tzu-Kuei Shen, Li-Wei Ko, Tzyy-Ping Jung, Chin-Teng Lin, "An EEG-based Self-Constructed Neural Fuzzy System to Estimate Driver's Cognitive State", *Australian Journal of Intelligent Information Processing Systems*: *Computational Neuroscience and Brain Computer Interface*, vol. 11, no. 3, 2010

[31] C. W. Chang, L. W. Ko, F. C. Lin, T. P. Su, T. P. Jung, C. T. Lin, and J. C. Chiou, "Drowsiness Monitoring with EEG-Based MEMS Biosensing Technologies," GeroPsych: *The Journal of Gerontopsychology and Geriatric Psychiatry*, vol. 23, no. 2, pp. 107-113, June 2010.

[32] Reymond G. and Kemeny A. "Motion cueing in the Renault driving

simulator," *Vehicle System Dynamics*, vol. 34, pp. 249-259, 2000.

[33] Reymond G., Kemeny A., Droulez J., and Berthoz A., "Role of lateral acceleration in curve driving: driver model and experiments on a real vehicle and a driving simulator," *Human Factors*, vol. 43, pp. 483-495, 2001.

[34] R. -S. Huang, T. -P. Jung, J. -R. Duann, S. Makeig and M. I. Sereno, "Imaging Brain Dynamics During Continuous Driving Using Independent Component Analysis," *35th Annual Meeting of the Society for Neuroscience*, Abstract, Washington D. C., the USA, 12-16 Nov. 2005

[35] R. -S. Huang, T. -P. Jung, and S. Makeig, "Multi-scale EEG Brain Dynamics during Sustained Attention Tasks," *IEEE International Conference on Acoustics*, Speech, and Signal Processing (ICASSP), pp. IV-1173-IV-1176, Honolulu, Hawaii, USA, 4 June 2007

[36] A. Delorme and S. Makeig, "EEGLAB: an open source toolbox for analysis of single-trial EEG dynamics including Independent Component Analysis," *Journal of Neuroscience Methods*, vol. 134, no. 1, pp. 9-12, Mar. 2004.

[37] T. W. Lee, Independent Component Analysis: Theory and Applications, Kluwer Academic Publishers, 1998.

[38] S. Javidi , D.P. Mandic, A. Cichocki, "Complex Blind Source Extraction From Noisy Mixtures Using Second-Order Statistics," *IEEE Transactions on Circuits and Systems I*, vol. 57, no. 7, pp. 1404-1416, Jul. 2010.

[39] Z. Xue, J. Li, S. Li and B. Wan, "Using ICA to Remove Eye Blink and Power Line Artifacts in EEG ," *in Innovative Computing, Information and Control*, First International Conference, vol. 3, pp. 107-110, 2006.

[40] T.P. Jung, S. Makeig, C. Humphries, T.W. Lee, M.J. McKeown,V. Iragui, and T.J. Sejnowski, "Removing Electroencephalographic Artifacts by Blind Source Separation," *Psychophysiology*, vol. 37, pp. 163-178, 2000.

[41] A. J. Bell and T. J. Sejnowski, "An information maximization approach to blind separation and blind deconvolution," *Neural Computation*, vol. 7, pp.1129-1159, 1995.

[42] J.F. Cardoso, "High-order contrasts for independent component analysis," *Neural Computation*, vol. 11, pp. 157-192, 1999.

[43] A. Hyvärinen, "Fast and Robust Fixed-Point Algorithms for Independent Component Analysis" *IEEE Transactions on Neural Networks,* vol. 10, pp. 626-634, 1999.

[44] J. Onton, M. Westerfield, J. Townsend, and S. Makeig, "Imaging human EEG dynamics using independent component analysis," *Methodological and Conceptual Advances in the Study of Brain-Behavior Dynamics: A Multivariate Lifespan Perspective*, vol. 30, pp. 808-822, 2006.

[45] C. Jutten, J. Herault, "Blind separation of sources, Part 1: an adaptive algorithm based on neuromimetic architecture," *Signal Processing*, vol. 24, pp. 1-10, 1991.

[46] P. Comon, C. Jutten, J. Herault, "Blind separation of sources, Part 2: problems statement," *Signal Processing*, vol. 24, pp.11-20, 1991.

[47] R. Linsker, "Improved local learning rule for information maximization and related applications," *Neural Networks*, vol. 18, pp. 261-265, 2005.

[48] S. Amari, T.P. Chen, A. Cichocki, "Stability analysis of learning algorithms for blind source separation," *Neural Networks*, vol.10, pp. 1345-1351, 1997.

[49] T.W. Lee, M. Girolami, T. J.Sejnowski, "Independent Component Analysis using an Extended Infomax Algorithm for Mixed Sub-Gaussian and Super-Gaussian Sources," *Neural Computation*, vol. 11, pp. 417-441, 1999.

[50] M. Shen, L. Lin, J. Chen, and C. Q. Chang, "A Prediction Approach for

Multichannel EEG Signals Modeling Using Local Wavelet SVM," *IEEE Transaction On Instrumentation and Measurement*, vol. 59, no. 5, pp. 1485-1492, May 2010.

[51] A. Alenezi, Scott A. Moses, Theodore B. Trafalis,"Real-time prediction of order flowtimes using support vector regression", *Computers & Operations Research*, vol. 35, no. 11, pp. 3489-3503, 2008.

[52] U. Thissen, M. Pepers, B. UstUn, W. J. Melssen, L. M. C. Buydens,"Comparing support vector machines to PLS for spectral regression applications", *Chemometrics and Intelligent Laboratory Systems*, vol. 73, no. 2, pp. 169-179, 2004.

[53] C. C. Chang and C. J. Lin, LIBSVM : a library for support vector machines. ACM Transactions on Intelligent Systems and Technology, 2:27:1--27:27, 2011. Software available at http://www.csie.ntu.edu.tw/~cjlin/libsvm.

[54] B. B. Chaudhuri and U. Bhattacharya, "Efficient training and improved performance of multilayer perceptron in pattern classification," *Neurocomputing*, vol. 34, pp. 11-27, 2000.

[55] I. Guler and E. D. Ubeyli, "Multiclass support vector machines for EEG-signals classification," *IEEE Trans. Infor. Tech. in Biomedicine*, vol. 11, no. 2, pp. 117-126, Mar. 2007.

[56] S. Haykin, Neural Networks: A Comprehensive Foundation. Upper Saddle River, N.J.: Prentice Hall, 1999. 2nd Edition.

[57] L. X. Wang and J. M. Mendel, "Fuzzy basis functions, universal approximation, and orthogonal least-squares learning," *IEEE Trans. Neural Networks*, vol. 3, pp. 807-814, Sept. 1992.

[58] L. X. Wang, Adaptive Fuzzy Systems and Control. Englewood Cliffs, NJ: Prentice-Hall, 1994.

[59] M. D. Buhmann. Radial Basis Functions: Theory and Implementations.

Cambridge University, 2003.

[60] C. F. Juang and C. T. Lin, "An online self-constructing neural fuzzy inference network and its applications," *IEEE Transactions on Fuzzy Systems*, vol. 6, no. 1, pp. 12-32, Feb. 1998.

[61] Conference of European Directors of Roads, "Distance Between Vehicles", May (2011), available on line:

http://www.cedr.fr/home/index.php?id=218/e_Distance_between_vehicles .pdf

[62] Road Safety of Authority, "Stopping Distances for Cars", available on line:

http://www.rulesoftheroad.ie/rules-for-driving/speed-limits/speed-limits_s topping-distances-cars.html
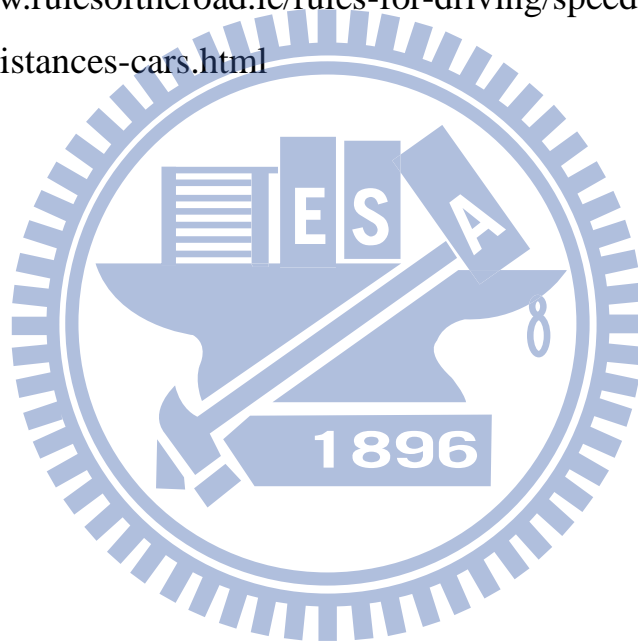
Publication List

## *Journal Paper*

[1] **Fu-Chang Lin**, Li-Wei Ko, Chun-Hsiang Chuang, Tung-Ping Su and Chin-Teng Lin, "Generalized EEG-based Drowsiness Prediction System by Using a Self-Organizing Neural Fuzzy System", *IEEE Transactions on Circuits and Systems I* (Accepted, 17th Dec. 2011).

[2] Chin-Teng Lin, **Fu-Chang Lin**, Shi-An Chen, Shao-Wei Lu, Te-Chi Chen, Li-Wei Ko, "EEG-based Brain-computer Interface for Smart Living Environmental Auto-adjustment", *Journal of Medical and Biological Engineering*, 30(4): 237-245, June 2010.

[3] C. W. Chang, L. W. Ko, **F. C. Lin**, T. P. Su, T. P. Jung, C. T. Lin, and J. C. Chiou, "Drowsiness Monitoring with EEG-Based MEMS Biosensing Technologies," GeroPsych: *The Journal of Gerontopsychology and Geriatric Psychiatry*, vol. 23, no. 2, pp. 107-113, June 2010.

## *Conference Paper*

[1] **F. C. Lin**, L. W. Ko, S. A. Chen, C. F. Chen, and C. T. Lin, "EEG-based Cognitive State Monitoring and Prediction by Using the Self-Constructing Neural Fuzzy System," Proceedings of the 2010 *IEEE International Symposium on Circuits and Systems* (ISCAS 2010), Paris, France, May 30 – June 2, 2010.